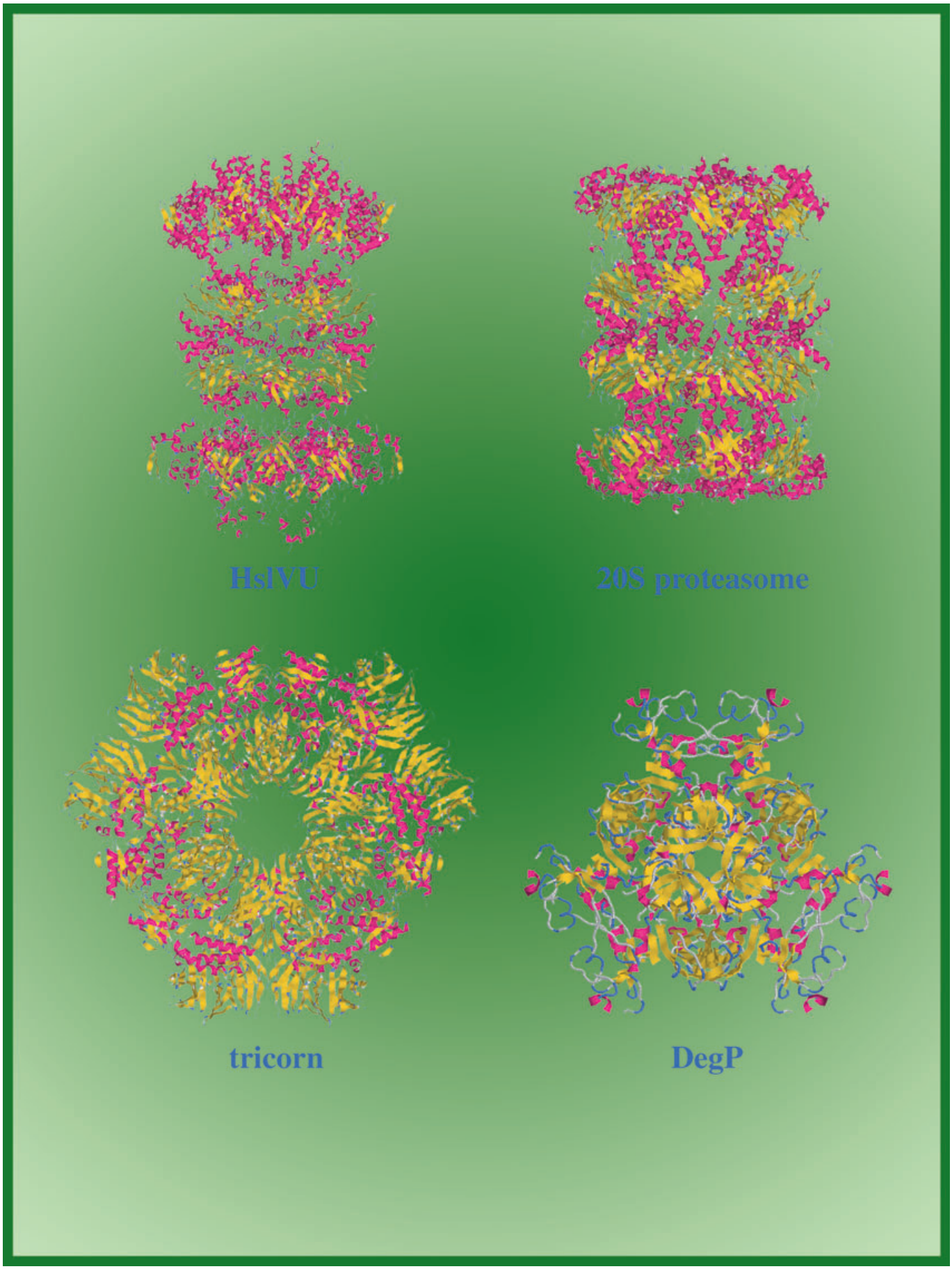

  DOI: 10.1002/cbic.200400313 *ChemBioChem* **2005**, *6*, 222 – 256

Molecular Machines for Protein Degradation

Michael Groll,*[a] Matthias Bochtler,[c, d] Hans Brandstetter,[e] Tim Clausen,[f] and Robert Huber[b]

One of the most precisely regulated processes in living cells is intracellular protein degradation. The main component of the degradation machinery is the 20S proteasome present in both eukaryotes and prokaryotes. In addition, there exist other proteasome-related protein-degradation machineries, like HslVU in eubacteria. Peptides generated by proteasomes and related systems can be used by the cell, for example, for antigen presentation. However, most of the peptides must be degraded to single amino acids, which are further used in cell metabolism and for the synthesis of new proteins. Tricorn protease and its interacting factors are working downstream of the proteasome and process the peptides into amino acids. Here, we summarise the current state of knowledge about protein-degradation systems, focusing in particular on the proteasome, HslVU, Tricorn protease and its interacting factors and DegP. The structural information about these protein complexes opens new possibilities for identifying, characterising and elucidating the mode of action of natural and synthetic inhibitors, which affects their function. Some of these compounds may find therapeutic applications in contemporary medicine.

Introduction

One of the biggest challenges in modern cell biology is to unveil the principles of intracellular protein synthesis and protein degradation. Functional analysis of structural data has significantly contributed to the recent progress in understanding interactions between elements of the protein-synthesis machinery and their regulation. At the same time, the picture of protein-degradation processes and interactions between the components involved is still incomplete. In eukaryotic cells most cytosolic and nuclear proteins are degraded by the ubiquitin (Ub)/proteasome pathway, which is responsible for protein quality control, antigen processing, signal transduction, cell-cycle control, cell differentiation and apoptosis. This pathway employs a complex enzymatic system to degrade proteins. Protein substrates are marked by covalent addition of a poly-Ub chain and are subsequently degraded by a 2500 kDa proteolytic molecular machine, known as the 26S proteasome. The discovery of ubiquitination was honored with the Nobel prize in Chemistry in the year of 2004, thereby highlighting the discovery of this important physiological regulatory mechanism. The 26S proteasome plays its role as the proteolytic machinery in this cascade of reactions by degrading previously marked substrate proteins. This multifunctional complex is built up from the 700 000 Da proteolytic core particle (CP, 20S proteasome) and two 900 000 Da regulatory particles (RPs, 19S complexes), which are responsible for substrate recognition, substrate unfolding and substrate translocation.

When the involvement of the Ub/proteasome protein degradation pathway in a vast number of cellular processes is considered, inhibitors of this system are promising candidates as antitumor or antiinflammatory drugs. After the discovery of the 20S proteasome, its mode of action was first analysed with nonspecific protease inhibitors. Specific inactivation of proteasomal active centres for a limited amount of time reduces cytotoxic effects, and this has been a major topic of proteasomal investigations lately. New synthetic and natural inhibitors have greatly facilitated the investigation of the proteasome in vivo as well as in vitro (see Section 2). The released structural information allowed the Millennium Pharmaceuticals company to develop the proteasome inhibitor Valcade (bortezomib), which passed the clinical phase III study this year and now represents a newly approved prescription drug against multiple myeloma. These and further experiments will certainly enhance interest in the proteasome as a potential target for drug development in medical research.

CPs are ubiquitous among all three kingdoms of life. However, in contrast to eukaryotes, archaea and actinomycetes contain a much more simply organised core particle (only one type of α and one type of β subunit; see Section 2), whereas eubacteria possess a proteasome-related system named HslV

[a] *Dr. M. Groll*
Present address:
Adolf-Butenandt-Institut Physiological Chemistry, LMU München
Butenandtstraße 5, Gebäude B, 81377 München (Germany)
Fax: (+49) 89-2180-77093
E-mail: michael.groll@bio.med.uni-muenchen.de

[b] *Prof. Dr. R. Huber*
Abteilung Strukturforschung, Max-Planck-Institut für Biochemie
Am Klopferspitz 18a, 82152 Martinsried/Planegg (Germany)

[c] *Dr. M. Bochtler*
Present address:
IIMCB, ul. Trojdena 4, 02-109 Warsaw (Poland)

[d] *Dr. M. Bochtler*
Present address:
MPI-CBG, Pfotenhauerstraße 108, 01309 Dresden (Germany)

[e] *Dr. H. Brandstetter*
Present address:
Proteros Biostructures GmbH
Am Klopferspitz 19, 82152 Martinsried (Germany)

[f] *Dr. T. Clausen*
Present address:
Institute of Molecular Pathology
Dr. Bohrgasse 7, 1030 Wien (Austria)

 DOI: 10.1002/cbic.200400313

(comprised of only one type of β subunit; see Section 1). Although subunits of the HslV complex show substantial structural and functional similarities to the corresponding subunits of archaeal and eukaryotic CPs, the general architecture and the assembly of the mature complexes differ significantly.

Despite all the differences, a common feature of the CPs and proteasome-related systems is the generation of peptide fragments with a length distribution of about 8–15 amino acid residues. As a rule, these peptides cannot be reused by the cell and have to be further degraded by proteases to single amino acids, which can be utilised for de novo protein synthesis. One example of this kind of protease in prokaryotes is the tricorn protease (TRI), which exists only in some archaea and eubacteria (see Section 3). Structural and functional analysis has shown that the tricorn protease acts as a carboxypeptidase with preferential di- and tripeptidase activity. Further degradation of these small peptides is performed by tricorn-interacting proteases, such as the aminopeptidases F1, F2 and F3. Since

Michael Groll was born in 1971 in Donauwörth, Germany. He studied chemistry in Munich, Germany, and then joined Prof. Robert Huber for postgraduate studies. In 1998, he received his PhD for crystallographic and biochemical studies on the 20S proteasome from S. cerevisiae*. He continued to work with Prof. Huber as a postdoctoral researcher, but also spent some time at Harvard Medical School in Prof. Finley's group. In 2004, he received his Habilitation from the "Charité" in Berlin for his work on structural and functional relationships between archaebacterial and eukaryotic 20S proteasomes. Since 2004, Michael Groll has been running an independent research group in the Adolf-Butenandt-Institut for Physiological Chemistry of LMU Munich.*

Matthias Bochtler was born in Nürnberg, Germany, in 1971. He studied physics in Munich and in Cambridge, UK, and then joined Prof. Robert Huber's group in Martinsried for a PhD in protein crystallography. In 2001, he accepted a joint appointment by the Max Planck Society and the Polish Academy of Sciences to start an independent research group in Warsaw, Poland. His research interests are focused on peptidases, proteases and protein degradation.

Biochemist Tim Clausen was born in 1969 in Flensburg, Germany. He graduated in biology from the University of Constance and then went on to Munich Technical University, where he obtained his PhD in 1997 for work with Prof. Robert Huber on pyridoxal-dependent enzymes. He continued with structural studies in Martinsried, and received his Habilitation from the University of Constance in 2001. During this time he has also become interested in proteases and chaperones. At present, Tim Clausen is running an independent research group at the Institute of Molecular Pathology (IMP) in Vienna, Austria.

Hans Brandstetter was born in Vilsbiburg, Germany, in 1964. He studied physics in Munich and then joined Prof. Robert Huber at the MPI in Martinsried. He graduated with a PhD thesis on the structural biology of blood coagulation factors IIa, IXa and Xa in 1994. Awarded an Alexander von Humboldt fellowship, Hans Brandstetter moved on to join the groups of Prof. Stephen J. Lippard and Prof. Christin A. Frederick at the Massachusetts Institute of Technology and the Dana Farber Cancer Institute/Harvard Medical School for structural and mechanistic studies on the methane monooxygenase system. On his return to the group of Prof. Robert Huber, his work focused again on proteases, including metalloproteinases, tricorn and the DP IV peptidase. Since 2003 Hans Brandstetter has served as the chief scientific officer to Proteros Biostructures.

Robert Huber was born in 1937 in Munich. He studied chemistry at the Technical University of Munich, where he also completed his PhD and Habilitation. Since 1972, he has been a member and scientific director at the Max-Planck-Institut for Biochemistry, and he has also served TU Munich as a professor since 1976. Prof. Huber has made major contributions to the understanding of the structure and function of biological macromolecules. He has studied proteases and their natural and synthetic inhibitors, metalloenzymes (iron, nickel, molybdenum, copper), proteins of the immune system (antibodies and antibody receptors), protein hormones and their receptors, protein kinases, enzymes of amino acid biosynthesis (PLP-containing enzymes), enzymes of cofactor and vitamin biosynthesis and proteins of energy and electron transfer. In addition, he has contributed to the development of instruments for data collection and to methods in protein crystallography, particularly Patterson methods, graphic methods and refinement, to the use of electron-rich metal clusters, and most recently to the methods and instruments for crystal annealing and improvement. His work has been recognised with numerous honorary doctorates, professorships, memberships in learned societies and awards, including the Otto-Warburg Medal, the Emil von Behring Medal, the Sir Hans Krebs Medal, the Linus Pauling Medal, the Max Tishler Prize and, in 1988, the Nobel Prize for Chemistry together with H. Michel and J. Deisenhofer.

the distribution of the tricorn protease among microbial genomes is limited, there should exist functional analogues. The recently identified tetrahedral aminopeptidase (TET) is able to degrade oligopeptides to single amino acids and can be considered as a functional equivalent of the tricorn protease. Structural data have revealed its molecular architecture and functional characteristics.

The four proteases discussed in this review display different regulatory mechanisms but show sequestration of their active sites inside molecular cages as a common structural principle, although the structures are assembled from different building blocks in different shapes and with varying symmetries. We focus in particular on structural, functional and mutational studies from our laboratories. Other cage-forming proteases and their regulatory components that have been structurally characterised are mentioned briefly.

1. The ATP-Dependent Protease HslVU

HslVU, presently the mechanistically best-characterised adenosine triphosphate (ATP) dependent protease, is the most recent addition to the set of known ATP-dependent proteases in bacteria. In contrast to other enzymes in this group, HslVU had eluded all attempts to isolate the ATP-dependent proteolytic activities from the bacterial cytosol, probably because of the lability of the complex. The first hint about the existence of this ATP-dependent protease emerged from a screen for bacterial heat shock genes that led to the identification[1] and sequencing[2] of the *hslVU* operon. The sequence data showed that HslU was an Hsp100 protein with a Walker ATPase motif, and they also revealed a remarkable similarity of HslV with the β subunits of archaebacterial and eukaryotic proteasomes, a fact suggesting that HslV could have protease activity.[2] The presence of both genes in the same operon suggested the possibility that they could form an ATP-dependent protease. This hypothesis was subsequently proven by the demonstration that ATP-dependent peptidase activity could be reconstituted from the recombinantly expressed and purified components.[3,4] HslVU was subsequently rediscovered several times. The enzyme was independently discovered in screens for proteins that could downregulate the heat shock response[5] and for suppressors of the SOS-mediated inhibition of cell division in *Escherichia coli*.[6] The observed biological responses in HslVU-overexpression or -deletion strains result from a decrease or increase in the steady levels of HslVU substrates.[7] HslVU, itself a heat shock protein, affects the heat shock response by degradation of the heat shock factor σ32[8,9] and affects the SOS response through the degradation of the cell-division inhibitor SulA.[9,10]

HslVU biochemistry and physiology

The physiological role of HslVU seems to be limited, probably because of overlapping substrate specificity with other ATP-dependent proteases in bacteria. In *E. coli*, HslVU deletion has no effect on the phenotype at standard growth temperature and affects growth and viability only at very high temperatures.[7] According to the protease database MEROPS, some bacterial species appear to lack an HslVU-type peptidase altogether.[11] Therefore, it came as a surprise that some HslV and HslU homologues were recently found in primordial eukaryotes, where they appear to be simultaneously present with genuine 20S proteasomes.[12] Low expression levels and the lability of the HslVU complex make work with proteins from wild-type strains difficult. Gratifyingly, the active protease can be reconstituted in vitro from overexpressed and purified components.[3] It requires ATP for the degradation of folded substrates and ATP or some of its analogues for the purification of small chromogenic peptides. As expected, the ATP-hydrolysis and proteolysis activities are mutually dependent.[13] In addition, the peptidase activity was found to depend in complex ways on the presence of various cations, especially K^+, in the buffers.[14]

HslV peptidase

On the sequence level, HslV shows sequence similarity with the β subunits of archaebacterial and eukaryotic proteasomes, a fact that was immediately noticed when the *E. coli* gene was sequenced[2] and was later shown to extend to other related eubacterial sequences.[15] Electron microscopy of recombinant HslV subsequently suggested that the particle formed a dimer of hexamers that appeared to enclose only one central cavity without antichambers, as in proteasomes.[16] The unexpected sixfold symmetry of HslV and the similarity of subunit fold with that of eukaryotic proteasomes were subsequently confirmed by X-ray crystallography.[17] The crystallographic data also showed that the contracted ring, as compared to that of proteasomes, resulted from small changes to the subunit–subunit interface, not from an entirely new mode of oligomerisation[17] (Figure 1).

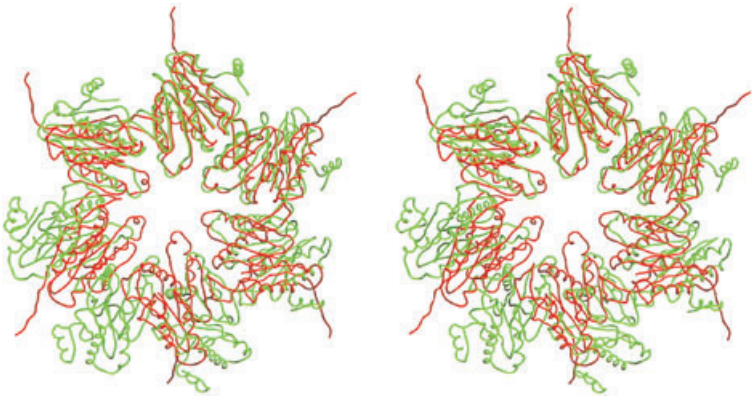

Figure 1. *Comparison of* E. coli *HslV and the* T. acidophilum *proteasome. A superposition of one hexameric ring of* E. coli *HslV (red) with one heptameric ring of the β subunit of the* T. acidophilum *proteosome (green) is shown in stereo representation. The subunits at the "top" of the ring have been overlayed optimally. The "tails" of the HslV subunits that point radially outwards are histidine tags and are thus cloning artefacts. Figure reproduced from ref. [17].*

All 12 active sites of HslV are located on the inner walls of the hollow particle. In the *E. coli* particle, each active site has neighbouring active sites 28 Å away on the same ring and 22 and 26 Å away on the opposite ring. The environment of the nucleophilic Thr1 looks similar to that in proteasomes, and the presence of a (putatively protonated) lysine residue near the active site probably helps to lower the pK_a value of the N-terminal α-amino group so that it is present in the unprotonated form that can act as the general base to accept a proton from Thr1.

Since the determination of the HslV crystal structure, two additional crystal structures from other species have also been determined. The highest resolution structure available to date is the crystal structure of the *Haemophilus influenzae* enzyme.[18] Intriguingly, this structure showed the presence of cation-binding sites near the active centres,[18] a finding that could subsequently be confirmed for the *Thermotoga maritima* enzyme[19] and that explains, at least in qualitative terms, the dependence of HslVU activity on various cations in solution. Overall, the crystal structures of the enzymes from *H. influenzae*[18] and *T. maritima*[19] are very similar to the original structure of the *E. coli* enzyme. Therefore, it came as a surprise that the HslV homologue from *Bacillus subtilis*, known as CodW, behaves rather differently. Although the enzyme contains a threonine residue that aligns with the active-site threonine of the *E. coli*, *H. influenzae* and *T. maritima* enzymes, it does not contain the glycine at the C terminus of the profragment, a residue that is believed to be required for efficient autocatalytic processing; indeed, the polypeptide chain is processed five residues upstream of the conserved threonine that is the active-site nucleophile in other species, to expose an N-terminal serine residue.[20] Whether this implies that the serine is in the spatial position normally filled by the threonine, thereby implying a discrepancy between the sequence-based and structure-based alignments, or whether it means that the accessory catalytic residues are either dispensible or anchored elsewhere on the sequence is currently not clear.

HslU ATPase

Based on the sequence, HslU can be easily classified as an ATPase due to the presence of conventional Walker A (phosphate-binding loop or P-loop) and Walker B (magnesium-binding) motifs. Beyond this simple classification, two competing models for HslU were proposed, which classified the enzyme either as a PDZ-domain-containing ATPase[21] or alternatively as a AAA(+)-type ATPase.[22] The crystal structure settled the issue in favour of the AAA(+) model.[23] AAA(+) ATPases consist essentially of two structural domains that are connected through a short linker. The nucleotide binds at the interface of the two domains. As first observed with HslU, the presence or absence of nucleotide induces different relative orientations between the two domains.[23] With the availability of many different nucleotide states of HslU, the model was later refined to include a dependence on the state of hydrolysis of the nucleotide.[24]

The nucleotide is in a strategic position both at the interface of the N and C domains of one subunit and at the interface of adjacent subunits. A combination of mostly conserved residues from the two subunits around the nucleotide creates a highly polar environment.[23] Two arginine residues have attracted particular attention. Arg393 of *E. coli* HslU is thought to act as the "sensor" that transmits information on the presence or absence of nucleotide and possibly on its identity to the C domain and thus controls the relative orientation of N and C domains in HslU. Another conserved arginine residue, Arg325, is anchored on the subunit that makes fewer contacts with the nucleotide and is a homologue of the proposed "arginine finger" in FtsH.[25] Although the term "arginine finger" (taken from the small guanosine triphosphate (GTP) binding proteins Ras and Rho) implies a direct catalytic role for this residue, its distance from the phosphate groups of the nucleotide argues more for an indirect role. A similar conclusion has since been reached for ClpA.[26] Experimentally, mutation of either of the two arginine residues abolishes all ATP-dependent proteolysis activity.[27] Loss of subunit interactions plays a major role in the loss of function: The "arginine sensor" mutant Arg325Glu is fully and the "arginine finger" mutant Arg393Glu is partially dissociated in gel-filtration experiments in the presence of salt.[27]

A very complex picture has emerged from biochemical and crystallographic studies designed to characterise the substrate binding sites in HslU. An essential role for the C terminus of HslU was first suggested on the basis of experimental studies that were designed based on the prediction of PDZ-like domains at the C terminus of HslU.[21] Although the prediction of PDZ-like domains later turned out to be in error, the conclusion about a role for the C terminus of HslU in substrate recognition was later corroborated with the description of a biochemically defined "sensor and substrate-discrimination domain (SSD)"[28] that is also present in other AAA(+) ATPases

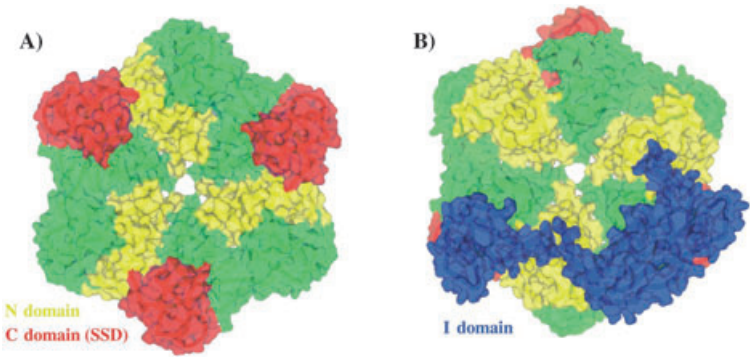

Figure 2. *HslU surface-coloured according to domain. A) View along the sixfold axis, seen from the side opposite to the I domains. B) View along the sixfold axis, seen from the side of the I domains. Every second subunit of the ring is coloured according to domain (N domain = yellow, I domain = blue, C domain or SSD domain = red), while the other subunits are coloured in green. The diagram is based on the trigonal crystals of* E. coli *HslU that contain nucleotide in every other subunit. The asymmetry and crystallographic packing effects are responsible for the broken sixfold symmetry of the I domains. Note that the I domains of three subunits at the top of the figure have been cut away in (B) to allow a view on the globular N and C domains.*

and was suggested to act as the "hook" for substrates.[29] When the crystal structure of HslU became available, the SSD domain turned out to coincide with the C domain. This finding is remarkable and not fully understood, since in all crystal structures of HslU the C domain primarily mediates oligomerisation contacts between HslU subunits. Its solvent-accessible regions are found on the periphery of the HslU ring, far outside the cavity that is formed by the protruding I domains (Figure 2). From the crystal structure,[23] it would appear likely that the protruding I domains, rather than the SSD domains, act as the "hook", although the ill-defined tertiary structure of the I domains makes specific interactions unlikely (Figure 2). In agreement with this model, it was found experimentally that the I domains are essential for the degradation of the folded substrate MBP-sulA.[27] A recent two-hybrid study is consistent with both points of view: it confirms the essential role of the C domain (SSD domain) in oligomerisation but also supports a role for the I domain and the SSD domain in substrate degradation. Presumably, if substrates are translocated through the central pore in HslU as electron-microscopy data suggest for ClpXP,[30] both the I domains and the globular part of the ring would come into contact with the substrate during substrate translocation, although the location of the C domains (SSD domains) on the periphery of the HslU ring would still need to be reconciled with this model.

The precise mode of recognition of substrates is even less clear for CodX, the HslU homologue from *B. subtilis*. In the absence of detergent, the I domains of two hexameric CodX rings contact each other, which leads to a head-to-head stacking of CodX rings and, presumably, the formation of a central cavity loosely surrounded by I domains. As the dimer of CodX rings can associate with the CodW protease on either side, repetitive, chain-type structures with alternating double rings of the peptidase CodW and the ATPase CodX can be formed.[31] The physiological significance of these high-molecular-weight assemblies is currently not clear.

ed a ratcheting mechanism in HslVU. This conclusion has since been confirmed by all HslU and HslVU crystal structures.[23,35–37] In all cases, HslU is hexameric and matches the oligomerisation state of HslV. For the first crystal structure of an HslU–HslV co-crystal, a controversial I-domain-mediated contact between HslU and HslV was reported.[38–40] The contact was suspicious from the very beginning because of the poor contact area, but it seemed compatible with the known low affinity between HslV and HslU and appeared to explain how the symmetry-mismatched ClpXP and ClpAP complexes could be formed. Although a crystallographic reinterpretation of our original data that attributed this docking mode to overlooked twinning[38,40] turned out to be itself in error,[39] it is now clear from the combined results of cryoelectron microscopy,[41] small-angle scattering analysis[36] and several additional crystal structures of the complex[35,36] that the physiological mode of interaction between HslU and HslV is with HslU I domains distal to HslV (Figure 3).

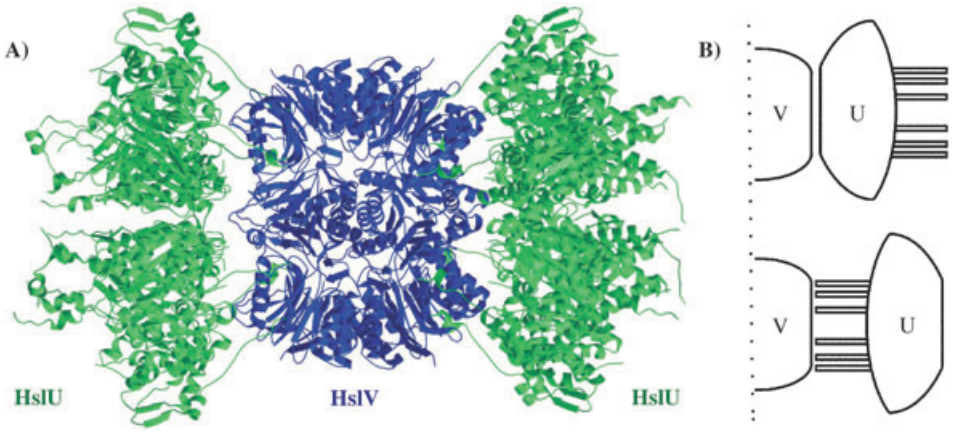

Figure 3. *HslVU complex. A) Crystal structure of the HslVU complex in the physiologically relevant form, drawn according to the coordinates in PDB file 1G3I.[36] Note the insertion of the C termini of HslU into clefts in HslV. B) Schematic comparison of the physiologically relevant binding mode, with I domains of HslU distal to HslV, with the originally reported mode of association, which has the I domains proximal to HslV.*

HslVU protease complex

A key theme in ATP-dependent proteolysis has been the issue of "symmetry-matched" versus "symmetry-mismatched" complexes. In the light of the clearly established symmetry mismatch of the ClpAP[32] and ClpXP[33] complexes, the unambiguous sixfold symmetry of HslV[16,34] in electron-microscopy images and the reports of a predominant HslU species with sixfold symmetry[16,34] came as a surprise because they excluded a ratcheting mechanism in HslVU. This conclusion has since been confirmed by all HslU and HslVU crystal structures.[23,35–37] In all cases, HslU is hexameric and matches the oligomerisation state of HslV. For the first crystal structure of an HslU–HslV co-crystal, a controversial I-domain-mediated contact between HslU and HslV was reported.[38–40] The contact was suspicious from the very beginning because of the poor contact area, but it seemed compatible with the known low affinity between HslV and HslU and appeared to explain how the symmetry-mismatched ClpXP and ClpAP complexes could be formed. Although a crystallographic reinterpretation of our original data that attributed this docking mode to overlooked twinning[38,40] turned out to be itself in error,[39] it is now clear from the combined results of cryoelectron microscopy,[41] small-angle scattering analysis[36] and several additional crystal structures of the complex[35,36] that the physiological mode of interaction between HslU and HslV is with HslU I domains distal to HslV (Figure 3).

Allosteric activation

In the absence of nucleotide, HslVU has residual activity at best, but the presence of several nonhydrolysable ATP analogues is sufficient to stimulate HslVU-driven proteolysis activity against substrates that do not require unfolding, a fact suggesting an allosteric effect of the nucleotide on HslU and, through HslU, also on HslV. This was further corroborated by the observation that a peptide vinyl sulfone only formed a covalent complex with HslV in the presence of HslU and nucleotide.[42] The details of this allosteric mechanism emerged from the crystal structure of HslVU from *H. influenzae*. In this case, but not in other crystal structures of the HslVU complex, the normally buried C termini of the HslU subunits distend and insert into the active-site clefts in HslV to reach out almost to the HslV active centres[36] (Figure 4). The crystal structure of HslVU in complex with a peptide vinyl sulfone inhibitor[43] and two independent biochemical studies[44] that demonstrated

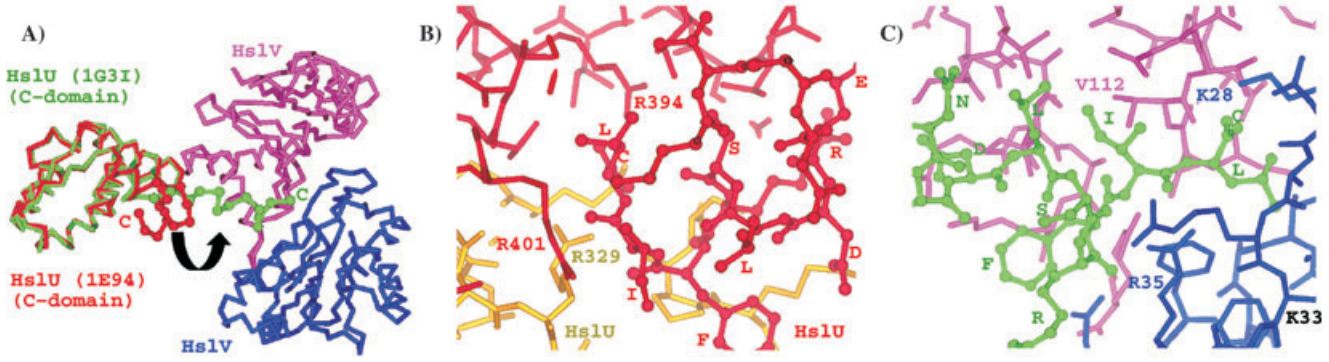

Figure 4. *HslVU activation mechanism. A) Cα trace of the superposition of the C domain of an HslU subunit (red) from the original* E. coli *HslVU complex onto that of the* H. influenzae *HslU subunit (green) from its complex. Two HslV subunits (pink and blue) from the* H. influenzae *complex are also shown to illustrate the binding of the C-terminal segment of* H. influenzae *HslU to the pocket between the HslV subunits (indicated also by a black curved arrow). B) Close-up of the C-terminal residues of an* E. coli *HslU subunit (red) from the complex. The carboxylate group of the terminal leucine residue forms salt bridges with Arg394 of the same subunit and with Arg329 of an adjacent (yellow) HslU subunit, which is not illustrated in (A) for clarity. C) Close-up of the C-terminal residues of an HslU subunit from the* H. influenzae *HslVU complex. Figure adapted from ref. [45].*

the activatory properties of the C-terminal tails of HslU further corroborated this mechanism. In the light of these data, it is remarkable that wild-type HslU in the presence of adenosine diphosphate (ADP) does not act as an activator for HslV, not even against unfolded or chromogenic substrates. A possible but experimentally untested explanation could be that the C termini of the HslU subunits are available for HslV binding only in the presence of activatory nucleotides.

Whatever the details of the allosteric activation mechanism, it is already clear that HslU primarily affects the conformation of the HslV active sites and not the accessibility of the HslV proteolytic chamber. Two independent lines of in vitro evidence support this conclusion. Firstly, an HslV mutant with a widened entrance channel does not show increased proteolytic activity in the absence of HslU, although it can still be activated like wild-type HslV by the presence of HslU.[45] Secondly, the recently determined crystal structure of the *H. influenzae* asymmetric HslVU protease in complex with an inhibitory peptide vinyl sulfone has the inhibitor bound only in HslV subunits that are in contact with HslU,[37] a fact strongly arguing against accessibility of the proteolytic chamber as the rate-limiting factor, at least under experimental conditions.

The eubacterial HslVU is distantly related in structure to the proteasome found in archaea, actinomycetes and eukaryotes. Surprisingly, however, the structural relationship is not reflected in the regulatory properties, as will be described in the following section which focuses on structural studies of the 20S proteasome and its activation, activity and inhibition.

2. The 20S Proteasome

The 20S proteasome complex

The 20S proteasome (core particle; CP) is a large, cylinder-shaped protease with the molecular weight of about 700 000 Da. It plays a crucial role in cellular protein turnover and is found in all three kingdoms of life. Electron micrographs of 20S proteasomes have revealed that it has molecular dimensions of about 160 Å in length and 120 Å in diameter.[46] The complex is formed by 28 protein subunits, which are arranged in 4 stacked rings, each comprising 7 subunits.[47] The detailed architecture of the CP was elucidated by crystal-structure analysis of the archaebacterial 20S proteasome from *Thermoplasma acidophilum* at 3.4 Å resolution.[48] The structural data showed that the CP has the shape of an elongated cylinder with three large cavities and narrow constrictions between them. The molecule has 72 point symmetry following an $\alpha_7\beta_7\beta_7\alpha_7$ stoichiometry. The two outer chambers are formed by α and β rings, whereas the central chamber containing the proteolytic active sites is composed of the β rings. The α and β subunits of the CP show similar folding, although the primary sequences of these subunits are quite different (Figure 5 A). The fold of the subunits is characterised by a sandwich of two five-stranded antiparallel β sheets, which are flanked by helical layers on the top and bottom. Archaebacterial proteasomes can be regarded as the prototype for the quaternary structure and topology of CPs, whereas the general architecture of eukaryotic CPs is much more complex.[49,50] These molecules represent the most elaborate versions of the CP, as the α and β subunits have each diverged into seven different subunits. Eukaryotic CPs show pseudo-sevenfold symmetry and consist of two equal parts ($\alpha_{1-7}\beta_{1-7}\beta_{1-7}\alpha_{1-7}$), which are related by twofold symmetry. The nomenclature of each subunit is defined according to the structural data from the yeast CP.[49] Residue numbers for these subunits are assigned on the basis of the alignment to *T. acidophilum* (Figure 5 B, C). All 14 different eukaryotic proteasomal subunits contain characteristic insertion segments and termini, which represent well-defined contact sites between related subunits and lead to their unique locations at special positions within the particle (Figure 5 D). Compared to the archaebacterial CPs which have 14 identical active sites, eukaryotic 20S proteasomes contain only three proteolytically active β-type subunits, β1, β2 and β5, whereas the other β-type subunits are inactive. In mammals, γ-interferon provokes the substitution of the three active β subunits (β1, β2 and β5) with three newly synthesised low-molecular-mass polypeptide (LMP) subunits

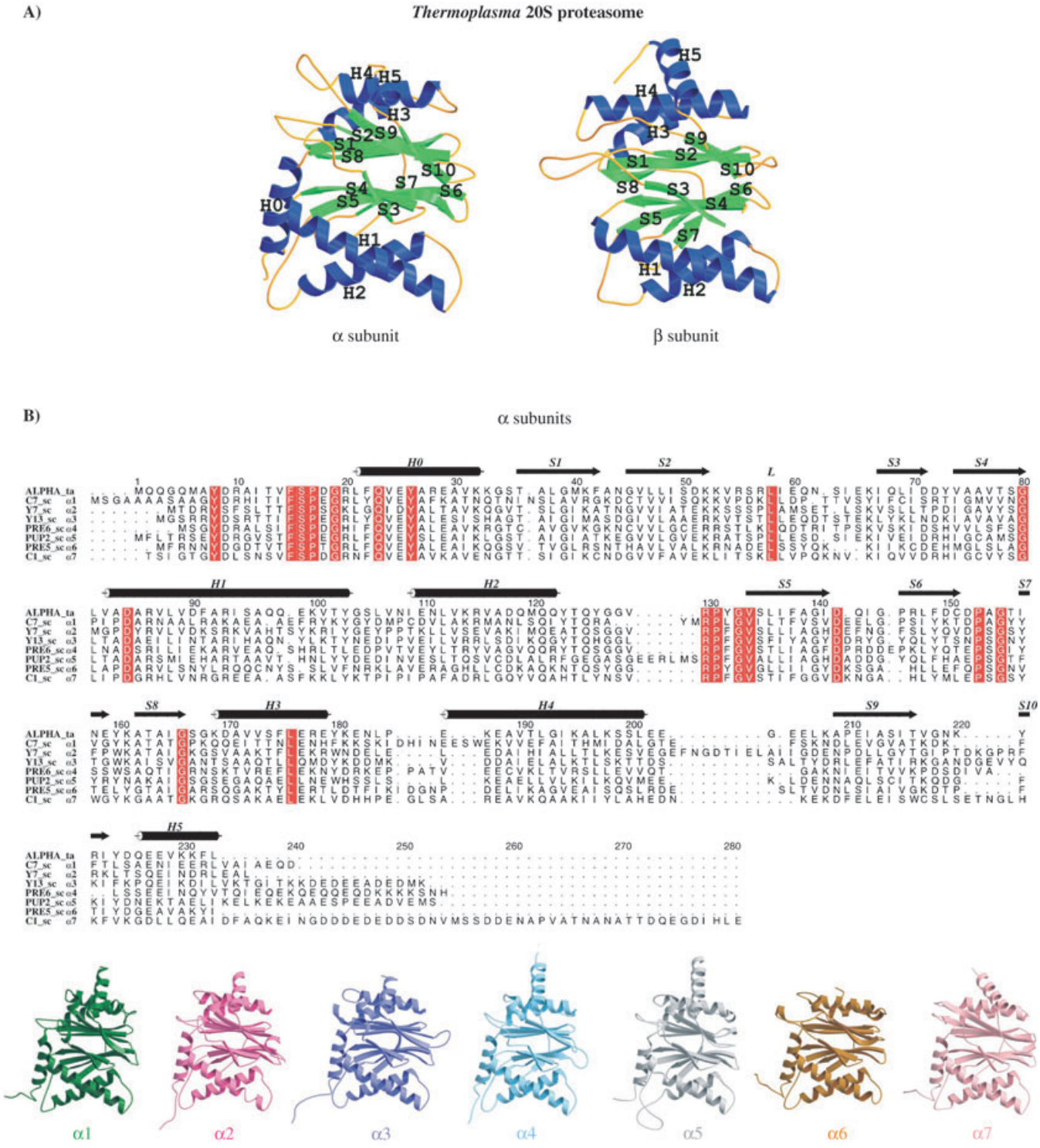

Figure 5. *A) Ribbon drawings of the α and β subunits from* T. acidophilum.[48] *Helices and β strands are coloured in blue and green, respectively, and secondary structure elements from helices H0–H5, as well as from β strands S1–S10, are labelled in black. B) Sequence alignment of the various α-type subunits of CPs from* T. acidophilum *and yeast. Conserved amino acids among all α-type subunits are highlighted against a red background; helices and β strands are shown as black cylinders and arrows, respectively. Below are the ribbon drawings of each of the different α-type subunits from* Saccharomyces cerevisiae. *Orientations of the subunits are similar to those illustrated in (A). Each α-type subunit contains specific insertions and terminal extensions, which cause their unique locations in the matured CP. C) Sequence alignment of the various β-type subunits in matured CPs from* T. acidophilum *and yeast. (Prosegments of the proteolytically active subunits are removed, subunits β6 and β7 are only shown with their partially processed precursor sequence.) The proteolytically active subunits β1, β2 and β5 are highlighted against green, yellow and blue backgrounds, respectively. Additionally, these subunits are aligned with their related constitutive and γ-interferon-inducible human β-type subunits. Positions 20, 31, 35 and 45 of the S1 specificity pocket of subunit β1 are coloured in orange, thereby illustrating the change of specificity in the inducible human immunosubunit. The labelling and representation of the ribbon drawings of the various β-type subunits from yeast is similar to that described in (B). D) Topology of the 28 subunits of the yeast CP drawn at atomic resolution and as spheres. The segment of the β–β′ rings shows Cα-chain tracings of subunits β1, β2, β3, β6′ and β7′, thereby highlighting their β–*cis* and β–trans–β interactions through characteristic contacts of insertion segments.*[49]

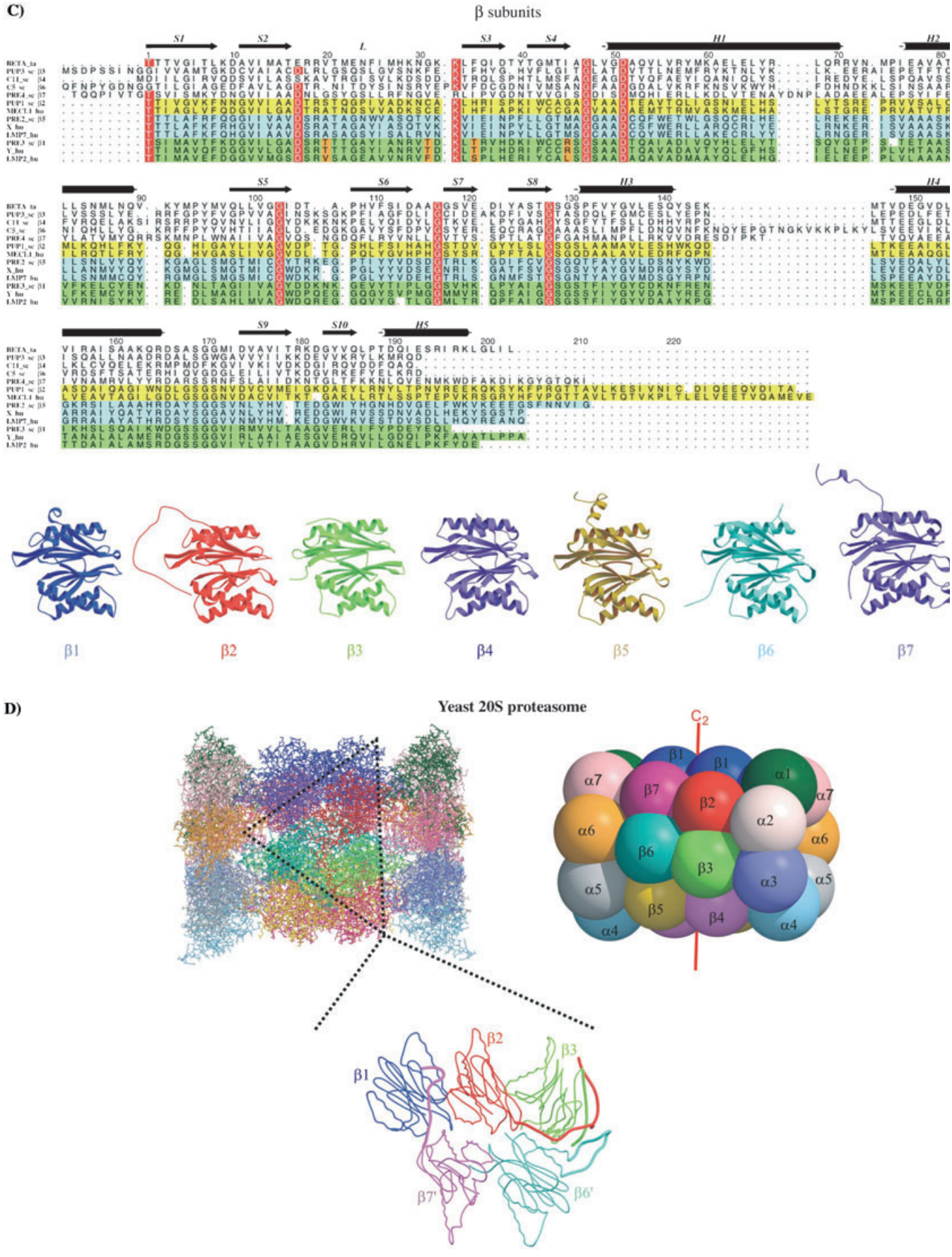

Figure 5. *(Cont.)*

termed β1i, β2i and β5i.[51,52] The incorporation of the γ-interferon-inducible subunits into the CP requires its de novo assembly and depends on the cell's development state and the tissue type.[53,54] Collectively, these γ-interferon-inducible subunits are referred to as the immunosubunits as they tune the CP for higher efficiency to generate specific antigenic peptides.[55] These epitopes are finally loaded onto major histocompatibility complex (MHC) class I proteins and initiate the immune response.

The proteolytic active centres

The crystal structure of the CP from *T. acidophilum* in complex with the competitive inhibitor *N*-acetyl-Leu–Leu–norleucinal (Calpain inhibitor I) showed for the first time that the proteolytic active centres in archaebacterial proteasomes are formed by the N-terminal threonine of each of the β subunits.[48] The functional aldehyde group of the inhibitor is covalently bound to the Thr1 Oγ atom as a hemiacetal. The tripeptide aldehyde adopts a β conformation and fills the gap between β strands by generating an antiparallel β-sheet structure. 20S proteasomes were the first known example of threonine proteases. Structural and mutational studies defined Thr1, Glu17 and Lys33 as the most important residues for the proteolytic system. Additionally, Ser129, Asp166 and Ser169 are close to the active-site threonine and seem to be required for the structural integrity of the proteolytic centre, as well as being involved in catalysis.[48,56] Crystal structures of the yeast 20S proteasomes as well as the characterisation of various mutants finally allowed the elucidation of the proteolytic mechanism in CPs.[49,57,58] These results demonstrate that the Thr1 Oγ atom reacts either with electrophilic functional groups of inhibitors or with peptide bonds of substrates, while the Thr1 N atom represents the proton acceptor (Figure 6 A). The N terminus of the nucleophilic threonine is hydrogen bridged to the Ser129 Oγ, Asp168 O and Ser169 Oγ atoms, whereas the Thr1 Oγ is hydrogen bonded to the Lys33 Nζ atom. The pK_a value and status of protonation of the ionisable groups is unknown, but the pattern of hydrogen bonds suggests that at least the Lys33 Nζ atom is charged. Indeed, in yeast, the conserved active substitution of Lys33 with Arg33 in subunit β5 leads to its inactivation. The structural superposition of this mutant with the wild-type shows a change of Arg33 only, which for sterical reasons has its guanidino group tilted relative to the amino group of the lysine residue to avoid a clash with Thr1.[58] This rearrangement is possibly associated with effects on the intrinsic pK_a values of the Thr1 Oγ and Thr1 N atoms, thus preventing the hydrolysis of substrates. Besides the nucleophilic N-terminal threonine, a nucleophilic water molecule, termed NUK, is also essential for proteolysis. It is in proximity to the Thr1 Oγ, Thr1 N, Ser129 Oγ and Gly47 N atoms. It had been missed in the electron-density map of the CP from *T. acidophilum* at lower resolution but was seen in the yeast CP[49] and penicillin acylase,[59] a member of the Ntn-hydrolase family (Ntn = N-terminal nucleophile). The water molecule is thought to serve as the proton shuttle between the Thr1 Oγ and Thr1 N atoms during substrate binding and to cleave the acyl-ester intermediate, thereby regenerating the Thr1 Oγ atom.

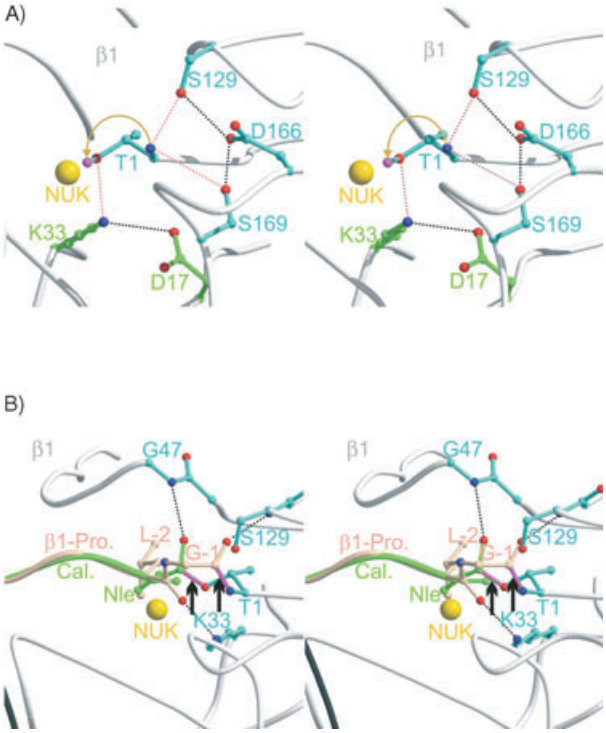

Figure 6. *Stereorepresentation of proteolysis and autolysis. A) The vicinity of residue Thr1 in subunit β1. The protein backbone is drawn as white coils, whereas residues that particularly contribute to the active site (Thr1, Asp17, Lys33, Ser129, Asp166 and Ser169) are shown as ball-and-stick structures. Lys33 is in a salt bridge to Asp17 (purple dots, both residues are coloured green) and is therefore presumably positively charged, thus lowering the pK_a value of the Thr1 Oγ atom electrostatic potential (black dots). Close to Thr1 are residues Ser129, Asp166 and Ser169 (coloured blue) which are required for the conformational stability of Thr1 (purple dots). A solvent molecule, NUK (shown as yellow sphere), is localised in the electron density close to the Thr1 Oγ and N atoms and presumably plays a role in the proton transfer (yellow arrow). B) Suggested mechanism for autolysis and substrate proteolysis exemplified at the active site of the yeast 20S proteasome subunit β1. The backbone is shown as white coils and Thr1 is drawn as as a blue ball-and-stick structure. Calpain inhibitor I and β1-propeptide are coloured green and pink, respectively. The superposition of wild-type β1 and β1 Thr1Ala main-chain atoms reveals a root-mean-square deviation of 0.19 Å, which allow the Ala residue in the mutant to be modelled with the Thr1 residue from the wild-type CP. Proteolysis and autolysis (black arrows) are initiated by proton transfer from the Thr1 Oγ atom to the water NUK (shown as a yellow sphere). The Gly47 N atom (blue sticks) is the major constituent of the oxyanion hole for inhibitors and substrates; it lowers the energy of the tetrahedral adduct transition state. The Ser129 N atom (blue sticks) is an essential part of the oxyanion hole for the carbonyl oxygen atom of Gly−1, whereas the Lys33 Nζ atom (blue sticks) stabilises the carbonyl oxygen atom of position −2 in the propeptide. Hydrogen bonds are indicated as black dots. Addition of the Thr1 Oγ to the Gly−1 C (autolysis) or Nle1 C atoms (proteolysis) is followed by ester bond formation, which is hydrolysed in both pathways by incorporation of the water NUK into the product.*[49,57,58]

Topology of proteasomal subunits

The topology of proteasomal subunits is not unique to proteasomes but rather to a set of hydrolases that have no recognisable sequence similarity to each other. Currently, there are already 19 documented crystal structures of Ntn-hydrolases de-

posited in the RCSB protein data bank. This class of proteins use their N-terminal residue as the nucleophile and are therefore termed Ntn-hydrolases.[60] Surprisingly, the active-site residues, including the aforementioned lysine residue are not conserved, a fact supporting the assignment of the common N-terminal amino group as the proton acceptor in proteolysis. However, all Ntn-hydrolases require a processing step which results in the exposure of the N-terminal amino group acting as the nucleophile. Therefore, 20S proteasomes have to follow a defined maturation pathway leading to the functionally active Ntn-protease complex. The prosegments of the β-subunit precursor complexes are removed by intramolecular autolysis during the consecutive maturation steps of the particle to result in the proteolytic active-protease complex (Figure 6B).[57,61,62]

Early and late assembly intermediates in 20S proteasomes

α Subunits from archaea assemble spontaneously into homo-oligomeric seven-membered rings, whereas their β subunits are synthesised as monomers and contain precursor sequences (Figure 7). The α ring alone has the same conformation as is found in the assembled 20S proteasome,[63] which illustrates that during proteasome maturation a stable and rigid framework is formed by the α rings. It is noteworthy that even the contact regions are not significantly different between free α subunits and αβ assemblies in the CP, a fact indicating pre-existing complementarities of the α–β contact surfaces. Therefore, the α ring represents an early assembly intermediate during core-particle maturation and serves as the nucleus for the β-subunit precursor complexes, thereby leading finally to the matured 20S complex. Surprisingly, it could be shown that adding β-subunit precursors from *Archaeoglobus fulgidus* to α subunits from *Aeropyrum pernix* generates a proteolytically active chimeric 20S proteasome.[63] This cross-maturation of chimeric CPs from phylogenetically distant archaea is evidence for a common assembly pathway of proteasomes from these organisms. 20S proteasomes in actinomycetes have been found to have a substantially smaller contact region between α subunits than the corresponding regions found in the CPs of archaea and eukaryotic cells, a fact suggesting that a smaller contact area between α subunits is probably the structural basis for the α subunits not assembling into rings when expressed alone.[64] The crystal structure of the CP from *Rhodococcus erythropholis* reveals that the propeptide of the β subunits acts as an assembly-promoting factor by linking its own β subunit to two adjacent α subunits. In eukaryotic CPs, the assembly of the 14 different subunits is supported by additional regulatory factors, which probably act as chaperones and are only transiently associated with the nascent complexes.[53,65] However, structural data for eukaryotic precursor complexes and assembly intermediates are so far not available. Analysis of all deposited β-subunit structures shows that the contact area between β subunits within a β ring is not sufficient for β-ring self-assembly without the additional contact provided by the α ring. An established order of assembly and maturation helps to prevent uncontrolled protein degradation within the cell. If β rings could preassemble, their active sites would not be sequestered and be accessible to protein substrates. One function of the β precursors is to correctly position half 20S proteasome complexes for the generation of the CP on the maturation pathway. The crystal structure of the proteolytically inactive *A. fulgidus* β Thr1Gly CP mutant, which is unable to mature, represents one of the last CP assembly intermediates in archaeal proteasomes.[63] It shows loosely associated $\alpha_7\beta_7$ half proteasomes, which are separated from each other by a gap of 4.5 Å, as compared to the wild-type structure of the mature enzyme (Figure 7). The $\alpha_7\beta_7\beta_7\alpha_7$ assembly intermediate confines almost completed active sites to the inner cavities of the complex and the maturation is finished by the subsequent autocatalytic processing step. Archaebacterial and eukaryotic CPs are homologous in sequence and structure[66] and eukaryotic 20S proteasomes are also assembled from half proteasomes, named 16S precursor complexes.[67] It appears likely

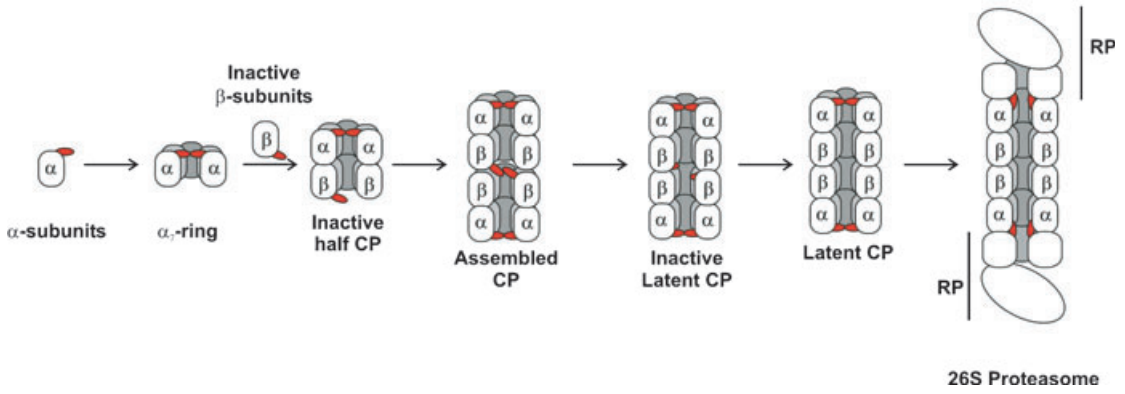

Figure 7. *Model of coupled regulation of proteasome assembly and inhibition. Proposed steps in the assembly of the CP are depicted. The inhibitory N-terminal sequences of the α and β subunits are represented in red. In the inactive half CP, inhibition is provided by the β-subunit propeptides (which directly block the proteolytic active sites). Inhibition by the α-subunit tails becomes effective only when the half CPs condense to form a closed chamber. The inactive CP is converted into the latent form upon autolysis of the β propeptides. The last step represents holoenzyme formation, which is accompanied by channel opening.*[57,62,63,68,98,99]

that the assembly pathway in eukaryotes, in particular the initial formation of the α ring, is similar to that in archaeal proteasomes. In the late assembly intermediates of eukaryotes, the various different propeptides from the β subunits and additional chaperones are essential to generate the two-fold symmetry that results in the fully active matured CP.[53,62,65,68] For example, in yeast, the propetide of subunit β5 has been shown to be essential for cell viability but is functional when expressed in trans (intermolecularly),[62] whereas deletion of the propetide of subunit β1 does not show any phenotype.[69] In cases where the propeptide of subunit β1 is replaced by ubiquitin, which liberates the N-terminal threonine immediately after expression, the subunit remains inactive. Structural analysis of the mutant proteasome showed no significant differences to the wild-type structure, except for extra electron density at the amino group of Thr1 of subunit β1, which was interpreted as an acetyl group and confirmed by mass spectroscopy.[58] In parallel, yeast mutagenesis has shown that all proteolytically active subunits maintain their activity by deleting their respective propeptides when the Nα-acetyltransferase is inactivated.[70] These observations support the above-mentioned proteolytic mechanism and assign the role of proton acceptor to the amino group of Thr1. The acetyl group is not cleaved by autolysis (see below), probably for steric and electronic reasons.

positioned to act as the general base and to promote the abstraction of the proton from the Thr1 hydroxy group, thereby initiating nucleophilic attack on the carbonyl carbon atom of the preceding peptide bond.[57] The structures of the active sites are therefore designed for both reactions, autolysis and substrate proteolysis. As shown for the yeast β1 Thr1Ala CP mutant, the conformation of the segment Leu−2 to Thr1 has a bulge at Gly−1 with a short hydrogen bond (2.5 Å) between the Leu−2 O and Thr1 N atoms; this is classified as a three residue γ turn (Figure 8). γ Turns show no significant sequence

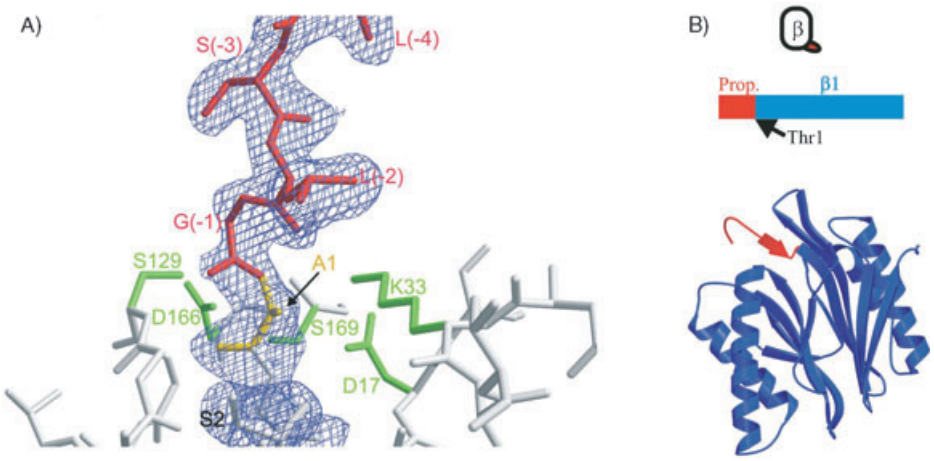

Figure 8. *Autolysis of β subunits—a late occurring assembly process of CPs. A) 20 Å sector around Ala1 of subunit β1 of the β1 Thr1Ala mutant from yeast. Residues are drawn in balls-and-stick representations (coloured in grey) except the prosegment of subunit β1 (coloured in red), the mutated Thr1Ala residue (coloured in yellow) and the amino acids responsible for autolysis and proteolysis (coloured in green). The experimental electron density of the Ser−3/Ser2 segment is shown in blue. B) Model of the chromosomally expressed subunit β1 (coloured in blue) with its propeptide (coloured in red); Thr1 is labelled in black. The ribbon drawing of the β1 Thr1Ala mutant from yeast confirms the proposed mechanism.*[57,58]

Autolytic mechanism in 20S proteasomes

All eukaryotic proteasomal β-type subunits have probably diverged from a single ancestor similar to the archaebacterial β subunit. The maturation of active eukaryotic and archaebacterial β subunits is independent of the presence of other active subunits and occurs by intrasubunit autolysis within the assembled particle.[57,58,68] The prosegments are removed by autolysis between residues Gly1 and Thr1, a process requiring a Gly–Thr site and catalytic residues. Designed mutants in eukaryotic CPs[61,71,72] and naturally occurring inactive proteasomal subunits altered at those sites are not processed. In eukaryotes, only three β-type subunits (β1, β2 and β5) are active and possess N-terminal threonine residues, whereas the remaining β-type subunits (β3, β4, β6 and β7) remain inactive and are found as precursors or intermediate processing products.[49,50] For the autolysis reaction, the N-terminal amino group is not available as a proton acceptor and is functionally replaced by the catalytic water molecule (NUK). NUK is ideally

preference and the conservation of Gly−1 in proteasomes may be to avoid steric interference of a side chain with the turn segment at position 168. The Thr1 Oγ atom is centrally positioned in the γ turn and is in proximity to the carbonyl carbon atoms of Leu−2 and Gly−1, such that further approach by a Thr1 side-chain rotation and pyramidalisation of the carbonyl carbon atoms follow the preferred trajectory of a nucleophilic addition reaction.[73] Addition leads to a hydroxazolidine intermediate, which may decay to the ester when the C–N bond is cleaved (see Figure 6B). The nucleophilic water molecule functions as the base in the addition reaction and, after a slight rearrangement, as a proton donor to the amido nitrogen atom when the C–N bond is cleaved and the ester is formed. It may finally be incorporated into the product when the ester is hydrolysed while the active site generates. The conservation of backbone geometry and the majority of the residues making up the active site in inactive β subunits indicate that early in evolution these subunits could have been proteolytically active. Later, these subunits lost their activity by mutations. Subunits β3, β4 and β6 lack at least the nucleophilic threonine in position 1, and β7 has Arg33 and Phe129 instead of Lys33 and Ser129, respectively. However, reactivation of inactive β-

type subunits by multiple mutations has failed so far,[58] whereas inactivation of individual active subunits is possible but causes severe phenotypes.[62,69]

Specificity of proteasomal subunits

The eukaryotic 20S proteasome has different protease activities. In vivo assays in eukaryotic cells have shown that the CP is able to cleave after almost every amino acid.[74,75] However, proteolytic activity against chromogenic substrates demonstrates only five distinct cleavage preferences, named chymotryptic-like (CL), tryptic-like (TL), peptidyl–glutamyl–peptide hydrolysing (PGPH), branched-chain amino acid preferring (BrAAP) and small neutral amino acid preferring (SNAAP) activity. Most of the subunits responsible for these cleavages could be defined by structural and functional mutagenesis in the yeast CP (Figure 9).[49,58,69] Thus, the bottom of the P1 pocket,

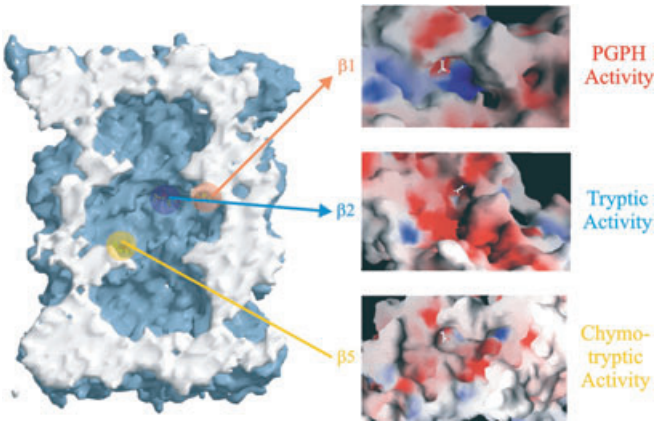

Figure 9. *Surface representation of the yeast 20S proteasome crystallised in the presence of calpain inhibitor I, clipped along the cylindrical pseudo-sevenfold symmetry axis. The accessible surfaces is depicted in blue and the cut surface in white. Inhibitor molecules are shown as space-filling models in green and indicate the proteolytically different active sites. The various proteolytic active centres are marked by a specific colour coding: orange = subunit β1, blue = subunit β2 and yellow = subunit β5. Cleavage preferences, termed PGPH-, tryptic- and chymotryptic-like activity, are zoomed and illustrated in surface representation; the nucleophilic Thr1 is presented as a ball-and-stick model. Basic residues are coloured in blue, acidic residues in red and hydrophobic residues in white.*[58]

which appears largely to determine its character, is formed by residue 45. Additionally, adjacent subunits in the β rings contribute to the S1 pockets further back and modulate their character. Subunit β1 contains Arg45 in the specificity pocket that preferentially interacts with glutamate P1 residues and is therefore associated with the PGPH activity of the CP, as also indicated by mutational analysis.[76,77] However, degradation experiments of yeast enolase have identified that subunit β1 has, beside its PGPH specificity, limited BrAAP activity.[78] A possible explanation for the dual cleavage specificity of this subunit is provided by the crystal-structure analysis of the CP–Calpain-inhibitor-I complex, which shows the hydrophobic norleucine side chain of the inhibitor projecting towards the Arg45 residue. The high-resolution structure of the complex displays additional electron density in the vicinity of Arg45 and was interpreted as a bicarbonate anion, which compensates for the unbalanced positive charge.[57] Subunit β2 has glycine as residue 45 and consequently a spacious S1 pocket confined at its bottom by Glu53. This subunit is suited for very large P1 residues of basic character and has the trypsin-like activity. This hypothesis was confirmed by mutational analysis.[58,68,69] The chymotrypsin-like activity can be attributed to subunit β5, which is shaped in particular by Met45. However, mutational analysis has shown that subunit β5 also has the tendency to cleave after small neutral and branched side chains; therefore, BrAAP and SNAAP activity can additionally be assigned to this subunit. One explanation for the various activities of subunit β5 is the mobility of Met45, which allows the alteration of the size of the S1 pocket. Met45 in the CP–Lactacystin complex adopts tight interactions with the isopropyl side chain of the inhibitor. On the other hand, the crystal structure of the CP–Calpain-inhibitor-I complex represents the Met45 side chain displaced by the bulky norleucine side chain of the inhibitor, thus making the S1 pocket more spacious.[49]

As mentioned before, in mammalian proteasomes, the constitutive proteolytic subunits are replaced by immunosubunits upon γ-interferon induction; the quantity and distribution of MHC class I molecules on the cell surface is thereby controlled.[79,80] The substitution of these subunits leads to the generation of oligopeptides that have an higher affinity to bind to MHC class I molecules by their C-terminal anchor residues. Surprisingly, the constitutive and related immunosubunits are almost identical in the amino acid sequences of their substrate-binding pockets, except for β1i, which contains two conspicuous differences in the S1 pocket, as compared to β1 (see Figure 5C). Modelling experiments with the coordinates of the CP from yeast revealed that these two exchanges firstly reduce the size of the S1 pocket (Thr21Phe) and secondly change the charge character of the pocket from positively charged to neutral (Arg45Leu). These specific substitutions can explain why the immunoproteasome has a reduced activity for cleavage after acidic amino acids, whereas the CL and BrAAP activity is drastically enhanced.[49] Interestingly, knock-out mutants of subunit β1i in mice have reduced MHC class I epitope presentation,[81–83] which might be due to the preference of MHC class I molecules to interact with peptides having basic or hydrophobic C-terminal anchor residues.[84] However, the substitutions of β2 and β5 with β2i and β5i do not indicate substantial modifications in the arrangement and specificities of the S1 pocket. Nevertheless, in vivo experiments in mice mutants lacking these immunosubunits show a severe defect in MHC class I presentation.[79] The available crystal structures of 20S proteasomes from yeast and bovine liver do not give an explanation for these observations.[49,50] However, it is likely that the conserved replacement of β2 and β5 includes restrictions in the flexibility and size of the specificity pocket, which will certainly alter the cleavage preference of substrates. As already mentioned, the size of the S1 pocket in subunit β5 varies in response to substrate binding. More structural and functional experiments are necessary to understand the functional consequences of the subunit exchange in mammalian

CPs. The different cleavage specificities of subunits may reflect physical constraints on the peptide substrate due to the slightly altered local structure around each active site, rather than a strict selectivity for the P1 residues of the substrate. In line with this idea, it has been shown that CPs can cleave protein substrates at every peptide bond, a fact showing that substrate residues other than P1 can influence degradation and neighbouring subunits can interfere with the function of the catalytic subunits.

Generation of oligopeptides

The length of the cleavage products made by proteasomes varies from 3–25 amino acids and has an average length distribution of 7–8 amino acids. The mechanism by which peptide-product length is controlled was unclear until recently. The crystal structure of the 20S proteasome from *T. acidophilum* suggested the presence of a molecular ruler given by the defined distances of Thr1 residues between adjacent β subunits. In these CPs the intervals between active-site residues are always about 30 Å; this allows binding of peptides of 8–12 amino acids in an extended conformation.[48] However eukaryotic CPs contain a reduced number of proteolytic active sites, and it is also possible to inactivate four of the six active β-type subunits, β1 and β2, by mutagenesis.[69] The distance between the remaining active β5 and β5′ threonines in this mutant CP is about 49 Å,[58] which would suggest products with an average length distribution of 15–18 amino acids if adjacent active-site distances were indeed defining the product size. Interestingly, the mutant proteasome degrades yeast enolase, which serves as a suitable substrate for 20S proteasomes because of its thermolability, to oligopeptides having an average length distribution of 8–15 amino acids, with an ability similar to that of the wild-type CP.[78] As expected, the fragments produced by the double mutant reveal a processive degradation mechanism, but they show differences in the cleavage pattern compared to wild-type proteasomes as the mutant is only able to cleave after hydrophobic residues. Surprisingly, the analysis of cleavage products at different times from wild-type and mutant CPs showed similar turnover rates, a result implying that the number of proteolytic active sites in proteasomes is not a limiting factor. The crystal structure of the yeast 20S proteasome had suggested the presence of further "non-Thr1" proteolytic active centres in the inner cavity of the CP, which were hypothesised to be important for the product length determination.[49] The hypothesis was based on the observation that the crystal structure of the yeast CP showed defined electron density of the partially processed intermediates of the inactive subunits β6 and β7, whose prosegments are anchored at the inner annulus of the central β–β chamber. Additionally, crystallographic analysis of various yeast CP mutants, in which proteolytically active threonine residues were inactivated by site-directed mutagenesis, still showed the characteristic length distribution of the partially processed propeptides observed in the wild-type crystal structure. However, N-terminal sequencing of the inactive β6 and β7 subunits in β2-inactivated proteasome mutants resulted in longer prosegments than those of wild-type CP and they were structurally disordered.[58] These observations excluded the presence of additional non-Thr1 endopeptidase cleavage sites in 20S proteasomes and indicate that partially processed propeptides rearrange to their final locations after they have been hydrolysed and CP maturation is completed. The experiments show that the substrate docks in specific channels, which exhibit binding sites for peptides 7–9 amino acids long (Figure 10). The maximum likelihood of substrate cleavage depends on the mean residence time at the proteolytic sites, so the related product-cleavage pattern is directly related to the affinity of the substrates for the individual binding clefts. Consistently, the active subunits differ in eukaryotic CPs only in their binding pockets, thereby yielding different cleavage specificities. Nevertheless, it must be emphasised that the CP complex does not represent

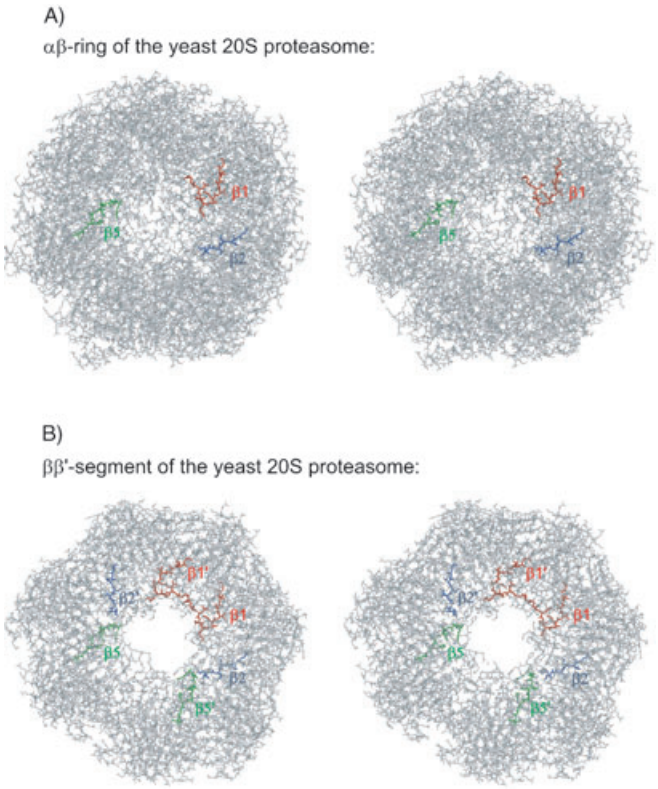

Figure 10. *Model of the eukaryotic CP at atomic resolution (coloured in grey) with the different docking sites for substrates to the various proteolytically active subunits β1, β2 and β5 (highlighted in red, blue and green, respectively). The model was prepared by using coordinates from the β1 Thr1Ala/β2 Thr1Ala double mutant from the yeast CP by replacing the coordinates of subunit β5 with coordinates from subunit β5 of the β5 Lys33Ala yeast CP mutant. The various prosegments have a defined length of 7–10 amino acids, whereas the remaining residues of the precursors are flexible and do not reveal clear electron densities. As shown in Figure 6B, the prosegments adopt a similar orientation (except Gly−1) to that found in the crystal structures of the yeast CP with various inhibitors. Therefore, the organisation of the precursors in the model mimics substrate docking. The arrangement of the propeptides is specific for each of the proteolytically active sites due to the unique topology of the CP and due to the specific structural constraints and cleavage preferences of the related active centres. A) $\alpha_7\beta_7$ Half CP from yeast, which illustrates the possible pathway of substrates entering the CP through the regulatory gate performed by the α ring. B) Segment of the β–β rings, which possesses the organisation of the proteolytic active centres and docking sites in the central chamber.*[58, 78]

a simple collection of various proteolytic specificities but that the whole structure of the proteolytic chamber imposes the characteristic appearance for product generation. However, a comparison of the crystal structures of the CP mutants with the wild-type structure shows no significant changes of subunit positions or backbone structure, and the activity assay against chromophoric substrates is not altered by the presence or absence of intact sites of other subunits. Also the covalent binding of subunit specific inhibitors has no influence on the remaining active sites and does not show noticeable structural changes.[49,85–87] All these observations argue against the existence of allosteric interactions between the active sites for product formation. The produced peptide fragments are generally further degraded to amino acids by endopeptidases or aminopeptidases,[88] which can then be reused for protein synthesis. Interestingly, some of the finally obtained peptides are stable against further hydrolysis. They are specially designed to be incorporated into MHC class I molecules and presented on the outer membrane to the extracellular space.[89]

Substrate access into eukaryotic 20S proteasomes by regulatory gating

The structural organisation of the proteasome segregates its proteolytic active sites from the cellular components by sequestering them within a central chamber formed by active β-type subunits.[90,91] This feature was first observed in the crystal structure of the *Thermoplasma* proteasome.[48] The architecture of this CP shows a transverse channel through the whole molecule. The α rings contain central entry ports with 13 Å diameters, which are constrained by turn-forming segments of Tyr126–Gly–Gly–Val in each individual α subunit, a fact suggesting that the rate-limiting factor for product generation is not substrate hydrolysis at the proteolytic active subunits but accessibility into the lumen of the CP (see previous section). The openings in the prokaryotic CP are slightly larger than the diameter of an α helix and are therefore not sufficiently wide enough to allow translocation of folded substrates. These constrictions are essential for cell viability as they represent an important check point for regulated and progressive degradation of substrates. Therefore, the compartmentalised geometry of CPs prevents unwanted degradation of endogenous proteins and favours the processive degradation of substrates by restricting the dissociation of partially digested polypeptides. By contrast, the hydrolytic chambers of eukaryotic CPs are quite inaccessible.[49] The N termini of the α subunits project into the ports seen in the prokaryotic CPs[48,63] and fill them up completely in several layers with tightly interdigitating side chains forming a central plug (Figure 11 A). Thus, substrate access into the interior chamber of eukaryotic CPs requires substantial rearrangements of the N-terminal residues of the α subunits. Intriguingly, the N-terminal residues 1–12 are disordered in the crystal structures of the CPs from *T. acidophilum* and *A. fulgidus*, which indicated for the first time a regular gating mechanism in at least the eukaryotic 20S proteasome.[49] Additionally, there are some narrow side windows, particularly at the interface of α and β rings. These openings are mainly in between the teeth-like helix H1–turn–helix H2 motifs of the α–β interface and point towards the active-site threonine residues. They are coated with polar and charged residue side chains, which may move to make openings of about 10 Å diameter and may allow passage of unfolded, extended peptide chains, possibly acting as exit channels for the generated fragments.[49] Unlike speculations about product release, substrate accessibility in eukaryotic CPs is clearly defined by the α rings. For example, the 19S regulatory particle, which confers ATP- and ubiquitin-dependence on proteolysis by the 20S proteasome, is attached proximally to the α rings.[92] This association results in a strong activation of peptide-bond hydrolysis.[93] Similarly, the proteasome activator PA28 (11S) is bound to the α subunits and accelerates peptide digestion[94–96] as well as the improvement of antigen processing.[97] Mutational and crystallographic analysis of the yeast 20S proteasome[98,99] as well as the crystal structure of the 11S regulator from *Trypanosome brucei* in complex with the yeast CP[96] led to the elucidation of the principle and mechanism of the formation of a gated channel into eukaryotic proteasome core particles. In the yeast proteasome mutant, the nine-residue tail (GSRRYDSRT) from the N terminus of subunit α3 was chromosomally deleted. This segment was chosen for deletion because it is situated on top of the molecule, extends across the pore of the CP and contacts all other N termini that are involved in the organisation of the plug.[49,98] The tail of subunit α3 itself is defined on the basis of the sequence alignment of archaeal and eukaryotic α-type subunits to the single *Thermoplasma* α subunit and corresponds to the sequence Met1–Thr13, which is disordered in the crystal structure of the CP from *T. acidophilum*.[48] The distortion of the N-terminal tails has also been observed in the crystal structure of the CP from *A. fulgidus* and accounts for the observation of a channel in prokaryotic proteasomes, whereas the irregular but well-defined structure appears to seal the chamber in the eukaryotic complex. The importance of the tails in the functions of the CP is indicated by the remarkable evolutionary conservation of these sequences across eukaryotes. Although each tail is conserved evolutionarily, the tail sequences are divergent from one α subunit to another. This divergence is correlated with dramatic structural heterogeneity among the tails. In contrast, sequences upstream of Thr13 are strongly conserved from one subunit to another and assume pseudo-sevenfold symmetry of the particle. As expected, deletion of the first nine amino acids of subunit α3 (hereafter termed the α3 ΔN mutant) causes a major structural perturbation.[98] Surprisingly, the α3 ΔN mutant does not show any obvious phenotype, although the crystal structure of this mutant has an axial channel through the molecule whose dimensions are comparable to those of the *T. acidophilum* channels[48] (Figure 11 B). The loss of electron density results from both the elimination of the N-terminal residues from subunit α3 and the disorder in the tails of the other subunits. Importantly, α3 is unperturbed within the mutant particle, a fact indicating that the deletion does not cause an assembly defect. The CP of the α3 ΔN mutant shows a strongly enhanced peptidase activity with three different fluorogenic peptide substrates, each specific to a different active site. Thus, the enhanced basal activity of the

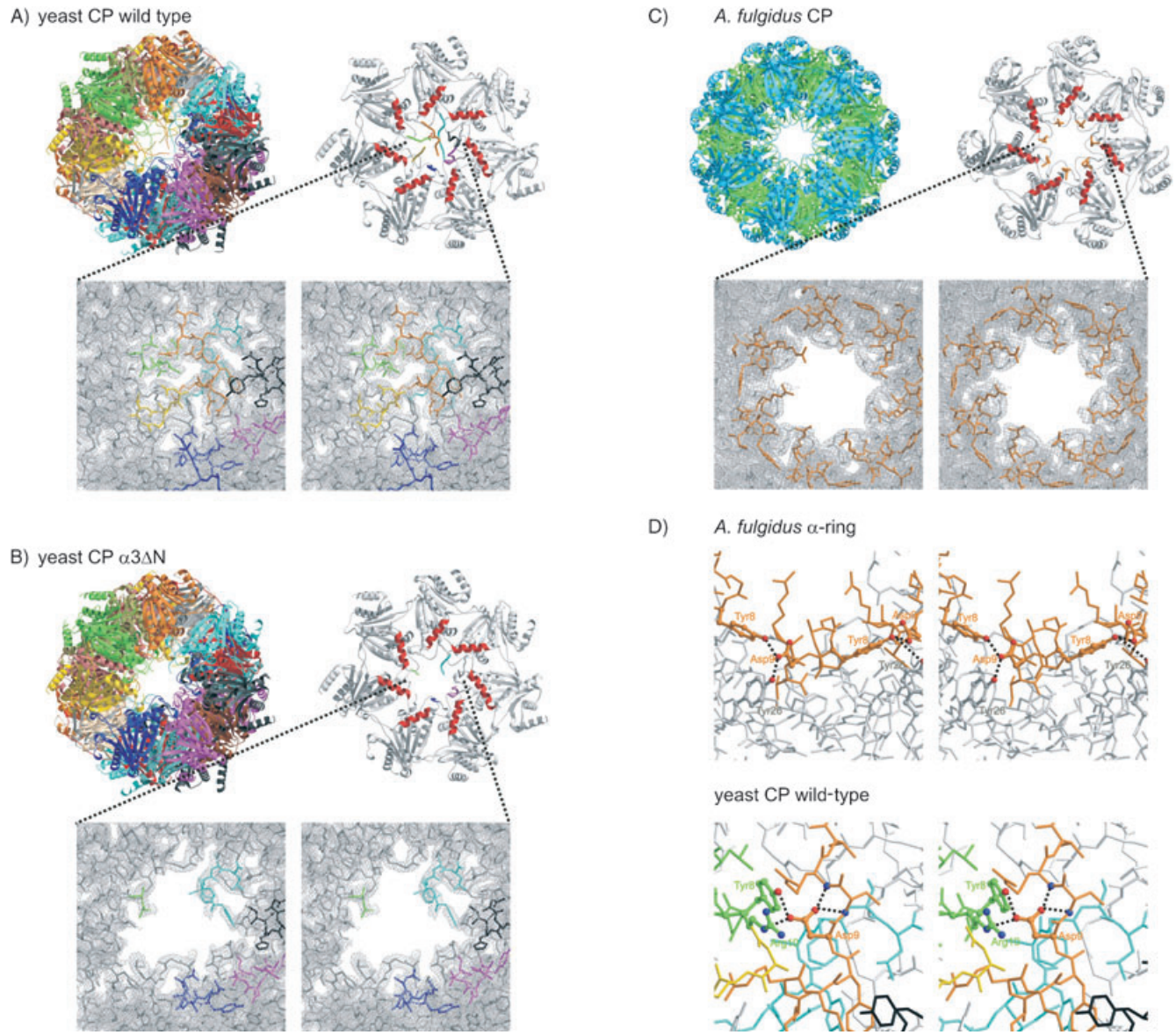

Figure 11. *Substrate access into and product release out of eukaryotic and prokaryotic CPs—similarities and differences. A) and B) Deletion of the α3 N-terminal segment in eukaryotic 20S proteasomes opens a central channel into the CP. Ribbon drawings of the wild-type (A) and the α3 ΔN mutant (B) 20S proteasomes and their related α rings. Subunits follow a specific colour coding (top view of the ribbon representation of the CPs). In the α ring, only the N-terminal tails (residues up to position 13) are drawn in their specific colour coding, whereas the remaining part of the molecule is coloured in grey. The helices H0, which posses specific docking sites for the various regulators, are highlighted in red. Each figure shows the electron-density maps of the α rings of the related yeast CPs (wild-type and mutant α3 ΔN). The maps are contoured at 1σ, with $2F_O-F_C$ coefficients after twofold averaging. The N-terminal segments are coloured as shown for the α ring. The regulatory gate in the yeast CP is built by a specific structural arrangement, termed the YDR motif, which is conserved among all eukaryotes and prokaryotes. C) Ribbon drawing of the CP from* A. fulgidus *(top view), with α subunits coloured in blue and β subunits coloured in green. The crystal structure of prokaryotic CPs show a transversal channel through the whole molecule. However, in the crystal structure of archaeal CPs, the first N-terminal residues, which include the YDR motif, are structurally disordered. In comparison, the crystal structure of the free α ring from* A. fulgidus *shows defined electron densities of the N-terminal segments which protrude outside of the body of the molecule. Mutational studies of the YDR motif in prokaryotes confirmed these structural observations and argue against the regulatory YDR gating mechanism that has been found in eukaryotic CPs. D) Stereodrawings of the open and closed channels from* A. fulgidus *and yeast. The N-terminal tails are rendered as in (A) and (C). The characteristic structural arrangement of the YDR motif is highlighted in bold sticks. Specific interactions within the YDR motif are shown by black dots. In eukaryotes, residues of the YDR element in the α3 and α4 subunits maintain the regulatory gate. In contrast, residues of the YDR motif in prokaryotic CPs interact specifically with the YDR motif of the adjacent α subunits and mainly contribute to the open axial channel.*

mutant cannot be due to allosteric activation of any individual active site. General allosteric activation can be excluded as well, because the detailed structures of the proteolytically active β-type subunits are indistinguishable in the mutant and wild-type particles. Eukaryotic 20S proteasomes can also be stimulated by mild chemical treatments, such as exposure to low levels of sodium dodecylsulfate (SDS).[100] Interestingly, SDS-mediated activation was not observed with the mutant complex; this suggests that SDS activation of wild-type CP is mediated by channel opening. These data indicate that the closed state of the channel seen in the crystal structure is also the predominate state in solution. Therefore, eukaryotic 20S

proteasomes exist in a self-inhibited state, in which the entry into the lumen of the particle is rate limiting for hydrolysis. The in vivo activity of the α3 ΔN 26S proteasome in degradation of ubiquitin–protein conjugates was found to be comparable to that of the wild-type by using β-galactosidase derivatives.[98,101] Additionally, the α3 ΔN deletion mutant had no significant effect on the stability or abundance of the 26S proteasome holoenzyme. Thus, formation of the wild-type 26S proteasome activates peptide hydrolysis within the CP to an extent comparable to that of SDS, a fact suggesting that in wild-type holoenzymes the repressive effect of the α3 tail is relieved. Remarkably, the addition of the synthetic peptide with the sequence of the α3 tail to the α3 ΔN mutant restores wild-type behaviour, whereas control peptides did not significantly inhibit the mutant.[98] Equally, the synthetic α3 peptide failed to inhibit the basal activity of the wild-type 20S proteasome. The α3-tail peptide inhibits all three proteolytic active centres of the α3 ΔN mutant, which is consistent with its blocking peptide entry into the proteolytic chamber. The region of the sequence that is responsible for the closed channel state was analysed by an alanine scan with the α3-tail peptide. Asp9 of subunit α3 could be identified as being essential in the stabilisation of the closed state of the channel. The observation is surprising, because the only sequence conserved from one α tail to another is Tyr8–Asp9–Arg10 (hereafter termed the YDR motif); this indicates a key structural role for this motif in the regulatory gating process. Conservation of Tyr8 is absolute, whereas Asp9 is present in six of the seven α tails and Arg10 is less well conserved. The structural data of the wild-type CP demonstrate that the $O^{\delta 1}$ atom of Asp9 on subunit α3 is in contact with Tyr8 and Arg10 of the neighbouring subunit α4. However, the $O^{\delta 2}$ atom of Asp9 interacts only with the nitrogen atoms of the backbone of the α3 N-terminal amino acids Ser10 and Arg11, thus maintaining the inhibitory effect of the synthetic α3-tail peptide on the α3 ΔN mutant by alanine modifications within these positions (Figure 11 D). The direct contacts formed between these residues in adjacent subunits may explain their correlated evolutionary conservation among all eukaryotes. The requirement for Asp9 is specific, because neither of the two most conservative substitutions for these residues, Asn and Glu, resulted in complete inhibition of peptidase activity, although Glu showed a partial inhibitory effect. The functional significance of Asp9 was further tested in yeast by introducing an Asp9Ala mutation in the chromosome.[98] In vitro peptidase assays on the Asp9Ala mutant CPs resulted in a derepression of the peptidase activity as strong as that of the α3 ΔN mutant. The close similarities between the Asp9Ala and α3 ΔN mutant 20S proteasomes suggest that the properties of the α3 mutants reflect the general properties of CPs in an open-channel stage. Thus, the channel may be driven into the open stage in various ways, and the detailed structure of the open conformation is apparently not critical for function. It is likely that the channel of the CP does not function as a selectivity filter and substrates may be committed to translocation within the regulatory particle prior to their entrance into the CP. So far, structural and mutational experiments indicate a dominant role of Asp9 of subunit α3 in the regulatory gating process; however, it is likely that the replacement of Tyr8 with Phe in subunit α4 has a similar effect.

Regulation of substrate accessibility into 20S proteasomes by the 19S regulatory particle

Activation of 20S proteasomes and other ATP-dependant protein complexes has often been attributed to allosteric regulation of their proteolytic active sites. However, the structural studies discussed provide no evidence for such a mechanism. Indeed, the regulatory particle (RP) functions as a gate opener in addition to its important roles in substrate recognition, unfolding and translocation.[91,102] Most probably, the six homologous ATPase subunits of the RP form a ring in which each subunit contacts the CP.[103] Thus, these molecules are well situated to influence the gating of the CP. Interestingly, substitutions in the ATP-binding motif of subunit Rpt2 of the RP lead to a severe reduction in peptide hydrolysis by the holoenzyme.[104] Lys229 is invariant in the nucleotide-binding pockets (Walker A motif) of AAA ATPases, where it interacts directly with the phosphate groups of ATP.[23,105,106] The conservative Lys229Arg mutation in Rpt2 is lethal, but the additional exchange of Ser241 to Phe makes the mutant viable, albeit associated with a severe peptide hydrolysis defect (hereafter termed the Rpt2RF mutant).[99] Substitutions equivalent to Lys229Arg in the other Rpt proteins are not lethal and do not significantly reduce peptide hydrolysis.[104] This indicates that the ATPase domain of subunit Rpt2 plays a major role in regulating the peptidase activity of CPs. Three models for the Rpt2 effect on peptide hydrolysis can be now considered. In model I, the mutation of the Rpt2 subunit influences the conformational functionality of the proteolytic active sites of the CP. However, as discussed before, allosteric regulation of these active sites has been shown to be unlikely by mutagenic and structural analysis. In model II, the mutation in subunit Rpt2 closes a hypothetical channel within the centre of the RP base, which blocks substrate access to the CP channel. As for model I, this hypothesis is unlikely to be true, as in mutant yeast strains containing the Rpt2RF regulatory particle and the α3 ΔN CP, the 26S proteasomes still mature and show similar peptide hydrolysis to that observed in wild-type cells. In model III, substrate access is controlled by the CP channel, which is closed in the Rpt2RF holoenzyme. With a constitutively open α3 ΔN CP, peptidase activity should be restored, as is observed.

Regulation of the molecular gate of eukaryotic 20S proteasomes by PA28

Peptide hydrolysis by the eukaryotic CP is also dramatically stimulated upon association with the 11S regulatory complex (also known as REG or PA28).[94,95,107] The main function of 11S complex is to enhance the production of antigenic peptides for presentation by MHC class I molecules.[108,109] The subunits of the 11S regulator share extensive sequence similarity, apart from a highly variable internal segment of 17–34 residues which may confer subunit-specific properties.[110] PA28α and PA28β preferentially form a heteromeric complex,[111–113] al-

though purified PAα forms a heptamer in solution[95] and has biochemical properties similar to the heteromeric PA28α/PA28β complex.[114] The crystal structure of human recombinant PA28α shows the molecule in its architecture as a heptameric barrel-shaped assembly, which contains a central channel with an opening of 20 Å diameter at one end and of 30 Å diameter at the presumed proteasome-binding surface.[110] The topology of PA28α is predominantly helical, with four long α helices, each containing 33–45 residues. The last ten C-terminal amino acids of PA28α have been identified as a binding/activation sequence for the proteasome CP.[96, 115] PA28 itself contains a central chamber with narrow constrictions at its poles. Therefore, substrate allocation is restricted, a fact implying that a check-point function for the specific selection of only unfolded substrates is performed by PA28. So far, crystallisation of a CP–11S complex from the same species has been unsuccessful. However, a chimeric 11S–CP–11S complex from yeast CP and *Tryponosoma* 11S/PA26 could be elucidated by crystallography.[96] The crystal structure of the complex explained the ability of 11S regulators to activate eukaryotic CPs from widely divergent species. It showed a symmetrical complex with regulator molecules bound at each end of the 20S barrel. The binding of the 11S regulator triggers the rearrangement of the α plug. Unlike the uncomplexed CP, all seven α-subunit N-terminal tails extend away from the CP and project into the pore of the regulator. The structural rearrangement of the α-subunit N-terminal tails is basically achieved by two features. First, the 11S activation loops impose a more stringent sevenfold symmetry on the CP, thereby straightening out the asymmetrically orientated α tails and pushing them away from the entrance gates. Second, the high-affinity binding between CP and 11S is accomplished by the C-terminal sequences of the regulator, which insert into pockets formed by the α subunits of the 20S proteasome. The fundamental contact is observed between the C-terminal main-chain carboxylate group of the 11S regulator and the N-terminal end of the helix H0 of the various α subunits. The strength of this interaction is amplified by the heptameric assembly of the CP–11S complex. Although up to now there have been no structural data available from 26S proteasome holoenzymes, it is unlikely that there is consensus in the activation mechanism of the CP by RP and 11S particle. Different modes of activation of the CP by these two regulators are indicated by the lack of sequence homology and oligomeric structure. The 11S regulator exhibits sevenfold symmetry, whereas the contact region of the RP contains six related ATPases.[116] The finding that an ATPase domain,[99] which is absent in the 11S regulators, can control CP gating is an additional important distinction between the regulation of CP gating by RP and 11S complexes.

Substrate access in prokaryotic proteasomes

In comparison to the eukaryotic CPs, the simpler prokaryotic CPs do not establish a multifunctional 26S proteasome and their genomes lack major parts of the RP. Remarkably, all sequenced archaebacterial CPs to date contain the characteristic YDR motif in their α subunits. This observation suggests that the regulatory gating mechanism in CPs is of universal importance among all species. However, the crystal structures of *T. acidophilum*[48] and *A. fulgidus*[63] show no defined electron densities at the N termini of their α subunits. Thus, prokaryotic CPs have a central channel through the whole molecule (Figure 11C). The strictly conserved YDR sequence among archaea, which forms the essential motif of the regulatory gate in eukaryotes, is part of the disordered segment. As confirmed by N-terminal Edman degradation, the primary sequences of the *Thermoplasma* and *Archaeoglobus* α subunits in the matured CPs did not show any degradation or posttranslational modifications in their termini. In contrast to prokaryotic CPs, the yeast 20S proteasome has ordered N-terminal tails of the α subunits which occupy unique positions not following any symmetry. Furthermore mutagenesis and structural analysis revealed that residue Asp9 of subunit α3 is the key element in the rigid construct of the central channel plug.[98] The lack of defined electron density in the crystal structures of the prokaryotic CPs is due to disorder within the subunits or to heterogeneity between the subunits. The resulting open channel is apparent, but it could in reality be filled with unstructured matter, which would abolish easy passage of the substrates. However, the yeast α3 Asp9Ala mutant has a 20-times enhanced proteolytic activity against chromgonic substrates compared to the wild-type CP and is also characterised by a disordered plug region. The *A. fulgidus* α Asp9Ala point mutant has no effect on the activity of chromogenic substrates,[63] a fact indicating that a stable plug is not formed in archaeal proteasomes; this contrasts with the role of the YDR motif of the eukaryotic CPs. The crystal structure of the free α ring from *A. fulgidus* allowed the N-terminal segments, including the YDR motif, to be traced and localised (Figure 11C). Surprisingly, the N-terminal tails project outwards from the body of the molecule and adopt the secondary structure of 3_{10} helices.[63] Therefore, the channel of the α ring is formed by the loop Tyr126–Gly–Gly of the individual α subunits, with a passage of 13 Å in diameter left at the centre. Interestingly, in the YDR motif, only Tyr8 makes hydrogen bonds to Asp9 of the adjacent α subunits, whereas Arg10 points towards the channel, thereby generating a strongly positive potential (Figure 11D). It is unclear whether the differences in this area between the free α rings and the α rings in CP are due to an allosteric effect that the β subunit exerts on the α subunit, but the conservation of other sections, in particular of the α–β contacts, argues against this. A more trivial reason may lie in the different buffer conditions used for crystallisation.

In comparison to archaeabacterial CPs, the more complex eukaryotic 20S proteasomes have the ability to establish a multifunctional 26S holoenzyme with the 19S regulatory particle. Binding of the RP to the CP activates the free CP from its repressed state, probably by opening the axial channel in a similar way to that seen and described in the α3 ΔN mutant. The central plug is constructed by the heterogeneous set of N-terminal tails and has the central YDR motif, which is strictly conserved. In the crystal structure of the wild-type CP from yeast, the carboxylate group of α3 Asp9 is seen to contact both Arg10 and Tyr8 of the neighbouring α4 subunit. It is notewor-

thy that a similar local interaction occurs in the α ring of *A. fulgidus*, in which Asp9 makes a strong hydrogen bond to Tyr8 of the adjacent α subunit, but the global structure of the N-terminal tail in the α ring of *Archaeoglobus* is entirely different from that of the plug-forming α-subunit tails in the eukaryotic 20S proteasome. Strict sequence conservation across eukaryotic species of the α-subunit N-terminal segments emphasises the importance of this structural element in eukaryotic proteasomes and suggests that the regulatory gate is an early invention in the evolution of eukaryotes. It is remarkable that the YDR motif appears to be present in all organisms but is different in tertiary structure and function between eukaryotes and prokaryotes.

Covalent inhibition of the 20S proteasome

The proteasome is particularly important for the regulated degradation of many critical proteins which control a vast array of biological pathways, including proliferation, differentiation and inflammation. Therefore, proteasome inhibitors are promising candidates as antitumor or anti-inflammatory drugs. After the discovery of the 20S proteasome, its mode of action was first analysed with nonspecific protease inhibitors. Recently, several molecules, with greater specificity against the CP, have become available to study several functions of the proteasome. These inhibitors have greatly facilitated the investigation of the proteasome in biological processes in vivo as well as in vitro.

One of the first found proteasome inhibitors was *N*-acetyl-Leu–Leu–norleucinal (Ac-LLnL-al; also called Calpain inhibitor I), which has been widely used to study proteasome functions in vivo, despite its lack of specificity.[117] This inhibitor binds reversibly to proteasomes and in the case of the eukaryotic CP abolishes the chymotrypsin-like and, to a lesser extent, the trypsin-like and postacidic activities. The crystal structure of the proteasome in complex with Ac-LLnL-al shows the inhibitor covalently bound to the Thr1 Oγ atom of all active subunits as a hemiacetal (Figure 12A). The compound therby adopts a β conformation and fills a gap between the strands, including residues 20, 21 and 47, respectively, to which it is hydrogen-bonded, generating an antiparallel β-sheet structure. The norleucine side chain projects into the S1 pocket, whereas the leucine side chain at P2 is not in contact with the protein. The leucine side chain at P3 closely interacts with amino acids of the adjacent β-type subunit. Thus, the specificity pockets of both S1 and S3 play a prominent role in inhibitor binding.[48,49] However, in vitro and in vivo analyses have demonstrated that the inhibitor inactivates primarily the

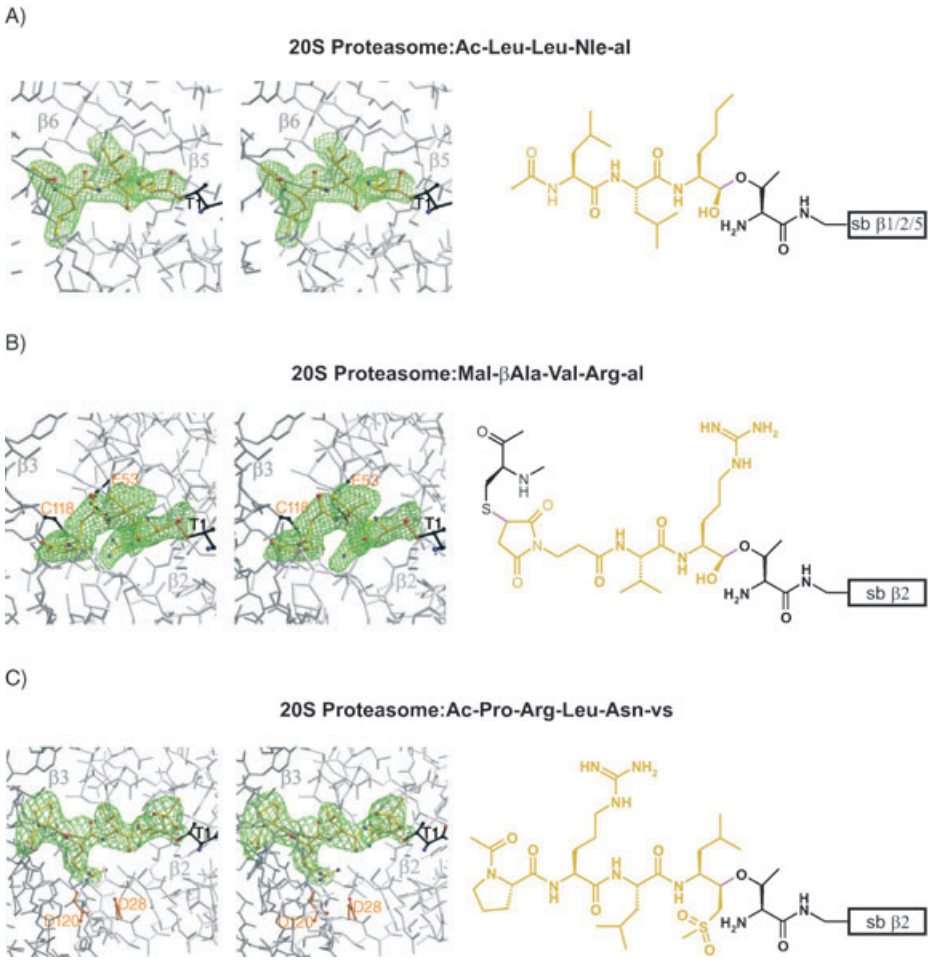

Figure 12. *Stereorepresentation of the yeast 20S proteasome subunits (coloured in white and grey) in complex with the synthetic inhibitors (coloured in yellow), Calpain inhibitor I (A), Mal-βAla-Val-Arg-al (B) and Ac-Pro-Arg-Leu-Asn-vs (C). Covalent linkages of the inhibitory compounds with the proteasomal subunits are drawn in pink. Electron-density maps (coloured in green) are contoured from 1σ in similar orientations around Thr1 (coloured in black) with $2F_O-F_C$ coefficients after twofold averaging. Apart from the bound inhibitor molecules, structural changes were only noted in the specificity pockets. Temperature-factor refinement indicates full occupancies of all inhibitor-binding sites. The inhibitors have been omitted for phasing. A) Calpain inhibitor I covalently bound to subunit β5. In contrast to the crystal structure of the CP–lactacystin complex (see Figure 13A), Met45 of subunit β5 is rearranged by 3 Å to avoid a clash with the Nle side chain of the inhibitor, thereby making the S1 pocket more spacious.[49] B) Mal-βAla-Val-Arg-al, a selective bivalent inhibitor, covalently bound to subunit β2. Residue Glu53 of subunit β2 (coloured in orange) is particularly responsible for the tryptic-like cleavage preference of this subunit. The electron density reveals the presence of an additional covalent bond between the functional maleinimide side chain of the inhibitor and Cys118 of subunit β3, thereby proving the bivalent binding mode of this compound.[121] C) Ac-Pro-Arg-Leu-Asn-vs, a specific vinyl sulfone inhibitor, covalently bound to subunit β2. Favourable hydrogen bonds between Asp28 of subunit β2, Cys118 and Asp120 of subunit β3 within the walls of the S3 pocket are coloured in orange. These residues are particularly responsible for the subunit specificity. Subunits β1 and β5 do not form stable complexes with this inhibitor, due differences in their S3 pockets.[87]*

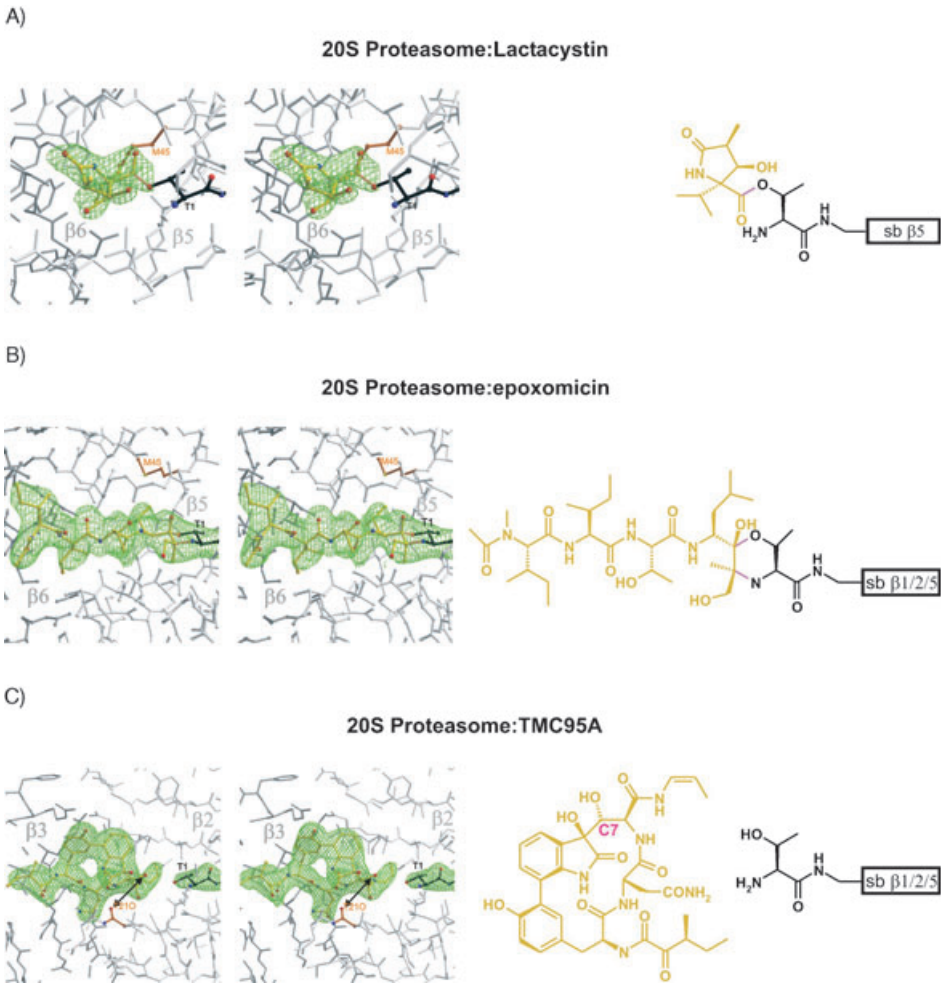

Figure 13. *Stereoview of yeast 20S proteasome subunits (white and grey) in complex with the natural inhibitors (yellow), lactacystin (A), epoxomicin (B) and TMC-95A (C). The layout of this figure is similar to that of Figure 12. A) Lactacystin covalently bound to subunit β5. The S1 pockets of subunit β1 and β2 differ from that of subunit β5 and do not interact with lactacystin. Met45 of subunit β5 (coloured in orange) specifically interacts with the branched side chain of lactacystin. In contrast to the crystal structure of the CP–calpain inhibitor I complex (see Figure 12A), Met45 minimises the size of the S1 pocket, thereby allowing optimal protein–ligand interactions, which account for the selectivity of this compound.[49] B) Epoxomicin, a natural* Streptomyces *metabolite, covalently bound to subunit β5. The electron density reveals the presence of a unique six-membered ring system. This morpholino derivative results from adduct formation between epoxomicin and the proteasomal N-terminal Thr1 Oγ and N atoms (both bonds are coloured pink). Met45 of subunit β5 is arranged similarly to that described in Figure 12A, thus making the S1 pocket more spacious for the Leu side chain of the inhibitor.[85] C) TMC-95A noncovalently bound to subunit β2. The natural specific 20S proteasome inhibitor from* Apiospora montagnei *binds near the proteolytic active site and occupies the specificity pockets of the CP. TMC-95A adopts an extended conformation without modifying the nucleophilic Thr1 and is found in all proteolytically active sites. Optimal binding to the 20S proteasome is due to the strained conformation of TMC-95A, caused by the presence of the cross-link between the tyrosine and the oxoindol side chain. The IC_{50} values for stereoisomers in position C7 of the TMC-95s (indicated by a black arrow) vary by two orders of magnitude. This observation is explained by the fact that, for effective binding, the hydroxy group must be in its S-isomeric state in order to avoid a steric clash with the carbonyl oxygen atom of residue 21 (orange).[86]*

chymotrypsin-like active site of the yeast 20S proteasome, although in the crystal structure the compound was found to bind to all proteolytic active centres when used at high concentrations.[48,49]

The first identified natural inhibitor against proteasome activity is lactacystin. This compound is made by *Streptomyces* sp. and was discovered by its ability to induce neurite outgrowth in a murine neuroblastoma cell line.[118] The incubation of cells in the presence of radioactive lactacystin resulted mainly in the labelling of subunit β5.[119] The natural compound effectively and irreversibly inhibits the chymotrypsin-like activity of the 20S proteasome. It also blocks the trypsin-like and the postacidic activities with lower potency. In aqueous solutions at pH 8, lactacystin is spontaneously hydrolysed into *clasto*-lactacystin β-lactone which represents the reactive compound inhibiting the CP.[120] The crystal structure of the complex between lactacystin and the yeast proteasome shows the molecule covalently bound only to subunit β5,[49] which is in accord with the observed chemical modification of subunit β5/β5i of the mammalian proteasome.[119] Bound lactacystin displays a host of hydrogen bonds with protein main-chain atoms (Figure 13A). The irreversible inhibition by lactacystin of the active site of the proteasome is due to the formation of an ester bond with the N-terminal threonine. Specificity for subunit β5 is explained by its apolar S1 pocket. A major function of the specificity pockets in CPs is to prolong the mean residence time of substrates at the proteolytic active sites by characteristic substrate–protein interactions. This is essential for the proteolytic step in order to allow completion of the reaction. The functional head group plays a significant role for inhibitor binding and may override other contributions. As mentioned, the Calpain inhibitor I binds, despite its hydrophobic side chains, to all proteolytic active sites through its aldehyde group, which is much more reactive than a lactone ring. Lactacystin, containing a less reactive head group, needs a longer time to react with the Thr1 Oγ atom and therefore requires strong interactions at S1. The dimethyl side chain of the inhibitor mimics a valine or a leucine residue and therefore only Met45 of subunit β5 is able to contribute effectively with its hydrophobic S1 pocket and to interact closely.

Previously discussed data gave impetus to the first structure-based design for inhibitor development of single proteolytic active sites in eukaryotic CPs.[121] As 20S proteasomes are

able to cleave substrates after almost each amino acid and all proteolytic active sites within the molecule follow a universal catalytic mechanism, peptide-based inhibitors cause some problems. However due to the knowledge of the crystal structure of the yeast 20S proteasome, it was possible to design and synthesise a specific bifunctional inhibitor against subunit β2, termed maleoyl-βAla–Val–Argininеal (Mal-βAVR-al). In the yeast CP, subunit β3 contains in position 118 a cysteine residue, which contributes mainly to the S3 specificity pocket of the proteolytic β2 active site. Thus, synthesis of a bivalent inhibitor, containing a malenimide group in the P3 site for covalent binding with the S3 thiol group and a C-terminal aldehyde group for hemiacetal formation with the Thr1 Oγ atom was envisaged. Structure-based modelling was required to obtain the characteristic distance of the malenimide side chain to the P1–P2 dipeptide aldehyde, and inclusion of the specificity of the S1 pocket allowed the activity of the inhibitor to be limited only to subunit β2. The crystal-structure determination of bound Mal-βAVR-al to the yeast CP reveals the inhibitor only bound to subunit β2 by hemiacetal formation and additionally confirms the presence of the covalent bond between the malenimide and the Cys118 residue of subunit β3[121] (see Figure 12B). Remarkably, Mal-βAVR-al shows an IC_{50} value of 0.5 μM for subunit β2, much lower than the IC_{50} value of 200 μM with Calpain inhibitor I, and represented a new type of inhibitor that is highly selective for the trypsin-like activity. Given that Cys118 is conserved among the known primary structures of eukaryotic CPs, the new inhibitor represents a promising tool for studying the mechanisms of substrate degradation of the protease complexes. However, the reactivity of the malenimide group towards thiols limits the use of the inhibitor only to in vitro assays.

A further approach to develop subunit-specific inhibitors for single proteolytic active subunits of the proteasomes was tried by using nonpeptide compounds. Based on the crystal structure of the yeast 20S proteasome, a unique topography of the six proteolytic active subunits in the central chamber was derived, with the active-site separation distances among the Thr1 residues defined. The structural data allowed the design of bi- or multivalent proteasome inhibitors containing a polymeric spacer of appropriate length to link two monovalent binding head groups and to yield homo- or heterobivalent inhibitors.[122] In first attempts, peptides for the spacer region were chosen, as they are comparable to unstructured polypeptide chains of unfolded proteins. However, peptides about the size of gastrin (17-mer) or secretin (27-mer) were found to be rapidly degraded by the CP and are therefore unsuitable. Next, poly(ethylene glycol) (PEG) was selected as the spacer element, as this represents a linear, flexible, solvated and protease-resistant polymer that mimics unfolded peptide chains, thus allowing access to the proteolytic chamber. Furthermore, this spacer is hydrophilic and therefore avoids formation of hydrophobic cores that would prevent the molecule from entering it. The spacer length was chosen to satisfy the inter- and intraring distances for occupation of the active sites. Finally the N termini of two tripeptide aldehydes were linked to the related PEG spacer, thereby resulting in a bivalent protease-resistant CP inhibitor. As expected, the crystal-structure analysis of the CP inhibitor complexes did not reveal a conformationally restricted PEG moiety in any part of the density due to structural distortion in the linker region. However, kinetic measurements against the proteolytic activity of the yeast CP showed that the bivalent inhibitors have IC_{50} values in the low nanomolar range, thus showing an increase in the potency by two orders of magnitude relative to the IC_{50} values of the monovalent analogues. Interestingly, this improved inhibition had already been achieved by using a heterogeneous polymeric spacer with a statistical length distribution from 19–25 monomers to bridge various distances between different active sites. Furthermore, the general principle of bivalency is not only restricted to the use of peptide aldehydes as binding head groups but could, in combination with more potent and selective monovalent inhibitors (see below), result in the design of specific inhibitors of the CP in the picomolar range. The question of whether PEG-linked bivalent inhibitors retain membrane permeability to an extent useful for intracellular tools has not been specifically addressed. However, PEG is known to be nontoxic, has low immunogenicity and low clearance rates, increases water solubility and may help in transmembrane transfer.

It has been shown that the α′,β′-epoxyketone peptide natural product epoxomicin potently and irreversibly inhibits the catalytic activity of the CP.[123] Unlike most other proteasome inhibitors, epoxomicin is highly specific for the proteasome and does not inhibit other proteases like calpain, trypsin, chymotrypsin, papain or cathepsins. The crystal structure of epoxomicin bound to the yeast CP reveals the molecular basis for selectivity of α′,β′-epoxyketone inhibitors.[85] The structure of the complex showed an unexpected morpholino formation between the N terminal threonine and epoxomicin, thereby providing the first insights into the unique specificity of epoxomicin for the proteasome (see Figure 13B). The morpholino-derivative formation is most likely a two step process. First, activation of the Thr1 Oγ atom is believed to occur by its N-terminal amino group acting as a base, either directly or through a neighbouring water molecule. Subsequent nucleophilic attack of the Thr1 Oγ atom on the carbonyl group of the epoxyketone pharmacophore would produce a hemiacetal, as is observed in the proteasome–Ac-LLN-al complex. The formation of the hemiacetal facilitates the second step in the formation of the morpholino adduct. In this cyclisation step, the N terminus of Thr1 opens the epoxide ring by an intramolecular displacement with consequent inversion of the C2 carbon. The observed specificity of epoxomicin for the proteasome is explained by the requirement for both an N-terminal amino group and a side-chain nucleophile for adduct formation with the epoxyketone pharmacophore. Thus, epoxomicin only interacts with the small class of Ntn-hydrolases. Nevertheless, epoxomicin, which represents a cell-permeable natural product, binds covalently to all proteolytic active subunits of the CP, therefore showing cytotoxicity.

Another class of proteasome inhibitors comprises peptides that possess a vinyl sulfone moiety.[42] These compounds bind to CPs irreversibly but are less reactive than aldehydes. Howev-

er, vinyl sulfones have similar limitations as the peptide aldehydes in so far as they have been reported also to bind and block intracellular cysteine proteases such as cathepsin S. The crystal structure of the proteasome–Ac-YLLN-vs complex shows covalent binding of the Thr1 Oγ atom of all active subunits to the β carbon atom of the vinyl sulfone group.[87] Previous work with libraries of peptide-based covalent inhibitors has identified structural elements that can be used to control the selectivity of synthetic inhibitors.[49,121,122] In parallel positional scanning, libraries of peptide vinyl sulfones were generated in which the amino acid located directly at the site of hydrolysis was held constant and sequences distal to that residue were varied across all natural amino acids.[124] These approaches provide the opportunity to make the vinyl sulfones specific against the active β2 subunit of the CP in altering the P3 and P4 positions, as indicated by Ac-PRLN-vs in comparison with Ac-YLLN-vs (Ac-PRLN-vs = acetyl-Pro–Arg–Leu–norleucine vinyl sulfone).[87] The crystal-structure analyses of the eukaryotic CP in complex with these vinyl sulfones suggest that favourable interactions between the P3 residue and the S3 pocket generated at the interface of neighbouring β subunits are responsible for inhibitor selectivity (see Figure 12C). Furthermore, the P1 residue was bound in the S1 pocket of each of the active sites, regardless of seemingly unfavourable electrostatic interactions. When these facts are taken together, it is possible to design a model in which specificity can be controlled predominantly by interactions at the S3 pocket for substrates with favourable interactions at this site and poor interactions at other sites. However, strong interactions at P1 may overcome the need for a favourable P3 residue. This model for substrate binding may aid in the development of inhibitors of the proteasome with tuneable selectivity for each of the active sites.

Noncovalent inhibition of the 20S proteasome

As proteasomes play an important role in many intracellular irreversible processes, such as mitosis, differentiation, signal transduction and antigen processing,[90] inhibitors that specifically block proteasomal activities may be promising candidates for tumor or inflammation therapy. However, all of the aforementioned proteasome inhibitors bind covalently to the active β subunits and usually cause cell death by induction of apoptosis.[125] Reversible and time-limited inactivation of the different proteasome activities may reduce the cytotoxic effects of these compounds. Recently, it was shown, that the natural products from *Apiospora montagnei*, the TMC-95s (TMC-95A, B, C and D), block the proteolytic activity of the CP selectively and competitively in the low nanomolar range.[126,127] The inhibitors consist of modified amino acids forming a heterocyclic ring system that is not related to any previously reported proteasome inhibitors. The crystal-structure analysis of the yeast CP in complex with TMC-95A shows the inhibitor bound at all three active sites[86] (see Figure 13C). The structure indicates a noncovalent linkage of TMC-95A to the active β subunits, without modifying their N-terminal threonines; this is in contrast to all previously structurally analysed proteasome–inhibitor complexes. TMC-95A displays a host of hydrogen bonds with the protein that give further stabilisation of the compound when bound. All these interactions are performed with main-chain atoms and strictly conserved residues of the CP, thereby revealing a common mode of proteasome inhibition amongst different species. The arrangement of TMC-95A in the CP is similar to the already reported aldehyde and epoxyketone inhibitors.[85] The *n*-propylene group of TMC-95A protrudes into the S1 pocket, making weak hydrophobic contacts with Lys33, whereas the S2 subsite is shallow and does not contribute in stabilizing TMC-95A, as already observed for the proteasome–Ac-LLnL-al adduct.[49] The side chain of the asparagine is inserted deeply into the S3 pocket and has been ascribed a major role in the differing IC_{50} values amongst the different activities. However, the stereoisomers of the TMC-95s dramatically influence the IC_{50} values, by two orders of magnitude; this is particularly noticeable for the hydroxy group seen in R1/R2, whereas the methyl group in R3/R4 has almost no effect on TMC-95 binding (Figure 14B). The crystal structure adequately explains this behaviour, as the hydroxy group in R1/R2 of the TMC-95 complex can only be accommodated as the *S* isomer. It is a surprise that during evolution the hydroxy group in R1/R2 of the TMC-95s was not replaced by a hydrogen atom, as this substitution would presumably have no effect for the binding affinity of these inhibitors.

The class of TMC-95 compounds specifically blocks the CP and does not inhibit other proteases like m-calpain, cathepsin L and trypsin.[126] The NMR spectroscopy structure of unbound TMC-95A in solution,[127] when superimposed with the structure bound to the CP, as determined by X-ray crystallography, shows a similar conformation.[86] The strained conformation of TMC-95s is stabilised suitably for optimal binding to the proteasome because of the cross-link between the tyrosine and the oxoindol side chain, (see Figure 13C). Binding does not require major rearrangements of ligand and protein and is favoured over more flexible ligands for entropic reasons.

Analysis of the TMC-95A structure overlaid with that of the vinyl sulfone peptide inhibiting only subunit β2 shows a remarkable overlap with both the backbone amides and the P1 and P3 residues, since TMC-95A interacts with the proteasome noncovalently (see Figure 14A). By presenting its functional groups in an optimal manner, covalent attachment to the catalytic nucleophile is no longer required. The combination of information from the crystal structures in complex with the CP inhibitors suggests the possibility of generating a scaffold based on the geometry of the bound TMC-95A that can present a variety of structures to the S1 and S3 pockets specific for each of the active sites of the CP. In particular, the P3 position offers itself for fine-tuning of the selectivity of compounds for individual β-subunits and designing reversible, selective and subunit-specific inhibitors of the CPs.

Much attention has been paid to the development of synthetic inhibitors and to the discovery of natural ligands because of the promising therapeutic potential of proteasome inhibition. The crystal structure of the CP–TMC-95A complex revealed the base for the minimum structural elements of TMC-95A for binding to the proteasome (see Figure 14B). In particu-

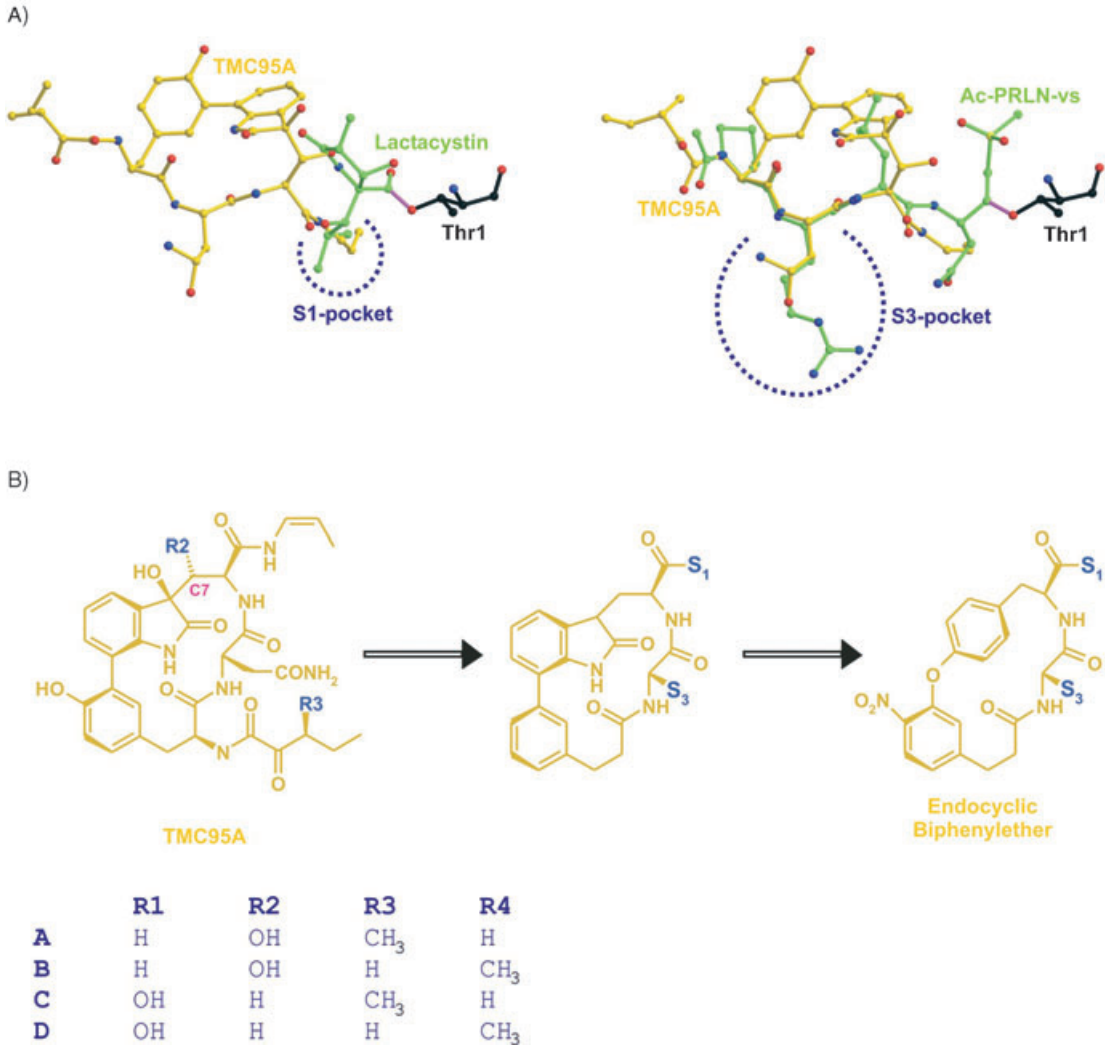

	R1	R2	R3	R4
A	H	OH	CH_3	H
B	H	OH	H	CH_3
C	OH	H	CH_3	H
D	OH	H	H	CH_3

Figure 14. *A) Superposition of TMC-95A and lactacystin and TMC-95A and Ac-Pro-Arg-Leu-Asn-vs bound to subunit β5 and subunit β2, respectively. Carbon atoms of TMC-95A are shown in yellow, of lactacystin and Ac-Pro-Arg-Leu-Asn-vs in green and of Thr1 in black; oxygen and nitrogen atoms are drawn in red and blue, respectively. The crystal structures of the related subunits were superimposed by using the program CCP4. The inhibitor structures were extracted and their arrangements compared. Lactacystin occupies the S1 pocket (coloured in blue) in a similar orientation to that of TMC-95A; Ac-Pro-Arg-Leu-Asn-vs occupies the S3 pocket (coloured in blue) in a similar orientation to that of TMC-95A.[49,87] B) Chemical structure of the TMC-95s including diastereomers A–D. From the crystal structure of the CP–TMC-95A complex, the lead-structure segment of TMC-95s, which contributes mostly to proteasome inhibition was derived. The S1 and S3 residues, shown in blue, mark specific amino acid residues that are major determinants for differential binding to proteasomal subunits. Simplification of the synthetically challenging structure of the TMC-95 lead by replacing the oxidised side-chain biaryl system with a endocyclic biphenylether is shown.[128–132]*

lar, the cyclic tripeptide of TMC-95A, which is constrained into a 17-membered ring structure by an endocyclic biaryl system, binds to the active-site clefts of the CP by hydrogen bonds, thereby adopting an antiparallel β-sheet structure. The remaining part of the inhibitory compound is not involved in direct interactions with the protein, except the oxoindol group of the tryptophan, which shows an additional hydrogen bond to the nitrogen backbone atom of residue 23. Thus, the conformationally restricted C-terminal (*Z*)-prop-1-enyl moiety as the P1 and the central asparagine as the P3 residue are the structural factors that dictate the differentiated affinity of TMC-95A for the three active sites. The lead structure sensibly facilitates synthetic access to TMC-95A analogues,[128,129] as the total synthesis of the natural TMC-95A compound is highly complex.[130–132] As a proof of concept the minimal core structure was decorated at the C terminus with an *n*-propyl group (on the norleucine side chain) as the P1 residue and at the N terminus with a benzyloxycarbonyl moiety as an N-protecting group, while the central Asn residue of TMC-95A was retained as the P3 residue.[132] However, the inhibitory potencies of the analogue showed a potency for subunit β5 that was 10-times reduced relative to that of the natural compound. This observation is a surprise, as the analogue contains an N-terminal benzylurethane instead of the alkyl-ketoamide group and only lacks the two hydroxy groups at the tryptophan moiety. According to the X-ray structure of the CP–TMC-95A complex these two modifications should not account for the significantly lower inhibition of the activity. Therefore, the replacement of the conformationally restricted and bent (*Z*)-prop-1-enyl group with the flexible *n*-propyl group as the P1 residue has to be the pri-

mary cause of this effect on the binding affinities. The crystal structures of the CP in complex with the TMC-95 analogue are perfectly superimposable with the CP–TMC-95A structures. An almost identical hydrogen-bonding network is established between the active-site cleft and the inhibitors with the only difference being the mode of insertion of the C-terminal *N*-alkyl chain into the S1 pocket. Here, the hydrophobic S1 pocket is optimally filled without any steric clashes by the (*Z*)-prop-1-enyl group of TMC-95A, while the *n*-propyl chain of the analogue is deeply inserted and thus clashes with the side chain of the subunit. In the case of the tryptic-like activity of subunit β2, the inhibitory potency of the analogue is lowered by a factor of three, as compared to the value for TMC-95A. Again, the structures of the bound inhibitors are almost superimposable and the hydrogen-bonding networks appear identical. Therefore, the structural observations suggest that the entropic loss related to the more flexible P1 residue in the analogue is responsible for the reduced potency. These results allowed the conclusion that the restricted conformational freedom of the cyclic tripeptide fully dictates the mode of insertion of the individual residues into the pockets of the active-site cleft and, correspondingly, the optimal occupancy of critical binding subsites.

In fact, the rigid display of the backbone severely limits the choice of groups acting as the P1 residue without steric clashes. Thus, the use of other, possibly less bulky and less rigid endocyclic clamps for conformational restriction of the peptide backbone is expected to allow a better orientation of groups interacting with the various subsites. Biaryl ethers of the isodityrosine type, which are also more easy to synthesise, are known to induce an identical conformational restriction to that of the biaryl system in TMC-95A when used as structural clamps in positions *i* and *i*+2 of cyclic peptides. The NMR-spectroscopy-derived conformation of the biarylether in solution clearly revealed that the *meta–para* junction through the ether group leads to a structure very similar to that of TMC-95A[133] (see Figure 14B). As a consequence, a TMC-95 analogue was prepared, with the biaryl group replaced with a biphenyl ether. Surprisingly, it was found that the new TMC-95 derivative showed an equipotent inhibition of the tryptic-like activity of yeast CP, as compared with TMC-95A,[134] (unpublished results). This observation makes the design of new reversible inhibitors, by the use of other, possibly even less bulky, endocyclic clamps for conformational restriction of the peptide backbone and for optimal orientation of groups interacting with the various subsites, attractive.

In some but not all archaea and eubacteria, the 20S proteasome is accompanied by another large cage-forming protease, the tricorn protease. Tricorn functionally interacts with the CP by cleaving proteasomal peptide products into smaller peptides, which are further degraded into single amino acids by associated factors. The structural and functional aspects of tricorn are described in the following section. The unexpected relationship between tricorn and the eukaryotic dipeptidyl peptidase IV revealed by these structural studies is also discussed in brief.

3. The Tricorn Protease and Its Structural and Functional Relationship with Dipeptidyl Peptidase IV

The tricorn protease, named for its tricorn-like shape, was first purified from the model organism *T. acidophilum* during a search for regulatory components of the 20S proteasome.[135] Even though the enzyme did not appear to regulate the 20S proteasome[135] and is now believed to act downstream, it attracted interest as a giant protease that exceeded the 20S proteasome in size. Genetic and biochemical characterisation showed that the enzyme was assembled from multiple copies of a single, 120 kDa polypeptide chain.[135] Six subunits each form homohexamers that assemble further into an icosahedral capsid with a molecular weight of 14.6 MDa.[135,136] The crystal structure of the 720 kDa tricorn hexamer is available.[137] It shows the mode of assembly of monomers, demonstrates that each monomer consists of five separate domains and suggests how the domains coordinate the specific steps of substrate processing and particularly substrate channeling to and from the active site.

Architecture of the tricorn protease

The hexameric *D*3-symmetric tricorn protein is assembled by two perfectly staggered and interdigitating trimeric rings with every subunit of one ring forming contacts almost exclusively with the two subunits of the other ring related by the molecular diads. The toroid structure has the shape of a distorted hexagon formed by a trimer of dimers (Figure 15). The overall dimensions of the molecule are 160 Å within the plane normal to the three-fold axis and 88 Å parallel to it. The conically shaped central pore connects with additional cavities formed by the individual subunits like spokes of a wheel (see Figure 15).

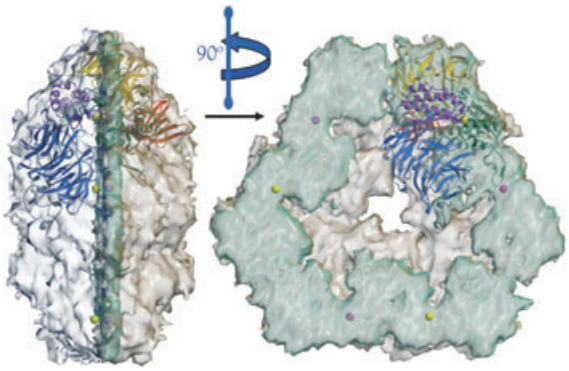

Figure 15. *Surface representation of the tricorn protease with the ribbon model of one subunit superimposed. The two orthogonal views are along the molecular twofold and threefold axes, respectively. The six solid spheres indicate the active-site positions. Figure reproduced from ref. [137].*

Single tricorn subunits can be divided further into five domains, namely a 6-bladed β propeller (β6) domain, a 7-bladed β propeller (β7) domain, a mixed α–β domain (C1), a PDZ-like

domain, and another mixed α–β domain (C2), that are arranged in this order along the polypeptide chain. Very unusually for β propeller domains, both β6 and β7 are topologically unclosed, an extremely rare feature otherwise observed only in the prolyl oligopeptidase (POP)[138] and DP IV protease.[139,140] The PDZ-like domain is interspersed between the two C-terminal mixed α–β domains. These C-terminal domains harbour the catalytic residues and exhibit the α–β hydrolase fold, again underlining the relationship of tricorn with DP IV and POP.

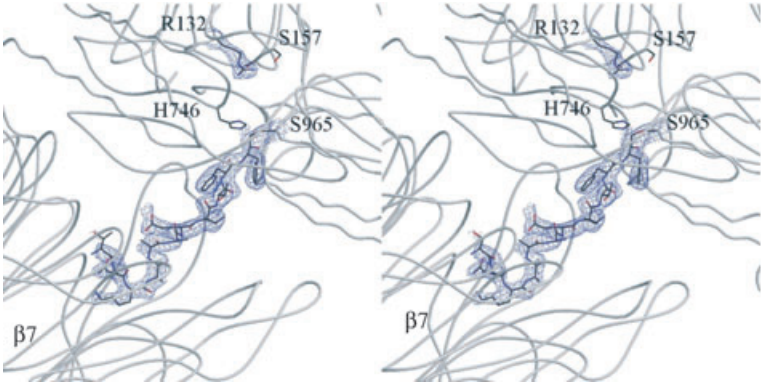

Figure 16. *Stereoview of a 13-mer chloromethyl ketone bound to the active site. With the exception of a few important residues in tricorn, which are presented in an all-atom representation, tricorn is represented as a smoothed Cα trace. For the inhibitor and Arg132, a key residue in tricorn, the experimental electron density is presented together with the final model. The peptide is clearly directed towards the β7 propeller.*

Catalytic residues and mechanism

To identify catalytically important amino acids, tricorn was cocrystallised[137] with a series of chloromethyl ketone based inhibitors, including the known tricorn inhibitors[135] tosyl-L-lysine chloromethyl ketone (TLCK) and tosyl-L-phenylalanine chloromethyl ketone (TPCK). In all cases, continuous electron density connecting to the side chain of Ser965 was observed and unambiguously fitted by the respective inhibitors. Ser965 is positioned at the entrance to helix H3 within subdomain C2. The amide nitrogen atom of Asp966, together with that of Gly918, forms the oxyanion hole which is occupied by a water molecule in the uninhibited structure. His746 is ideally positioned to activate the catalytic Ser965 at a hydrogen-bonding distance of 2.7 Å. Although a covalent linkage between a chloromethyl ketone inhibitor and the catalytic histidine of a serine protease could be expected,[141] no such linkage was found in any of the complexes of tricorn with trichloromethyl ketone inhibitors. Thus, in this respect, tricorn is more similar to cysteine peptidases.[142] A crucial role for Ser965 and His746 in activity is supported by mutagenesis data: both the single-site mutants Ser965A and His746A are amidolytically inactive.[137] His746 is correctly oriented by the Oγ atom of Ser745, which in turn is polarised by Glu1023. Thus, Ser965, His746, Ser745 and Glu1023 can be described as a catalytic tetrad. The arrangement of Ser965, His746 and the oxyanion hole suggests that peptide-bond hydrolysis follows the classical steps for trypsin-like serine proteases, namely the formation of the tetrahedral adduct, the acyl-enzyme complex and hydrolysis.

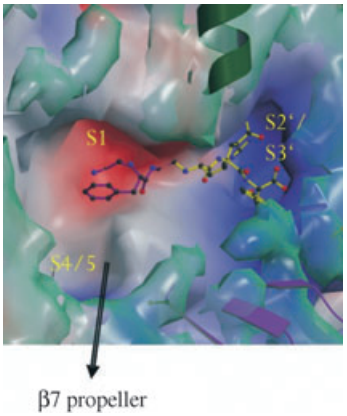

Figure 17. *Detailed active-site view and substrate recognition as deduced from experimental complex structures. The substrate C terminus is anchored by Arg131 and Arg132.*

Tricorn specificity

Tricorn has been shown to exhibit both tryptic and chymotryptic specificities.[135] The X-ray crystal structure reveals that specificity for basic P1 residues is conferred by Asp936, which is provided by the diad-related subunit (Figures 16 and 17), thus linking the mode of assembly (trimer of dimers) with function. Intriguingly, in the uninhibited high-resolution crystal structure, the acidic S1 specificity-determinant residue Asp936 was mobile. In the TPCK complex structure, the side chain of Asp936 adopts an alternative rotamer to allow the TPCK phenyl ring to freely access the hydrophobic niche formed by Tyr946, Ile969, Val991 and Phe1013. Thus, it appears that, due to its flexibility, Asp936 can serve as a substrate-specificity switch to accomodate both hydrophobic and basic P1 residues. The SO_2 group of TPCK and TLCK interacts with the NH moiety of Ile994, thereby already suggesting the strand Glu993–Pro996 as the unprimed substrate-docking site. These substrate-recognition sites are rather unrestricted, in agreement with tricorn's generally broad substrate specificity.[135,143] Experimentally, it was found that a negative charge was not tolerated at at positions P3, P4 and P5 of a synthetic fluorogenic 7-amino-4-methylcoumarin (AMC) substrate.[143] The crystal structure does not indicate any steric or electrostatic conflicts, if a canonical binding mode of these substrates is assumed. It is conceivable that discrimination against these substrates resulted from unproductive binding with inverted strand polarity, which in turn could be due to the inverted polarity of these substrates which lack a free C terminus and are N-terminally succinylated.

Tricorn accepts substrates with a rather broad variety of sequences upstream of the scissile peptide bond but it places restrictions on the length of substrates downstream of the scissile peptide bond. These restrictions are due to a prominent

cluster of basic residues (Arg131, Arg132) in tricorn that delimit the binding site of the substrate C terminus. These basic residues, positioned on a flexible loop (as discussed in detail below), together with the primed site topology, clearly mark tricorn as a carboxypeptidase. The geometric dimensions explain tricorns preferential di- and tricarboxypeptidase activity, while the cleavage of longer peptides will require some conformational rearrangement and is energetically less favourable. Single amino acids cannot be cleaved from a substrate, because the P1′ residue is unable to anchor its carboxylate group on the basic backstop residues (see Figures 16 and 17).

Each of the three C-terminal domains (C1, PDZ, C2) is remarkably similar to the respective domains (A, B and C) found in the D1 processing protease (D1P) of photosystem II. The root-mean-square deviations between the Cα positions of these domains are 2.2, 2.3 and 2.7 Å with 84, 86 and 135 matching amino acids, respectively. A weak homology between these domains is recognisable in the primary sequences (11, 19 and 20% identities). The relative arrangement of these domains, however, differs very much between tricorn and D1P; With the C2 domain aligned to the C domain of D1P, the orientation of the C1 domain differs from that of the D1P A domain by 35°. Analogously, the required transformation to align the PDZ-like domains includes a 96° rotation. The rotation axes of these transformations are unrelated to each other. In addition, proper alignment of the PDZ-like domain requires a 30 Å translation. The catalytic serine residues (Ser965 and Ser372, respectively) are positioned on topologically equivalent positions at the helix entrance in the C2 or C domain (tricorn and D1P, respectively). Furthermore, the amides forming the oxyanion hole (Gly918, Asp966 and Gly318, Aln373 in tricorn and D1P, respectively) superimpose to within 1 Å. As in other T-cell serine (Tsp) like proteases, the residue serving as a general base in D1P is a lysine (Lys372) residing within the C domain of D1P, while it is a histidine in tricorn (His746) which resides in tricorn's C1 domain. The relative arrangement of the C1 and C2 domains in tricorn must, for that reason, remain very restricted to allow proper catalysis.

A role of the PDZ domain in substrate recognition has been shown for Tsp[144] and was analogously suggested for the tricorn protease.[145] While the Gly–Leu–Gly–Phe substrate-recognition element is structurally conserved (Arg764–Ile–Ala–Cys767 in tricorn), as pointed out earlier, it appears unlikely for a number of reasons that the tricorn PDZ domain will participate in substrate recognition in a similar manner to that suggested for D1P:[146] 1) The putative substrate-binding site, as defined by the crystal structures of the C-terminal peptides complexed with PDZ domains,[147,148] is partly occupied by the outer strands of blade 3 of β6 within the same subunit; 2) the generally conserved arginine (Arg247) involved in recognition of the carboxylate group of the peptide C terminus corresponds to a hydrophobic residue in tricorn (Ile851); iii) the orientation and position of the tricorn PDZ domain differs so strongly from that seen in D1P that any analogy based on the sequential domain arrangement is invalidated on the basis of their respective three-dimensional domain arrangements. Instead, the PDZ domain mainly serves to scaffold the subdomains as described earlier and, in addition, might be involved in the recognition of associating component proteins.

Substrate access and product egress through β propellers

The comparison with POP, including the open Velcro topology,[138] suggests an important role for the β propellers in substrate access to and product exit from the active site[139] (Figure 18). Both the β6 and β7 propeller axes are directed towards the active site of the protein, almost intersecting near Ser965. The arginine anchor (Arg131, Arg132) obstructs the otherwise direct connection from the active-site chamber to the exterior through the β6 propeller. Based on these data, it has been proposed that the β6 propeller channel represents one, if not the, major rear exit from the catalytic chamber.[149] This model is supported by the properties of the tricorn point mutant Leu184Cys. The point mutant has a wider pore in the β6 domain and is indeed more active than the wild-type. After modification of the introduced thiol group with *N*-ethylmaleimide (NEM), the activity of the mutant enzyme towards fluorogenic substrates is significantly reduced (< 50%) compared with the wild-type protein.[137,149] The substrate entrance and product exit paths are indicated in Figure 19.

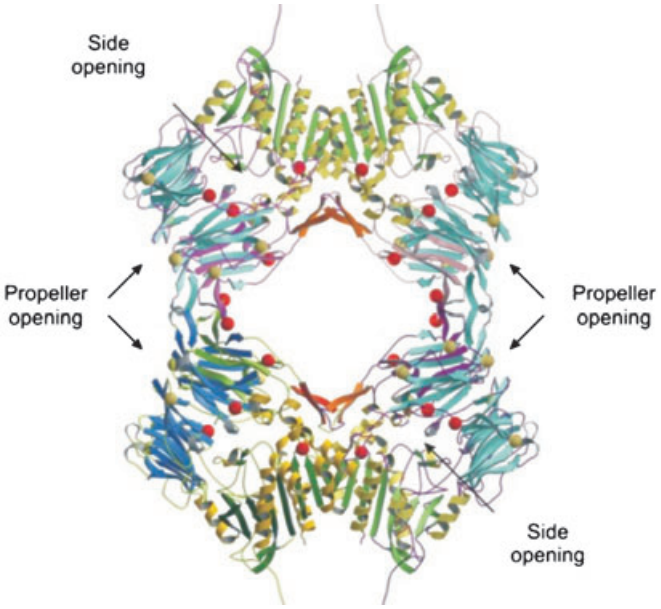

Figure 18. *Ribbon representation of the tetrameric DP IV. The tetramer results from a dimerisation of dimers and has 222 symmetry. Potential glycosylation sites are marked as grey spheres, and sites that were modified in the crystal structure are marked as red spheres. Figure reproduced from ref. [139].*

The crystal structures of the chloromethyl ketone based inhibitor complexes suggested the strand Glu993–Pro996 as a recognition strand for the unprimed substrate residues. This strand extrapolates towards the β7 channel (see Figure 14). The channel through the β7 propeller provides a significantly shorter route from the catalytic chamber to the outside of the protein (60 Å) than the alternative route through the central pore (83 Å). The latter path to the active site has multiple branchings and dead ends. Therefore, the β7 channel might be utilised by the enzyme for the preferred substrate passage

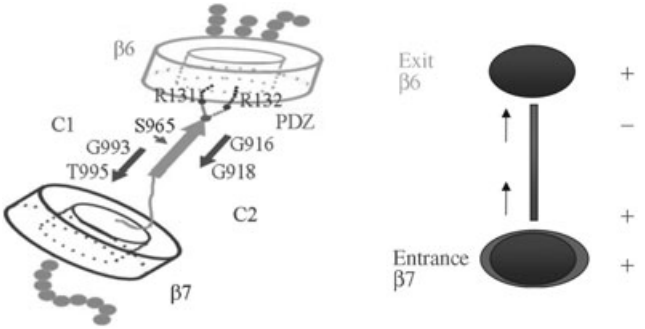

Figure 19. *Cartoon of the model for electrostatically driven processive substrate turnover.[149] A) The blue and yellow cylinders represent the seven- and six-bladed β propeller domains, respectively. Substrates to the β7 domain and products from the β6 domain are represented as strings of green dots. Single green dots represent individual amino acids. Figure reproduced from ref. [149]. B) Schematic representation of the electrostatic potential along the suggested path for substrates.*

to the active site. It is wide open but capped on its outside by four basic residues (Arg369, Arg414, Arg645, Lys646) which are only partially charge compensated by one acidic residue (Asp456). This locally positive lid to the β7 propeller channel is encircled by acidic residues (Asp333, Asp335, Asp372, Asp456, Asp506, Asp508, Glu592 and Glu663). Except from Glu663, which is located on the hairpin connecting-strands 3 and 4 of blade 7, all of these charged amino acids are positioned between strands 1 and 2 of the respective β7 blades. The resulting charge distribution mimics an electrostatic lens, whereby peptides are preorientated with their C termini towards the central basic propeller lid. Once the entrance to the β7 channel is opened by a concerted side-chain movement of Arg369, Arg414, Arg645 and Lys646, possibly assisted by main-chain movements of Ala643–Lys646 (blade 7), a peptide is able to enter the channel in an extended conformation where it will find multiple docking sites on the unsaturated inner strands of the β7 propeller blades. A similar substrate gating/filter mechanism through a seven-bladed β propeller has been suggested for the prolyl oligopeptidase,[138,150] and there is precedence for a β hairpin binding into a seven-bladed propeller.[151] The preferred substrate entry through the β7 propeller channel is in line with the point mutation Arg414Cys, located in the β7 channel. Derivatisation of the introduced thiol group with maleimide markedly decreased the fluorogenic activity of this mutant to about 50% of the wild-type activity.[137]

Tricorn cleaves substrates in a processive mode,[149] a fact indicating that only completely digested products will leave the inner protein chambers, while larger products will be retained and processed as preferred substrates. The structure suggests several mechanisms to maintain "one-way" processing. Basic lids (Arg414, Arg645, Lys646 and Arg131–Arg132) are placed at the entrances to the β6 and β7 channels. The topology and size of the inner cavities favour an extended conformation of the substrate and the C terminus of the substrate will be attracted to the basic β6 lid, thereby presenting the substrate's scissile bond at the active-site Ser965 residue for proteolyis. In one possible scenario, the primed product residues are released by the enzyme through the "rear exit" to the active site formed by the β6 propeller, which is gated by Arg131–Arg132. The arginine gate is located on a helical loop containing three glycines (Gly126, Gly130, Gly139) and not restrained to its position by any protein contacts. These glycines might function as hinge residues that allow the gate to move into a sufficiently voluminous cavity of mixed polarity (see Figure 17).

The unprimed side of the substrate is held in place by a series of interactions with the protein. In addition to the observed ionic (Asp936) or hydrophobic S1 interaction site (Tyr946, Ile969, Val991, Phe1013), the P1 main chain is held by its interaction with the oxyanion hole (Gly918, Asp966). P2–P4 residues will presumably utilise unsaturated main-chain hydrogen bonds at the strand Ile994–Pro996 and further interactions might occur in the β7 propeller channel, as described in galactose oxidase[151]. The modelling studies and suggested substrate binding at the primed and unprimed sides are fully experimentally confirmed by crystal structure studies with C- and N-terminally extended covalently bound inhibitors.[149]

Tricorn reportedly cooperates with three additional proteins, termed interacting factors F1, F2 and F3, to degrade oligopeptides sequentially to yield free amino acids.[152] F1 is a prolyl iminopeptidase with 14% sequence identity to the catalytic domain of prolyl oligopeptidase (POP), which has an additional propeller domain.[138,152] Guided by the structural scaffold of the latter structure, we speculate that F1 docks onto the six-bladed β propeller of the tricorn core protein. As in POP, the substrate would enter F1 through the propeller channel in this model. While a physical interaction of F1 with tricorn has been suggested,[153] the exact mode of interaction of tricorn with F1, F2 and F3 has not been detailed so far. There is also evidence for functional but not physical interaction of tricorn with the proteasome.[153] A physical interaction between these molecules by aligning their respective central pores would imply a symmetry mismatch. While such a physical interaction would be consistent with the geometric dimensions of both molecules, its existence needs to be experimentally confirmed and characterised.

The structural and functional relation of tricorn with DP IV

The situation in the tricorn protease is closely resembled by dipeptidyl peptidase IV (DP IV) where an eight-bladed topologically open β propeller and a side opening provide entrance to and exit from the active site (see Figure 18). Similarly to tricorn, DP IV is a serine protease with low but significant structural homology to the family of α/β-hydrolases. We superimposed the catalytic core elements, including the active-site serine and histidine residues, the strictly conserved helix following the active-site serine (Ser630–Ala642 and Ser965–Leu977, respectively) and tricorn's five-stranded parallel β sheet onto the equivalent strands of the eight-stranded DP IV sheet. Both sheets have identical polarity. Significantly, both tricorn propellers come to superimpose onto the two DP IV openings, with the tricorn β7 propeller on the DP IV β8 propeller and the tricorn β6 propeller on the side exit, as schematically indicated in Figure 20. This similarity suggests that the β8 propeller provides substrate access to and the side-opening offers product

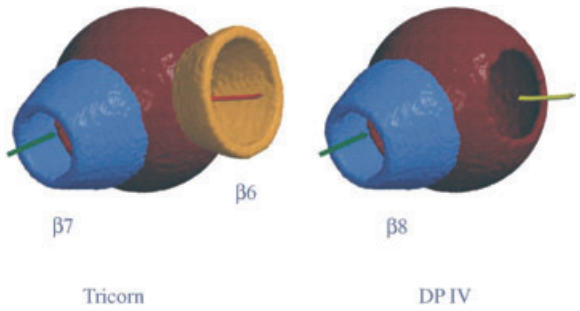

Figure 20. *Schematic representation of the active-site access and product egress in tricorn and DP IV. Figure reproduced from ref. [139].*

release from the DP IV active site. This tricorn-derived model is able to explain the high substrate selectivity critical for the DP IV function of activating or inactivating regulatory peptides. Passage through the β-propeller tunnel requires the substrates to unfold, thereby providing their "finger print" to DP IV. Once the amino terminus of the peptide approaches the active site, it is still held in place by its C terminus interacting with the β propeller, which may contribute to conformationally activate the substrate for cleavage. After the nucleophilic attack the acyl-enzyme intermediate forms, while the primed product is directly released through the side exit. This explains why degradation of glucagon by DP IV is not processive but occurs sequentially in two independent steps (glucagon 3–29 and glucagon 5–29).[154] Clearly, the final determination of the functional roles of the DP IV openings awaits further experiments.

In the last chapter, DegP, a bacterial cage-forming protease which has homologues in all kingdoms of life, is described. It differs from the other enzymes in its extreme flexibility and in its potential to change overall shape and internal structure. Structural flexibility is translated into function and into the unique property of DegP to act predominantly as a chaperone or as a protease according to the temperature. DegP is a Janus-faced molecule that appears as a helper or killer as cells need it.

4. The DegP Protease Chaperone: A Molecular Cage with Bouncers

Cells have developed a sophisticated system of molecular chaperones and proteases to reduce the amount of unfolded or aggregated proteins.[155] Chaperones recognise hydrophobic stretches of polypeptides that become surface exposed as a consequence of misfolding or unfolding. If refolding attempts fail, irreversibly damaged polypeptides are removed by proteases.

E. coli contains several intracellular proteases that recognise and degrade abnormally folded proteins. The biochemical and structural features of these ATP-dependent proteases have been studied extensively (see Section 1). However, relatively little is known about proteases that are responsible for the degradation of nonnative proteins in the periplasmic compartment of Gram-negative bacteria. Such a function has been attributed to the heat shock protein DegP, also commonly referred to as HtrA or Protease Do. While most factors involved in protein quality control are ATP-dependent heat shock proteins,[156] DegP fulfills this role without consuming chemical energy.[157] DegP homologues are found in bacteria, fungi, plants and mammals. Some, but not all, are classical heat shock proteins. They are localised in extracytoplasmic compartments and have a modular architecture composed of an N-terminal segment believed to have regulatory functions, a conserved trypsin-like protease domain and one or two PDZ domains at the C terminus.[158] PDZ domains are protein modules that mediate specific protein–protein interactions and bind preferentially to 3–4 residues at the C-terminal of the target protein.[159] Prokaryotic DegPs have been attributed for tolerance against thermal, osmotic, oxidative and pH stress, as well as to pathogenicity.[160] A number of DegP substrates are known. These are either largely unstructured proteins such as casein, small proteins that tend to denature, hybrid proteins or proteins that entered a nonproductive folding pathway.[157,161,162] Stably folded proteins are normally not degraded. In addition to its protease activity, DegP has a general chaperone function. The dual functions switch in a temperature-dependent manner, with the protease activity being most apparent at elevated temperatures.[162] The ability to switch between refolding and degradation activity and the large variety of known substrates make DegP a key factor in the control of protein stability and turnover.

The DegP protomer, a PDZ protease

DegP from *E. coli* was crystallised at low temperatures in its chaperone conformation and analysed.[163] The protomer can be divided into three functionally distinct domains, namely a protease and two PDZ domains, PDZ1 and PDZ2 (Figure 21). Like other members of the trypsin family, the protease domain of DegP has two perpendicular β-barrel lobes with a C-terminal helix. The catalytic triad is located in the crevice between the two lobes. While the core of the protease domain is highly conserved, there are striking differences in the surface loops L1, L2 and L3 (for nomenclature, see ref. [164]), which are important for the adjustment of the catalytic triad (Asp105, His135, Ser210) and the specificity pocket S1. The enlarged loop LA protrudes into the active site of a molecular neighbour, where it intimately interacts with loops L1 and L2. The resulting loop triad, LA*–L1–L2, completely blocks the substrate-binding cleft and results in a severe deformation of the proteolytic site with formation of the catalytic triad, the oxyanion hole and the S1 specificity pocket abolished. Thus, the protease domain of the DegP chaperone is present in an inactive state, in which substrate binding and catalysis is prevented.[163] The structure of the PDZ domains of DegP is similar to that of PDZ domains of bacterial origin.[146] Compared to the canonical 4+2 PDZ β sandwich,[147] the DegP PDZ domains show a circularly permuted secondary structure, in which the N- and C-terminal strands are exchanged. Furthermore, they contain a 20-residue insertion following the first β strand (including helix f) that is important for inter- and intramolecular contacts within the oligomer. In analogy to other PDZ domains, PDZ1 and/or PDZ2 should be involved in substrate binding. PDZ1 contains

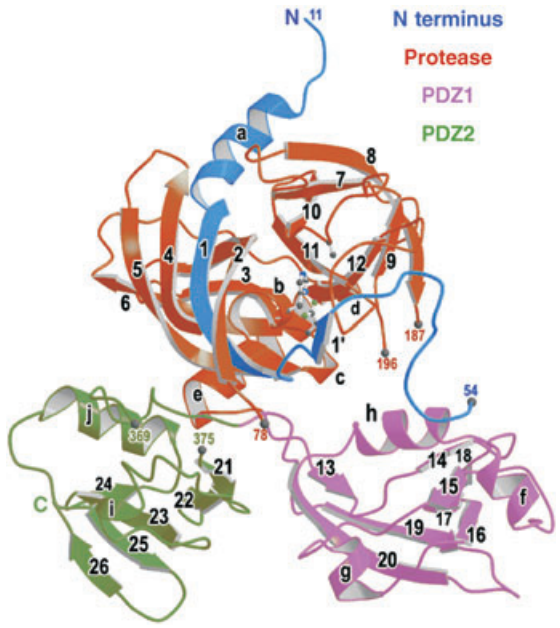

Figure 21. *Structure of the DegP protomer in ribbon representation. Colour is according to domain and residues of the catalytic triad are shown as ball-and-stick models. The nomenclature of secondary structure elements, the termini of the protein and regions that were not defined by electron density is indicated.*

a deep binding cleft for substrate, which is mainly constructed by strand 14, its N-terminal loop (the so-called carboxylate-binding loop) and helix h. The carboxylate-binding loop is located in a highly positively charged region and is formed by an Glu–Leu–Gly–Ile motif, which is similar to the frequently observed Gly-Leu-Gly-Phe motif.[147] Binding specificity is mainly conferred by the specific configuration of the 0, −2 and −3 binding pockets,[165] where pocket 0 anchors the side chain of the C-terminal residue. In PDZ1, all pockets are built by mainly hydrophobic residues. The thermal motion factors point to the flexibility of strand 14 and its associated carboxylate-binding loop, thereby indicating the plasticity of the binding site. Thus, PDZ1 seems to be well adapted to bind various stretches of hydrophobic peptide ligands. Unlike PDZ1, the occluded binding site of PDZ2 is unlikely to be involved in substrate recognition.

The DegP hexamer can adopt an open and a closed form

In the crystallographic asymmetric unit, two DegP molecules (A and B) were observed, which build up two distinct hexamers (Figure 22). Both hexamers are formed by staggered association of two trimeric rings. Hexamer A is a largely open structure with a wide lateral passage penetrating the entire complex (see Figure 22 A), whereas hexamer B corresponds to the closed form, in which a cylindrical 45 Å cavity containing the proteolytic sites is completely shielded from solvent (see Figure 22 B). In both cases, the top and bottom of the DegP cage are constructed by the six protease domains, whereas the twelve PDZ domains generate the mobile sidewalls. The height of the cavity is determined by three molecular pillars, which are formed by the enlarged LA loops of the protease domain. The PDZ domains are able to adopt different conformations and represent side doors that may open. This en bloc mobility enables the PDZ domains to function as tentacular arms that capture substrates and deliver them into the inner cavity. This structural organisation is strikingly different from the other cage-forming proteases, where substrates enter the central cavity through narrow axial or lateral pores, as described in Sections 1–3.

DegP, a chaperone

E. coli DegP has the ability to stabilise and support the refolding of several nonnative proteins in vivo and in vitro.[162,166] Possible binding sites for misfolded proteins are located within the inner cavity (Figure 23). The solvent-accessible height of this chamber is 15 Å at its centre and increases to 18 Å near the outer entrance. Due to these geometric constrictions, substrates must be partially unfolded to reach the active site (see Figure 23). As in other chaperones of known structure, the DegP cavity is lined by hydrophobic residues. Two major hydrophobic grooves can be distinguished, which are mainly

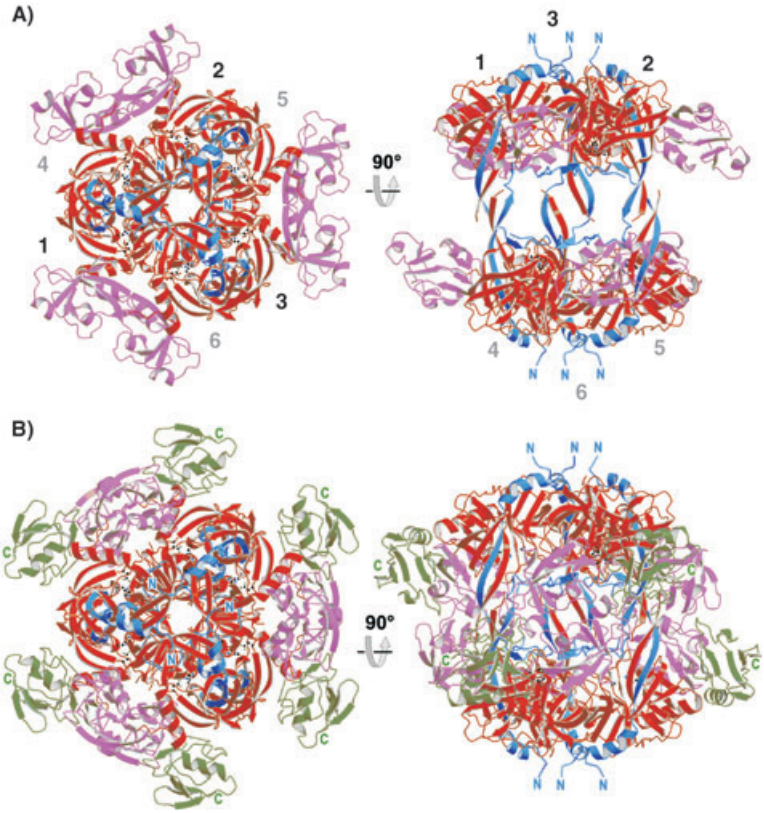

Figure 22. *Structure of the DegP hexamer. Top and side views of the hexamer constructed by molecules A and B. Both hexamers are approximately equal in size with a height of 105 Å and a diameter of 120 Å. The nomenclature of the individual monomers and their termini is given. Figure adapted from ref. [163].*

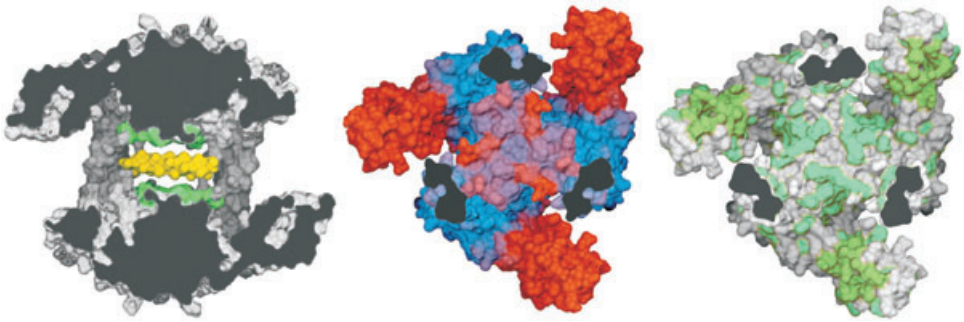

Figure 23. *Properties of the inner cavity. Half cut presentations of molecule A (left: side view; middle and right: top views) with cut regions shown in dark grey. Left: Surface representation of the internal tunnel illustrating its molecular-sieve character. Access is restricted to single secondary-structure elements as shown by the modeled polyalanine helix (coloured yellow). Middle: Top view of the ceiling of the inner cavity with mapped thermal motion factors to show its plasticity. Flexible regions are coloured red, rigid regions are blue. Right: Formation of the hydrophobic binding patches within the cavity. Hydrophobic residues of the protease domain are shown in cyan and the nonpolar peptide-binding groove of PDZ1 is coloured green.*

constructed by residues of loop LA and L2. Notably, the hydrophobic binding sites of the PDZ1 domains are properly orientated to augment the number of potential binding patches. The alternating arrangement of polar and hydrophobic surfaces, both within one trimeric ring and between trimeric rings, should allow the binding of exposed hydrophobic side chains as well as of the peptide backbone of substrates. Taken together, the ceilings of the DegP cavity represent docking platforms for partially misfolded proteins. Both platforms are structurally flexible and should thus allow binding of diverse polypeptides.

The protease form

The protease conformation of DegP is still elusive, as crystallisation of a substrate-like inhibitor complex has failed and maintenance of a stably folded protein precludes long-term experimentation at elevated temperatures where it displays protease activity. We propose a profound rearrangement of the LA*–L1–L2 loop triad into the canonical conformation of active serine proteases, ready for substrate binding. This may be initiated by a collapse of the hydrophobic LA platforms and an enlargement of the hydrophobic contacts caused at high temperature.

Working model for an ATP-independent heat shock protein

Cage-forming proteases and chaperones can be ATP-dependent or -independent. In the former group, ATPase activity is important for recognition of target proteins, for their dissociation and unfolding, for their translocation within the complex and for various gating mechanisms. The present crystal structure indicates why these functions are not relevant for DegP. DegP preferably degrades substrates that are per se partially unfolded and that might accumulate under extreme conditions.[157,167] Alternatively, threading of substrate through the inner chamber could promote unfolding into an extended conformation. Removal of higher order structural elements may reinitiate substrate folding after exit from DegP. By binding to the C terminus or the β-hairpin loop of a protein, the PDZ domains could properly position the substrate for threading it into the central cavity. After accessing this chamber, the fate of the unfolded protein depends on the interplay and structural organisation of loops LA, L1 and L2. Recruitment of PDZ domains for the gating mechanism should permit a direct coupling of substrate binding and translocation within the DegP particle. This two-step binding process is similar to that of other cage-forming proteins, such as the proteasome or the Clp proteases. Here, two binding sites (chambers) exist, the first of which primarily determines substrate specificity.

Conclusion and Outlook

From HslVU to other bacterial ATP-dependent proteases

HslVU is still the best-characterised ATP-dependent protease at the mechanistic level, but partial structural information for other ATP-dependent bacterial proteases has also become available, especially for the activatory domains. Very recently, separate structures of the Lon protease domain[168] and of the small, mostly helical α domain of the Lon AAA(+) module[169] have been published. The structure of ClpP, the protease core of the ATP-dependent proteases ClpAP and ClpXP, has already been available for quite some time.[170] More recently, the activatory components ClpA[26] and ClpX[171] have been crystallised, although only as the monomeric proteins and not as the physiologically occurring oligomers. For the essential, membrane-spanning metalloprotease FtsH, structural information at the atomic resolution is available for the ATPase domain but is still lacking for the protease component.[172,173] Although atomic-resolution structures of the active complexes would be highly desirable, numerous unsuccessful efforts in our and other hands suggest that this will be difficult. Even in the absence of full structural information on the ATP-dependent proteases, many conclusions can already be drawn. In particular, it is already clear that great variability in the protease domains contrasts with strong similarity of the ATPase domains in ways that were not originally anticipated.

Although the protease domains all share the multimeric architecture with a central channel or pore, there is no further similarity, either at the level of fold or in the active-site architecture. HslV is an Ntn-hydrolase[60] with an N-terminal threonine nucleophile.[17,174] ClpP is a serine protease that belongs to the crotonase superfamily of enzymes, a large class of enzymes that catalyse a variety of chemical reactions that all require the stabilisation of an intermediate by an oxyanion hole.[175] The crystal structure of the protease domain of *E. coli* Lon shows that this domain has yet another fold and a serine–

lysine dyad in the active site.[168] No structure is available for FtsH, but an HEXXH motif in the sequence and the experimental identification of a Zn^{2+}-chelating glutamate ligand place the protease domain of FtsH in MEROPS clan MA(E), together with other metallopeptidases such as thermolysin, angiotensin-converting enzyme, and thimet oligopeptidase.[11]

In contrast to the proteolytic core complexes, the activatory components of HslVU, ClpXP, ClpAP, Lon and FtsH are structurally related and belong to the AAA(+) family of ATPases.[22] The activators are separate subunits in HslVU, ClpXP and ClpAP and occur in one polypeptide chain with the peptidase domains in Lon and in FtsH. In HslU, ClpX, Lon and FtsH, only one copy of the AAA(+) module is present per subunit, whereas ClpA has two such modules.[22] In addition to the common AAA(+) domain, the different ATPases contain additional, enzyme-specific domains. In HslU, a mostly helical I domain is inserted into the AAA(+) module.[23] ClpX contains an N-terminal domain that was shown to bind zinc[176] and to act as a dimerisation module.[177] Like ClpX, ClpA contains a non-AAA(+) domain at its N terminus, and like the N-terminal domain in ClpX, this domain also has the capability to bind zinc.[26] However, unlike the N domain of ClpX, the N domain of ClpA is almost entirely helical and consists of two four-helix tandem motifs.[26]

In both ClpA and ClpX, the N-terminal non-AAA(+) motifs serve as "docking modules" for accessory proteolysis factors that modulate or change the activity of the proteolytic complex itself.[178] The N domain of ClpX interacts specifically with the adaptor protein SspB that stimulates the degradation of SsrA-tagged proteins.[179] The tag is jointly recognised by the SspB–ClpXP complex, where SspB interacts with the N-terminal and central regions of the SsrA tag and leaves the C-terminal region for interaction with ClpX.[180,181] The C-terminal region of SspB shares considerable homology with the corresponding region in RssB, another ClpX adaptor protein.[179] It appears that RssB promotes the degradation of a specific substrate, namely a subunit of RNA polymerase known as σ^S.[182] Very recently, it was shown biochemically that the adapter protein and the ATPase recognise distinct sites in the substrate.[183] ClpA has its own adaptor protein, ClpS. At least in vitro, ClpS switches ClpAP activity away from SsrA-tagged towards heat-aggregated proteins.[184] Two independent crystal structures of ClpS in complex with the N domain of ClpA are available.[26,185] They explain the specificity of ClpS for ClpA over other related Clp proteins, especially ClpB.[185] Although the membrane-protein complex HflKC is mostly exposed to the periplasmic face of the *E. coli* membrane, and although the periplasmic part of FtsH is rather small, genetic and biochemical data indicate that HflKC can form a complex with FtsH and suggest that HflKC modulates FtsH activity.[186,187] PinA has been described as a modulator of Lon-dependent protein degradation. However, instead of promoting degradation, it inhibits it by forming a tight complex with Lon's N-terminal region.[188–190]

Mechanistically, bacterial ATP-dependent proteases can be divided into two broad classes, the symmetry-matched complexes HslVU, Lon and FtsH on the one hand and the symmetry-mismatched complexes ClpXP and ClpAP on the other hand. In HslVU, the best-understood system, structural, functional and mutagenesis data suggest allosteric activation of the protease active sites by the C termini of the activator molecules.[36,44,45] In the crystal structure of the HslVU complex, the C termini of all subunits insert into their binding sites in protease. If this feature was essential, a similar activation mechanism should not be possible in the ClpAP and ClpXP systems. This does not seem to be the case, because there is strong biochemical evidence that an internal loop in ClpX could be the functional equivalent of the C terminus in HslU.[191] Although allosteric effects are clearly also involved in the activation of the Lon and FtsH proteases, the details require further investigation.

From the 20S to the 26S proteasome

The ATP-independent 20S proteasome is now fairly well characterised, and its maturation, catalytic mechanism, broad substrate specificity, regulation and interactions with a broad variety of inhibitors have been described in detail. This is in stark contrast to the available data on the ATP-dependent 26S proteasome, which has, so far, only been imaged at much lower resolutions by electron microscopy and 3D-image reconstruction.[192] Difficulties with crystallisation have to do with the size of the complex, which approaches >2.5 MDa, and probably more importantly with the lability of the 19S cap. So far, it is known that the ATP-dependent 19S regulators can be regarded as a complex of two major subcomplexes, the "base" and the "lid".[193] All six AAA(+) ATPases that occur in the 19S cap are part of the base complex.

Thus, the 20S-proteasome–base complex is in some ways reminiscent of bacterial HslVU, even though there are important differences. Firstly, the 20S proteasome, but not HslV, has antichambers in addition to the central proteolytic chamber. Secondly, bacterial HslV has sixfold symmetry, whereas eukaryotic 20S proteasomes have pseudo-sevenfold symmetry and are thus at least formally symmetry-mismatched with the six different ATPases in the cap. Although the analogy with all bacterial ATP-dependent proteases suggests a six-membered ring in the base of the 19S cap, two-hybrid-experiment data support a more complex model that places only four of the six AAA(+) ATPases in a ring. Finally, allosteric activation, not channel opening, appears to be essential for HslV activation. In contrast, there is no evidence for allosteric active-site activation in 20S proteasomes, but there is strong evidence that the activators control "gating" into the 20S particle.[98] At present, it is not clear whether the "insertion mechanism", shared among the very different ATP-dependent proteases HslVU and ClpXP, has an equivalent in 26S proteasomes. Although there is firm structural evidence for the role of the C termini of an ATP-independent proteasome activator in gating,[96] no such evidence is available for the C termini of AAA(+) ATPases in the 19S cap. Thus, the mechanism of 20S proteasome activation remains open for further investigation.

Despite many differences, the 20S-proteasome–base complex is likely to be similar to the bacterial peptidase HslVU in some ways. Although the details are controversial, it is general-

ly assumed that several AAA(+) ATPases will form a ring, and the analogy with HslVU suggests that the ATPase subunits could be in direct contact with the 20S core particle. Two-hybrid-experiment data support this model, because they reveal a number of interactions among proteasomal ATPases and between ATPases and 20S core subunits.[194] As there is no ubiquitin system in bacteria or archaea, the model systems shed no light on the "lid" complex that seems to lack homologues in these simpler organisms. Thus, currently the most detailed structural information is derived from high-resolution electron-microsopy data[192] and from an exhaustive protein–protein interaction map of the *Caenorhabditis elegans* 26S proteasome.[194] In the light of the intriguing similarities between the proteasomal 19S cap, the COP9 signalosome and the translation-initiation factor eIF3,[103] structural information on the 19S cap at atomic resolution could either come directly from a crystal of this complex regulatory molecule or could result more indirectly from the determination of the crystal structure of either of the two other complexes.

In analogy to tricorn, which serves as a scaffold for interacting proteases, it is becoming increasingly clear that the 19S cap serves as a scaffold for some ubiquitin isopeptidases that deubiquitinate substrates prior to their degradation. In some cases, the association is so tight that the isopeptidases are regarded as integral parts of the 26S proteasome. This is true for Rpn11, a ubiquitin-metalloisopeptidase that appears to be present in all eukaryotic proteasomes.[195] It is also true for Uch37, a conventional ubiquitin hydrolase with a cysteine nucleophile that was found in eukaryotic proteasome preparations but that appears to lack a homologue in yeast.[196] More recently, it was shown that Ubp6 (USP14 in mammals) is activated by and physically associated with 26S proteasomes,[197] thereby prompting the suggestion that it could be an integral part of physiologically occurring proteasomes that was lost in previous purification protocols of the 26S particle.[198] A physical association with proteasomes has also been reported for Doa4, another class II ubiquitin hydrolase.[199] In contrast to other non-ATPase subunits of the 19S cap, rough structural models can be built for the ubiquitin hydrolases that are part of the 19S cap or are associated with it: from the HAUSP[200] structure, it is known that conventional class II ubiquitin hydrolases belong to the papain family of cysteine peptidases, and the Rpn11 can partially be modeled after the structure of an archaebacterial protein of unknown function.[201] Given the loose association of 19S cap subunits, it is possible that more structural information on this complex will emerge from structures of individual subunits or their homologues rather than from a single crystal structure of the 19S cap or of the related COP9 signalosome.

From tricorn to structurally and functionally related proteases

Tricorn represents a striking example for molecular coevolution: the enzyme and its downstream peptidase share not only similarities of the α–β hydrolase fold but also analogies in the structure and mechanism of their catalytic machineries. The activities of the two enzymes compliment each other: Two tricorn arginine residues serve to recognise and anchor the C termini of substrates and thus explain the carboxypeptidase activity of tricorn. In contrast, two glutamate residues in F1 anchor the N termini of substrates, thereby making F1 an aminopeptidase.

Quite unexpectedly, the eukaryotic DP IV exhibits striking structural similarities with these archebacterial protein-degradation enzymes, both with respect to the catalytic machinery and the characteristic open-Velcro β propeller topology. By contrast, the function of DP IV is related to delicately regulating the blood-glucose level and is thus very much diverged from its archebacterial ancestors involved in "high-throughput degradation". Nonetheless, important analogies and conclusions about the substrate–product passage through these highly complex proteases can be drawn.

Functional eukaryotic tricorn analogues appear to be structurally unrelated to tricorn. It is currently believed that proteasome degradation products are digested by prolyl oligopeptidase, thimet oligopeptidase and a giant peptidase, tripeptidyl peptidase II.[202,203] Tripeptidyl peptidase II has several features in common with tricorn. It is a serine protease as well, and like tricorn it forms defined, giant, high-molecular-weight assemblies that far exceed the proteasome in size.[204] Apart from these similarities, tricorn and tripeptidyl peptidase II are quite different. Their sequences and folds are so unrelated that the two enzymes are classified in different clans in MEROPS.[11] The helical features in the ultrastructure of tripeptidyl peptidase II have nothing in common with the regular icosahedral tricorn, and most importantly, there is currently no experimental evidence for any role of tripeptidyl peptidase II as a scaffold to physically assemble components of the protein-degradation machinery.

From DegP towards proteins that tip the balance between refolding and degradation

DegP can act either as a chaperone or as a protease. According to the current working model, the switch depends on a conformational change from the low-temperature conformation with occluded active sites to the hypothetical high-temperature conformation with accessible active sites. Thus, the switch depends primarily on DegP and less so on substrates or cofactors. This simple model contrasts with more complex mechanisms to explain the balance between protein degradation and protein refolding in eukaryotes.

In direct analogy to DegP, it has been reported that many ATP-dependent proteases, including the proteasome, can act as chaperones if the protease activity is artificially ablated. Although this observation has been made multiple times in vitro, its in vivo significance is not clear, and interactions between genuine chaperones and the protein-degradation machinery appear to be the key factor that tips the balance between protein degradation and refolding. The idea of cross-talk between chaperones and the protein-degradation machinery has received strong support from the discovery of specific factors, such as CHIP ("C terminus of Hsc70 interacting pro-

tein"),[205] BAG-1 ("Bcl-2-associated athanogene-1")[206,207] or VCP ("valosin-containing protein"),[208] that interact with chaperones or act as chaperones and have also been demonstrated to be directly involved in ubiquitin-mediated protein degradation.

A physical association of components of the protein-degradation machinery with chaperones makes mechanistic sense. Chaperones select for aberrant proteins. Thus, the protein-degradation machinery is most likely to find these proteins in association with chaperones and cochaperones. Moreover, proteins that are encountered in complex with a chaperone are difficult to refold, simply because proteins that are refolded efficiently are quickly released from chaperones. Thus, a protease can be more selective for truly "difficult" cases if it targets aberrant proteins that occur in complex with chaperones. Substrates could either be recognised specifically or simply be targeted for degradation because of their persistent association with chaperones. As both the key chaperones and the 26S proteasome are abundant proteins, and because currently prominent proteins at the interface of chaperones and the protein-degradation machinery are rare proteins, we expect that more factors that have a role in the decision between protein degradation and protein refolding remain to be discovered.

Acknowledgements

M.B. thanks Dr. Ravishankar Ramachandran, Molecular & Structural Biology division, Central Drug Research Institute, Lucknow, India, for a critical reading of his contribution to the manuscript.

Keywords: molecular machines · proteasomes · protein degradation · protein structures · structure–activity relationships

[1] S. Chuang, F. Blattner, *J. Bacteriol.* **1993**, *175*, 5242 – 5252.
[2] S. E. Chuang, V. Burland, G. Plunkett, D. L. Daniels, F. R. Blattner, *Gene* **1993**, *134*, 1 – 6.
[3] M. Rohrwild, O. Coux, H. C. Huang, R. P. Moerschell, S. J. Yoo, J. H. Seol, C. H. Chung, A. L. Goldberg, *Proc. Natl. Acad. Sci. USA* **1996**, *93*, 5808 – 5813.
[4] S. Yoo, J. Seol, D. Shin, M. Rohrwild, M. Kang, K. Tanaka, A. Goldberg, C. Chung, *J. Biol. Chem.* **1996**, *271*, 14035 – 14040.
[5] D. Missiakas, F. Schwager, J. Betton, C. Georgopoulos, S. Raina, *EMBO J.* **1996**, *15*, 6899 – 6909.
[6] M. Khattar, *FEBS Lett.* **1997**, *414*, 402 – 404.
[7] M. Kanemori, K. Nishihara, H. Yanagi, T. Yura, *J. Bacteriol.* **1997**, *179*, 7219 – 7225.
[8] D. Missiakas, F. Schwager, J. M. Betton, C. Georgopoulos, S. Raina, *EMBO J.* **1996**, *15*, 6899 – 6909.
[9] M. Kanemori, H. Yanagi, T. Yura, *J. Bacteriol.* **1999**, *181*, 3674 – 3680.
[10] I. Seong, J. Oh, S. Yoo, J. Seol, C. Chung, *FEBS Lett.* **1999**, *456*, 211 – 214.
[11] N. Rawlings, E. O'Brien, A. Barrett, *Nucleic Acids Res.* **2002**, *30*, 343 – 346.
[12] B. Couvreur, R. Wattiez, A. Bollen, P. Falmagne, D. Le Ray, J. Dujardin, *Mol. Biol. Evol.* **2002**, *19*, 2110 – 2117.
[13] J. H. Seol, S. J. Yoo, D. H. Shin, Y. K. Shim, M. S. Kang, A. L. Goldberg, C. H. Chung, *Eur. J. Biochem.* **1997**, *247*, 1143 – 1150.
[14] H. Huang, A. Goldberg, *J. Biol. Chem.* **1997**, *272*, 21364 – 21372.
[15] A. Lupas, P. Zwickl, W. Baumeister, *Trends Biochem. Sci.* **1994**, *19*, 533 – 534.
[16] M. Rohrwild, G. Pfeifer, U. Santarius, S. A. Muller, H. C. Huang, A. Engel, W. Baumeister, A. L. Goldberg, *Nat. Struct. Biol.* **1997**, *4*, 133 – 139.
[17] M. Bochtler, L. Ditzel, M. Groll, R. Huber, *Proc. Natl. Acad. Sci. USA* **1997**, *94*, 6070 – 6074.
[18] M. Sousa, D. McKay, *Acta Crystallogr. Sect. D Biol Crystallogr.* **2001**, *57*, 1950 – 1954.
[19] H. K. Song, M. Bochtler, M. K. Azim, C. Hartmann, R. Huber, R. Ramachandran, *Biophys. Chem.* **2003**, *100*, 437 – 452.
[20] M. Kang, B. Lim, I. Seong, J. Seol, N. Tanahashi, K. Tanaka, C. Chung, *EMBO J.* **2001**, *20*, 734 – 742.
[21] I. Levchenko, C. K. Smith, N. P. Walsh, R. T. Sauer, T. A. Baker, *Cell* **1997**, *91*, 939 – 947.
[22] A. Neuwald, L. Aravind, J. Spouge, E. Koonin, *Genome Res.* **1999**, *9*, 27 – 43.
[23] M. Bochtler, C. Hartmann, H. K. Song, G. P. Bourenkov, H. D. Bartunik, R. Huber, *Nature* **2000**, *403*, 800 – 805.
[24] J. Wang, J. J. Song, I. S. Seong, M. C. Franklin, S. Kamtekar, S. H. Eom, C. H. Chung, *Structure (Cambridge, MA, US)* **2001**, *9*, 1107 – 1116.
[25] K. Karata, T. Inagawa, A. J. Wilkinson, T. Tatsuta, T. Ogura, *J. Biol. Chem.* **1999**, *274*, 26225 – 26232.
[26] F. Guo, L. Esser, S. Singh, M. Maurizi, D. Xia, *J. Biol. Chem.* **2002**, *277*, 46753 – 46762.
[27] H. Song, C. Hartmann, R. Ramachandran, M. Bochtler, R. Behrendt, L. Moroder, R. Huber, *Proc. Natl. Acad. Sci. USA* **2000**, *97*, 14103 – 14108.
[28] C. Smith, T. Baker, R. Sauer, *Proc. Natl. Acad. Sci. USA* **1999**, *96*, 6678 – 6682.
[29] S. Wickner, M. Maurizi, *Proc. Natl. Acad. Sci. USA* **1999**, *96*, 8318 – 8320.
[30] J. Ortega, S. Singh, T. Ishikawa, M. Maurizi, A. Steven, *Mol. Cell.* **2000**, *6*, 515 – 521.
[31] M. Kang, S. Kim, P. Kwack, B. Lim, S. Ahn, Y. Rho, I. Seong, S. Park, S. Eom, G. Cheong, C. Chung, *EMBO J.* **2003**, *22*, 2893 – 2902.
[32] M. Kessel, M. R. Maurizi, B. Kim, E. Kocsis, B. L. Trus, S. K. Singh, A. C. Steven, *J. Mol. Biol.* **1995**, *250*, 587 – 594.
[33] R. Grimaud, M. Kessel, F. Beuron, A. Steven, M. Maurizi, *J. Biol. Chem.* **1998**, *273*, 12476 – 12481.
[34] M. Kessel, W. Wu, S. Gottesman, E. Kocsis, A. Steven, M. Maurizi, *FEBS Lett.* **1996**, *398*, 274 – 278.
[35] J. Wang, J. Song, M. Franklin, S. Kamtekar, Y. Im, S. Rho, I. Seong, C. Lee, C. Chung, S. Eom, *Structure (Cambridge, MA, US)* **2001**, *9*, 177 – 184.
[36] M. C. Sousa, C. B. Trame, H. Tsuruta, S. M. Wilbanks, V. S. Reddy, D. B. McKay, *Cell* **2000**, *103*, 633 – 643.
[37] A. Kwon, B. Kessler, H. Overkleeft, D. McKay, *J. Mol. Biol.* **2003**, *330*, 185 – 195.
[38] J. Wang, *J. Struct. Biol.* **2001**, *134*, 15 – 24.
[39] M. Bochtler, H. Song, C. Hartmann, R. Ramachandran, R. Huber, *J. Struct. Biol.* **2001**, *135*, 281 – 293.
[40] J. Wang, *J. Struct. Biol.* **2003**, *141*, 7 – 8.
[41] T. Ishikawa, M. Maurizi, D. Belnap, A. Steven, *Nature* **2000**, *408*, 667 – 668.
[42] M. Bogyo, J. S. McMaster, M. Gaczynska, D. Tortorella, A. L. Goldberg, H. Ploegh, *Proc. Natl. Acad. Sci. USA* **1997**, *94*, 6629 – 6634.
[43] M. Sousa, B. Kessler, H. Overkleeft, D. McKay, *J. Mol. Biol.* **2002**, *318*, 779 – 785.
[44] I. Seong, M. Kang, M. Choi, J. Lee, O. Koh, J. Wang, S. Eom, C. Chung, *J. Biol. Chem.* **2002**, *277*, 25976 – 25982.
[45] R. Ramachandran, C. Hartmann, H. Song, R. Huber, M. Bochtler, *Proc. Natl. Acad. Sci. USA* **2002**, *99*, 7396 – 7401.
[46] J. Harris, *Biochim. Biophys. Acta* **1968**, *150*, 534 – 537.
[47] R. Hegerl, G. Pfeifer, G. Puhler, B. Dahlmann, W. Baumeister, *FEBS Lett.* **1991**, *283*, 117 – 121.
[48] J. Löwe, D. Stock, B. Jap, P. Zwickl, W. Baumeister, R. Huber, *Science* **1995**, *268*, 533 – 539.
[49] M. Groll, L. Ditzel, J. Löwe, D. Stock, M. Bochtler, H. D. Bartunik, R. Huber, *Nature* **1997**, *386*, 463 – 471.
[50] M. Unno, T. Mizushima, Y. Morimoto, Y. Tomisugi, K. Tanaka, N. Yasuoka, T. Tsukihara, *Structure (Cambridge, MA, US)* **2002**, *10*, 609 – 618.
[51] S. Frentzel, I. Kuhn-Hartmann, M. Gernold, P. Gott, A. Seelig, P. M. Kloetzel, *Eur. J. Biochem.* **1993**, *216*, 119 – 126.
[52] M. G. Brown, J. J. Monaco, *Enzyme Protein* **1993**, *47*, 343 – 353.
[53] P. C. Ramos, J. Hockendorff, E. S. Johnson, A. Varshavsky, R. J. Dohmen, *Cell* **1998**, *92*, 489 – 499.
[54] E. Krüger, P. Kloetzel, C. Enenkel, *Biochimie* **2001**, *83*, 289 – 293.

[55] P. Kloetzel, *Nat. Rev. Mol. Cell Biol.* **2001**, *2*, 179 – 187.
[56] E. Seemüller, A. Lupas, D. Stock, J. Löwe, R. Huber, W. Baumeister, *Science* **1995**, *268*, 579 – 582.
[57] L. Ditzel, R. Huber, K. Mann, W. Heinemeyer, D. H. Wolf, M. Groll, *J. Mol. Biol.* **1998**, *279*, 1187 – 1191.
[58] M. Groll, W. Heinemeyer, S. Jager, T. Ullrich, M. Bochtler, D. H. Wolf, R. Huber, *Proc. Natl. Acad. Sci. USA* **1999**, *96*, 10976 – 10983.
[59] H. J. Duggleby, S. P. Tolley, C. Hill, E. J. Dodson, G. Dodson, P. C. Moody, *Nature* **1995**, *373*, 264 – 268.
[60] J. A. Brannigan, G. Dodson, H. J. Duggleby, P. C. Moody, J. L. Smith, D. R. Tomchick, A. G. Murzin, *Nature* **1995**, *378*, 416 – 419.
[61] G. Schmidtke, R. Kraft, S. Kostka, P. Henklein, C. Frommel, J. Löwe, R. Huber, P. M. Kloetzel, M. Schmidt, *EMBO J.* **1996**, *15*, 6887 – 6898.
[62] P. Chen, M. Hochstrasser, *Cell* **1996**, *86*, 961 – 972.
[63] M. Groll, H. Brandstetter, H. Bartunik, G. Bourenkow, R. Huber, *J. Mol. Biol.* **2003**, *327*, 75 – 83.
[64] Y. Kwon, I. Nagy, P. Adams, W. Baumeister, B. Jap, *J. Mol. Biol.* **2004**, *335*, 233 – 245.
[65] E. Witt, D. Zantopf, M. Schmidt, R. Kraft, P. M. Kloetzel, E. Kruger, *J. Mol. Biol.* **2000**, *301*, 1 – 9.
[66] M. Groll, T. Clausen, *Curr. Opin. Struct. Biol.* **2003**, *13*, 665 – 673.
[67] G. Schmidtke, M. Schmidt, P. M. Kloetzel, *J. Mol. Biol.* **1997**, *268*, 95 – 106.
[68] S. Jäger, M. Groll, R. Huber, D. H. Wolf, W. Heinemeyer, *J. Mol. Biol.* **1999**, *291*, 997 – 1013.
[69] W. Heinemeyer, M. Fischer, T. Krimmer, U. Stachon, D. H. Wolf, *J. Biol. Chem.* **1997**, *272*, 25200 – 25209.
[70] C. S. Arendt, M. Hochstrasser, *EMBO J.* **1999**, *18*, 3575 – 3585.
[71] P. Chen, M. Hochstrasser, *EMBO J.* **1995**, *14*, 2620 – 2630.
[72] E. Seemüller, A. Lupas, W. Baumeister, *Nature* **1996**, *382*, 468 – 471.
[73] R. Huber, W. Bode, *Acc. Chem. Res.* **1978**, *11*, 114 – 122.
[74] M. Orlowski, S. Wilk, *Arch. Biochem. Biophys.* **2000**, *383*, 1 – 16.
[75] C. S. Arendt, M. Hochstrasser, *Proc. Natl. Acad. Sci. USA* **1997**, *94*, 7156 – 7161.
[76] W. Hilt, D. H. Wolf, *Trends Biochem. Sci.* **1996**, *21*, 96 – 102.
[77] T. P. Dick, A. K. Nussbaum, M. Deeg, W. Heinemeyer, M. Groll, M. Schirle, W. Keilholz, S. Stevanovic, D. H. Wolf, R. Huber, H. G. Rammensee, H. Schild, *J. Biol. Chem.* **1998**, *273*, 25637 – 25646.
[78] A. K. Nussbaum, T. P. Dick, W. Keilholz, M. Schirle, S. Stevanovic, K. Dietz, W. Heinemeyer, M. Groll, D. H. Wolf, R. Huber, H. G. Rammensee, H. Schild, *Proc. Natl. Acad. Sci. USA* **1998**, *95*, 12504 – 12509.
[79] H. J. Fehling, W. Swat, C. Laplace, R. Kuhn, K. Rajewsky, U. Muller, H. von Boehmer, *Science* **1994**, *265*, 1234 – 1237.
[80] C. Sibille, K. G. Gould, K. Willard-Gallo, S. Thomson, A. J. Rivett, S. Powis, G. W. Butcher, P. De Baetselier, *Curr. Biol.* **1995**, *5*, 923 – 930.
[81] J. Driscoll, M. G. Brown, D. Finley, J. J. Monaco, *Nature* **1993**, *365*, 262 – 264.
[82] M. Gaczynska, K. L. Rock, A. L. Goldberg, *Enzyme Protein* **1993**, *47*, 354 – 369.
[83] L. Van Kaer, P. Ashton-Rickardt, M. Eichelberger, M. Gaczynska, K. Nagashima, K. Rock, A. Goldberg, P. Doherty, S. Tonegawa, *Immunology* **1994**, *1*, 533 – 541.
[84] V. Engelhard, *Curr. Opin. Immunol.* **1994**, *6*, 13 – 23.
[85] M. Groll, K. B. Kim, N. Kairies, R. Huber, C. M. Crews, *J. Am. Chem. Soc.* **2000**, *122*, 1237 – 1238.
[86] M. Groll, Y. Koguchi, R. Huber, J. Kohno, *J. Mol. Biol.* **2001**, *311*, 543 – 548.
[87] M. Groll, T. Nazif, R. Huber, M. Bogyo, *Chem. Biol.* **2002**, *9*, 1 – 20.
[88] T. N. Akopian, A. F. Kisselev, A. L. Goldberg, *J. Biol. Chem.* **1997**, *272*, 1791 – 1798.
[89] K. L. Rock, A. L. Goldberg, *Annu. Rev. Immunol.* **1999**, *17*, 739 – 779.
[90] M. Bochtler, L. Ditzel, M. Groll, C. Hartmann, R. Huber, *Annu. Rev. Biophys. Biomol. Struct.* **1999**, *28*, 295 – 317.
[91] M. Groll, R. Huber, *Int. J. Biochem. Cell. Biol.* **2003**, *35*, 606 – 616.
[92] J. M. Peters, Z. Cejka, J. R. Harris, J. A. Kleinschmidt, W. Baumeister, *J. Mol. Biol.* **1993**, *234*, 932 – 937.
[93] L. Hoffman, G. Pratt, M. Rechsteiner, *J. Biol. Chem.* **1992**, *267*, 22362 – 22368.
[94] C. W. Gray, C. A. Slaughter, G. N. DeMartino, *J. Mol. Biol.* **1994**, *236*, 7 – 15.
[95] M. A. Kania, G. N. Demartino, W. Baumeister, A. L. Goldberg, *Eur. J. Biochem.* **1996**, *236*, 510 – 516.
[96] F. G. Whitby, E. I. Masters, L. Kramer, J. R. Knowlton, Y. Yao, C. C. Wang, C. P. Hill, *Nature* **2000**, *408*, 115 – 120.
[97] M. Groettrup, A. Soza, U. Kuckelkorn, P. M. Kloetzel, *Immunol. Today* **1996**, *17*, 429 – 435.
[98] M. Groll, M. Bajorek, A. Köhler, L. Moroder, D. M. Rubin, R. Huber, M. H. Glickman, D. Finley, *Nat. Struct. Biol.* **2000**, *7*, 1062 – 1067.
[99] A. Köhler, P. Cascio, D. S. Leggett, K. M. Woo, A. L. Goldberg, D. Finley, *Mol. Cell* **2001**, *7*, 1143 – 1152.
[100] B. Dahlmann, M. Rutschmann, L. Kuehn, H. Reinauer, *Biochem. J.* **1985**, *228*, 171 – 177.
[101] A. Bachmair, D. Finley, A. Varshavsky, *Science* **1986**, *234*, 179 – 186.
[102] D. Voges, P. Zwickl, W. Baumeister, *Annu. Rev. Biochem.* **1999**, *68*, 1015 – 1068.
[103] M. H. Glickman, D. M. Rubin, O. Coux, I. Wefes, G. Pfeifer, Z. Cjeka, W. Baumeister, V. A. Fried, D. Finley, *Cell* **1998**, *94*, 615 – 623.
[104] D. M. Rubin, M. H. Glickman, C. N. Larsen, S. Dhruvakumar, D. Finley, *EMBO J.* **1998**, *17*, 4909 – 4919.
[105] C. U. Lenzen, D. Steinmann, S. W. Whiteheart, W. I. Weis, *Cell* **1998**, *94*, 525 – 536.
[106] R. C. Yu, P. I. Hanson, R. Jahn, A. T. Brünger, *Nat. Struct. Biol.* **1998**, *5*, 803 – 811.
[107] W. Dubiel, G. Pratt, K. Ferrell, M. Rechsteiner, *J. Biol. Chem.* **1992**, *267*, 22369 – 22377.
[108] M. Groettrup, A. Soza, M. Eggers, L. Kuehn, T. P. Dick, H. Schild, H. G. Rammensee, U. H. Koszinowski, P. M. Kloetzel, *Nature* **1996**, *381*, 166 – 168.
[109] T. P. Dick, T. Ruppert, M. Groettrup, P. M. Kloetzel, L. Kuehn, U. H. Koszinowski, S. Stevanovic, H. Schild, H. G. Rammensee, *Cell* **1996**, *86*, 253 – 262.
[110] J. R. Knowlton, S. C. Johnston, F. G. Whitby, C. Realini, Z. Zhang, M. Rechsteiner, C. P. Hill, *Nature* **1997**, *390*, 639 – 643.
[111] C. A. Realini, M. C. Rechsteiner, *Adv. Exp. Med. Biol.* **1996**, *389*, 51 – 61.
[112] J. D. Mott, B. C. Pramanik, C. R. Moomaw, S. J. Afendis, G. N. DeMartino, C. A. Slaughter, *J. Biol. Chem.* **1994**, *269*, 31466 – 31471.
[113] J. Y. Ahn, N. Tanahashi, K. Akiyama, H. Hisamatsu, C. Noda, K. Tanaka, C. H. Chung, N. Shibmara, P. J. Willy, J. D. Mott, C. A. Slaughter, G. N. DeMartino, *FEBS Lett.* **1995**, *366*, 37 – 42.
[114] C. Realini, W. Dubiel, G. Pratt, K. Ferrell, M. Rechsteiner, *J. Biol. Chem.* **1994**, *269*, 20727 – 20732.
[115] C. P. Ma, P. J. Willy, C. A. Slaughter, G. N. DeMartino, *J. Biol. Chem.* **1993**, *268*, 22514 – 22519.
[116] M. H. Glickman, D. M. Rubin, V. A. Fried, D. Finley, *Mol. Cell. Biol.* **1998**, *18*, 3149 – 3162.
[117] A. Vinitsky, C. Cardozo, L. Sepp-Lorenzino, C. Michaud, M. Orlowski, *J. Biol. Chem.* **1994**, *269*, 29860 – 29866.
[118] S. Omura, T. Fujimoto, K. Otoguro, K. Matsuzaki, R. Moriguchi, H. Tanaka, Y. Sasaki, *J. Antibiot.* **1991**, *44*, 113 – 116.
[119] G. Fenteany, R. F. Standaert, W. S. Lane, S. Choi, E. J. Corey, S. L. Schreiber, *Science* **1995**, *268*, 726 – 731.
[120] L. R. Dick, A. A. Cruikshank, A. T. Destree, L. Grenier, T. A. McCormack, F. D. Melandri, S. L. Nunes, V. J. Palombella, L. A. Parent, L. Plamondon, R. L. Stein, *J. Biol. Chem.* **1997**, *272*, 182 – 188.
[121] G. Loidl, M. Groll, H. J. Musiol, L. Ditzel, R. Huber, L. Moroder, *Chem. Biol.* **1999**, *6*, 197 – 204.
[122] G. Loidl, M. Groll, H. J. Musiol, R. Huber, L. Moroder, *Proc. Natl. Acad. Sci. USA* **1999**, *96*, 5418 – 5422.
[123] L. Meng, R. Mohan, B. H. Kwok, M. Elofsson, N. Sin, C. M. Crews, *Proc. Natl. Acad. Sci. USA* **1999**, *96*, 10403 – 10408.
[124] T. Nazif, M. Bogyo, *Proc. Natl. Acad. Sci. USA* **2001**, *98*, 2967 – 2972.
[125] P. M. Kloetzel, *Cancer Gene Ther.* **1998**, *5*, 1297 – 1298.
[126] Y. Koguchi, J. Kohno, M. Nishio, K. Takahashi, T. Okuda, T. Ohnuki, S. Komatsubara, *J. Antibiot.* **2000**, *53*, 105 – 109.
[127] J. Kohno, Y. Koguchi, M. Nishio, K. Nakao, M. Kuroda, R. Shimizu, T. Ohnuki, S. Komatsubara, *J. Org. Chem.* **2000**, *65*, 990 – 995.
[128] M. Kaiser, M. Groll, C. Renner, R. Huber, L. Moroder, *Angew. Chem.* **2002**, *114*, 817 – 820; *Angew. Chem. Int. Ed.* **2002**, *41*, 780 – 783.
[129] M. Kaiser, C. Siciliano, I. Assfalg-Machleidt, M. Groll, A. Milbradt, L. Moroder, *Org. Lett.* **2003**, *5*, 3435 – 3437.

[130] S. Lin, S. Danishefsky, *Angew. Chem.* **2002**, *114*, 530 – 533; *Angew. Chem. Int. Ed.* **2002**, *41*, 512 – 515.
[131] B. Albrecht, R. Williams, *Proc. Natl. Acad. Sci. USA* **2004**, *101*, 11 949 – 11 954.
[132] M. Kaiser, M. Groll, C. Siciliano, I. Assfalg-Machleidt, E. Weyher, J. Kohno, A. Milbradt, C. Renner, R. Huber, L. Moroder, *ChemBioChem* **2004**, *5*, 1256 – 1266.
[133] J. Janetka, P. Raman, K. Satyshur, G. Flentke, D. Rich, *J. Am. Chem. Soc.* **1997**, *119*, 441 – 442.
[134] M. Kaiser, A. Milbradt, C. Siciliano, I. Assfalg-Machleidt, W. Machleidt, M. Groll, C. Renner, L. Moroder, *Chem. Biodiversity* **2004**, *1*, 161 – 173.
[135] T. Tamura, N. Tamura, Z. Cejka, R. Hegerl, F. Lottspeich, W. Baumeister, *Science* **1996**, *274*, 1385 – 1389.
[136] J. Walz, A. J. Koster, T. Tamura, W. Baumeister, *J. Struct. Biol.* **1999**, *128*, 65 – 68.
[137] H. Brandstetter, J. Kim, M. Groll, R. Huber, *Nature* **2001**, *414*, 466 – 470.
[138] V. Fülöp, Z. Böcskei, L. Polgar, *Cell* **1998**, *94*, 161 – 170.
[139] M. Engel, T. Hoffmann, L. Wagner, M. Wermann, U. Heiser, R. Kiefersauer, R. Huber, W. Bode, H. Demuth, H. Brandstetter, *Proc. Natl. Acad. Sci. USA* **2003**, *100*, 5063 – 5068.
[140] H. Rasmussen, S. W. Branner, F. C. N. Wagtmann, *Nat. Struct. Biol.* **2003**, *10*, 19 – 25.
[141] W. Bode, I. Mayr, U. Baumann, R. Huber, S. Stone, J. Hofsteenge, *EMBO J.* **1989**, *8*, 3467 – 3475.
[142] A. Eichinger, H. Beisel, U. Jacob, R. Huber, F. Medrano, A. Banbula, J. Potempa, J. Travis, W. Bode, *EMBO J.* **1999**, *18*, 5453 – 5462.
[143] T. Tamura, N. Tamura, F. Lottspeich, W. Baumeister, *FEBS Lett.* **1996**, *398*, 101 – 105.
[144] K. Beebe, J. Shin, J. Peng, C. Chaudhury, J. Khera, D. Pei, *Biochemistry* **2000**, *39*, 3149 – 3155.
[145] C. Ponting, M. Pallen, *FEMS Microbiol. Lett.* **1999**, *179*, 447 – 451.
[146] D. Liao, J. Qian, D. Chisholm, D. Jordan, B. Diner, *Nat. Struct. Biol.* **2000**, *7*, 749 – 753.
[147] J. Morais Cabral, C. Petosa, M. Sutcliffe, S. Raza, O. Byron, F. Poy, S. Marfatia, A. Chishti, R. Liddington, *Nature* **1996**, *382*, 649 – 652.
[148] D. Doyle, A. Lee, J. Lewis, E. Kim, M. Sheng, R. MacKinnon, *Cell* **1996**, *85*, 1067 – 1076.
[149] J. Kim, M. Groll, H. Musiol, R. Behrendt, M. Kaiser, L. Moroder, R. Huber, H. Brandstetter, *J. Mol. Biol.* **2002**, *324*, 1041 – 1050.
[150] V. Fülöp, Z. Szeltner, L. Polgar, *EMBO Rep.* **2000**, *1*, 277 – 281.
[151] N. Ito, S. Phillips, C. Stevens, Z. Ogel, M. McPherson, J. Keen, K. Yadav, P. Knowles, *Nature* **1991**, *350*, 87 – 90.
[152] P. Göttig, M. Groll, J. Kim, R. Huber, H. Brandstetter, *EMBO J.* **2002**, *21*, 5343 – 5352.
[153] N. Tamura, F. Lottspeich, W. Baumeister, T. Tamura, *Cell* **1998**, *95*, 637 – 648.
[154] J. Pospisilik, S. Hinke, R. Pederson, T. Hoffmann, F. Rosche, D. Schlenzig, K. Glund, U. Heiser, C. McIntosh, H. Demuth, *Regul. Pept.* **2001**, *96*, 133 – 141.
[155] S. Wickner, R. Maurizi, S. Gottesman, *Science* **1999**, *286*, 1888 – 1893.
[156] S. Gottesman, S. Wickner, M. Maurizi, *Genes Dev.* **1997**, *11*, 815 – 823.
[157] B. Lipinska, M. Zylicz, C. Georgopoulos, *J. Bacteriol.* **1990**, *172*, 1791 – 1797.
[158] T. Clausen, C. Southan, M. Ehrmann, *Mol. Cell.* **2002**, *10*, 443 – 455.
[159] M. Sheng, C. Sala, *Annu. Rev. Neurosci.* **2001**, *24*, 1 – 29.
[160] M. Pallen, B. Wren, *Mol. Microbiol.* **1997**, *26*, 209 – 221.
[161] H. Kolmar, P. Waller, R. Sauer, *J. Bacteriol.* **1996**, *178*, 5925 – 5929.
[162] C. Spiess, A. Beil, M. Ehrmann, *Cell* **1999**, *97*, 339 – 347.
[163] T. Krojer, M. Garrido-Franco, R. Huber, M. Ehrmann, T. Clausen, *Nature* **2002**, *416*, 455 – 459.
[164] J. Perona, C. Craik, *Protein Sci.* **1995**, *4*, 337 – 360.
[165] Z. Songyang, A. Fanning, C. Fu, J. Xu, S. Marfatia, A. Chishti, A. Crompton, A. Chan, J. Anderson, L. Cantley, *Science* **1997**, *275*, 73 – 77.
[166] R. Misra, M. Castillo Keller, M. Deng, *J. Bacteriol.* **2000**, *182*, 4882 – 4888.
[167] K. Strauch, K. Johnson, J. Beckwith, *J. Bacteriol.* **1989**, *171*, 2689 – 2696.
[168] I. Botos, E. Melnikov, S. Cherry, J. Tropea, A. Khalatova, F. Rasulova, Z. Dauter, M. Maurizi, T. Rotanova, A. Wlodawer, A. Gustchina, *J. Biol. Chem.* **2004**, *279*, 8140 – 8148.
[169] I. Botos, E. Melnikov, S. Cherry, A. Khalatova, F. Rasulova, J. Tropea, M. Maurizi, T. Rotanova, A. Gustchina, A. Wlodawer, *J. Struct. Biol.* **2004**, *146*, 113 – 122.
[170] J. Wang, J. A. Hartling, J. M. Flanagan, *J. Struct. Biol.* **1998**, *124*, 151 – 163.
[171] D. Kim, K. Kim, *J. Biol. Chem.* **2003**, *278*, 50 664 – 50 670.
[172] H. Niwa, D. Tsuchiya, H. Makyio, M. Yoshida, K. Morikawa, *Structure (Cambridge, MA, US)* **2002**, *10*, 1415 – 1423.
[173] S. Krzywda, A. Brzozowski, C. Verma, K. Karata, T. Ogura, A. Wilkinson, *Structure (Cambridge, MA, US)* **2002**, *10*, 1073 – 1083.
[174] A. Lupas, F. Zuhl, T. Tamura, S. Wolf, I. Nagy, R. De Mot, W. Baumeister, *Mol. Biol. Rep.* **1997**, *24*, 125 – 131.
[175] P. Babbitt, J. Gerlt, *J. Biol. Chem.* **1997**, *272*, 30 591 – 30 594.
[176] B. Banecki, A. Wawrzynow, J. Puzewicz, C. Georgopoulos, M. Zylicz, *J. Biol. Chem.* **2001**, *276*, 18 843 – 18 848.
[177] L. Donaldson, U. Wojtyra, W. Houry, *J. Biol. Chem.* **2003**, *278*, 48 991 – 48 996.
[178] D. Dougan, A. Mogk, B. Bukau, *Cell. Mol. Life Sci.* **2002**, *59*, 1607 – 1616.
[179] D. Dougan, E. Weber-Ban, B. Bukau, *Mol. Cell.* **2003**, *12*, 373 – 380.
[180] H. E. Song, M. J. Eck, *Mol Cell.* **2003**, *12*, 75 – 86.
[181] I. Levchenko, R. Grant, D. Wah, R. Sauer, T. Baker, *Mol. Cell.* **2003**, *12*, 365 – 372.
[182] Y. Zhou, S. Gottesman, J. Hoskins, M. Maurizi, S. Wickner, *Genes Dev.* **2001**, *15*, 627 – 637.
[183] A. Studemann, M. Noirclerc-Savoye, E. Klauck, G. Becker, D. Schneider, R. Hengge, *EMBO J.* **2003**, *22*, 4111 – 4120.
[184] D. Dougan, B. Reid, A. Horwich, B. Bukau, *Mol. Cell.* **2002**, *9*, 673 – 683.
[185] K. Zeth, R. Ravelli, K. Paal, S. Cusack, B. Bukau, D. Dougan, *Nat. Struct. Biol.* **2002**, *9*, 906 – 911.
[186] Y. Akiyama, M. Ehrmann, A. Kihara, K. Ito, *Mol. Microbiol.* **1998**, *28*, 803 – 812.
[187] A. Kihara, Y. Akiyama, K. Ito, *EMBO J.* **1996**, *15*, 6122 – 6131.
[188] J. Hilliard, L. Simon, L. Van Melderen, M. Maurizi, *J. Biol. Chem.* **1998**, *273*, 524 – 527.
[189] J. Hilliard, M. Maurizi, L. Simon, *J. Biol. Chem.* **1998**, *273*, 518 – 523.
[190] S. Roudiak, T. Shrader, *Biochemistry* **1998**, *37*, 11 255 – 11 263.
[191] Y. Kim, I. Levchenko, K. Fraczkowska, R. Woodruff, R. Sauer, T. Baker, *Nat. Struct. Biol.* **2001**, *8*, 230 – 233.
[192] J. Walz, A. Erdmann, M. Kania, D. Typke, A. J. Koster, W. Baumeister, *J. Struct. Biol.* **1998**, *121*, 19 – 29.
[193] M. H. Glickman, D. M. Rubin, H. Fu, C. N. Larsen, O. Coux, I. Wefes, G. Pfeifer, Z. Cjeka, R. Vierstra, W. Baumeister, V. Fried, D. Finley, *Mol. Biol. Rep.* **1999**, *26*, 21 – 28.
[194] A. Davy, P. Bello, N. Thierry-Mieg, P. Vaglio, J. Hitti, L. Doucette-Stamm, D. Thierry-Mieg, J. Reboul, S. Boulton, A. Walhout, O. Coux, M. Vidal, *EMBO Rep.* **2001**, *2*, 821 – 828.
[195] R. Verma, L. Aravind, R. Oania, W. McDonald, J. R. Yates, E. Koonin, R. Deshaies, *Science* **2002**, *298*, 611 – 615.
[196] Y. A. Lam, W. Xu, G. N. DeMartino, R. E. Cohen, *Nature* **1997**, *385*, 737 – 740.
[197] A. Borodovsky, B. Kessler, R. Casagrande, H. Overkleeft, K. Wilkinson, H. Ploegh, *EMBO J.* **2001**, *20*, 5187 – 5196.
[198] D. Leggett, J. Hanna, A. Borodovsky, B. Crosas, M. Schmidt, R. Baker, T. Walz, H. Ploegh, D. Finley, *Mol. Cell.* **2002**, *10*, 495 – 507.
[199] F. Papa, A. Amerik, M. Hochstrasser, *Mol. Biol. Cell* **1999**, *10*, 741 – 756.
[200] M. Hu, P. Li, M. Li, W. Li, T. Yao, J. Wu, W. Gu, R. Cohen, Y. Shi, *Cell* **2002**, *111*, 1041 – 1054.
[201] H. Tran, M. Allen, M. Bycroft, *Biochemistry* **2003**, *42*, 11 460 – 11 465.
[202] E. Wang, B. Kessler, A. Borodovsky, B. Cravatt, M. Bogyo, H. Ploegh, R. Glas, *Proc. Natl. Acad. Sci. USA* **2000**, *97*, 9990 – 9995.
[203] B. Tomkinson, *Trends Biochem. Sci.* **1999**, *24*, 355 – 359.
[204] B. Rockel, J. Peters, B. Kuhlmorgen, R. Glaeser, W. Baumeister, *EMBO J.* **2002**, *21*, 5979 – 5984.
[205] C. B. Scheufler, A. G. Bourenkov, S. Pegoraro, L. Moroder, H. Bartunik, F. Hartl, I. Moarefi, *Cell* **2000**, *101*, 199 – 210.
[206] S. Takayama, J. C. Reed, *Nat. Cell Biol.* **2001**, *3*, E237 – E241.
[207] H. Sondermann, C. Scheufler, C. Schneider, J. Hohfeld, F. Hartl, I. Moarefi, *Science* **2001**, *291*, 1553 – 1557.
[208] R. M. Dai, C.-C. H. Li, *Nat. Cell Biol.* **2001**, *3*, 740 – 744.

Received: September 6, 2004

